# Effects of Knee Brace on Anterior Cruciate Ligament Strain During Drop-Landing

by

Gajendra Hangalur

A thesis
presented to the University of Waterloo
in fulfillment of the
thesis requirement for the degree of
Master of Applied Science
in
Mechanical Engineering

Waterloo, Ontario, Canada, 2014

# AUTHOR'S DECLARATION

I hereby declare that I am the sole author of this thesis. This is a true copy of the thesis, including any required final revisions, as accepted by my examiners.

I understand that my thesis may be made electronically available to the public.

# Abstract

Knee is one of the most commonly injured joint in the human body and majority of the injuries are associated with ligaments which have detrimental effects on joint's stability and function. Bracing has often been used as a prominent measure to restrain an unstable joint and for individuals with anterior cruciate ligament (ACL) injury as a post-operative treatment measure. However, it is not known if the brace would protect the ACL of an uninjured person during dynamic activities by reducing the strain in the ACL.

Primary objective of this research study was to investigate the effects of knee brace on ACL during dynamic activities. Hence a combined in-vivo/ in-vitro methodology was used to assess the influence of "CTi-Custom" knee brace on ACL strain during drop-landing activity. Motion capture was performed on the drop-landing activity of a high-risk subject with and without knee brace worn. These in-vivo kinetic and kinematic parameters were subsequently input into a biomechanical model to calculate muscle forces that span the knee joint. A hybrid surrogate knee model was prepared using cast foam shell that was wrapped around a cadaver knee specimen to form an artificial interface for mounting a custom fit knee brace during in-vitro simulation. A strain gauge was instrumented on ACL of hybrid surrogate cadaver specimen and mounted on a dynamic knee simulator, where kinematics and muscle forces were applied replicating braced and unbraced drop-landing conditions. This simulation was performed with and without the brace mounted on the cadaver knee specimen and the ACL strain was measured.

Observing biomechanical model outputs it was evident that muscle forces for braced and unbraced conditions were different and the knee brace appeared to reduce the ACL antagonist muscle forces thereby dissipating energy, consequently reducing the peak GRF and the internal joint forces. The peak strain in the ACL was radically different for braced (8% strain) and unbraced (18% strain) conditions. However, when unbraced kinetics/kinematics was simulated with brace mounted on the cadaver knee, the ACL strain was not different from the unbraced condition. This enabled us to conclude that the custom fit knee braces reduce the strain in the ACL of high-risk subjects thus preventing them from potential ACL injury. However, any decrease in the ACL strain observed while wearing the brace was due to the brace altering the muscle firing pattern rather than due to the mechanical restraint offered by the brace. This reinforces previous research findings that brace affects proprioceptive feedback and alters the muscle firing pattern.

# Acknowledgements

With eternal grace of God, I would like to say that every ounce of success in my life has been due to influence of others around me. Firstly I would like to thank my Supervisor Dr. Naveen Chandrashekar for giving me an opportunity to conduct research at University of Waterloo and for also providing me with help and guidance through some of the toughest phases of my life and research tenure. In addition, I would also like to acknowledge our industry partners of research Össur Inc. and The knee Centre, Calgary (Karl Hager Limb & Brace Canada) for providing us with custom fit braces to conduct research.

My special thanks to Dr. Andrew Laing for his guidance during the research, Micah Nicholls of Össur Inc for conducting analysis while selecting high risk subject and my fellow students Elora Brenneman, Amanda Shorter, Peter Meitus and Ryan Bakker for their assistance throughout my research phase. I would also like to express gratitude to the University of Waterloo Engineering machine shop staff, Neil Griffett and Tom Gawel for their technical assistance in the Lab. Furthermore, I would also like to thank Steve Smith (plant manager at ORBIS Canada) for providing me assistance and flexibility at work to make a living while pursuing my Master's degree.

I want thank NSERC (National Sciences and Engineering Research Council of Canada) for awarding me "Alexander Graham Bell Canada Graduate Scholarship" to complete my Master's degree. Finally I would like to acknowledge unconditional love of my family and friends who were relentlessly praying for me, motivating me and constantly lifting my spirits as I stumbled through many difficulties. I would not have been here today without them or their unconditional love.

# Dedication

I would like to dedicate this thesis to my beloved late sister Deepa K.S.

# Table of Contents

# List of Figures

# List of Tables

# Abbreviations

ACL: Anterior Cruciate Ligament

GRF: Ground Reaction force

3D: Three Dimension

PCL: Posterior Cruciate Ligament

DVRT: Differential Variable Reluctance Transducer

GCS: Global Coordinate System

ISB: International Society of Biomechanics

LVDT: Linear Variable Displacement Transducer

ATT: Anterior Tibial Translation

ATR: Axial Tibial Rotation

PKB: Prophylactic Knee Brace

MVC: Maximum Voluntary Contraction

C3D: Binary File format used in Biomechanics

PID: Potential, Integral and Differential Parameters of a closed loop system

EMG: Electromyography

VKLD: Vermont Knee Laxity Device

HEST: Hall Effect Strain Transducer

MCL: Medial Collateral Ligament

LCL: Lateral Collateral Ligament

GT: Greater Trochanter

LM: Lateral Malleoli

GUI: Graphic User Interface

AMB: Anteromedial Bundle of ACL

PLB: Posterolateral Bundle of ACL

NMM: New Muscle Moment Arm

IMF: Individual Muscle-unit Force (derived from Anybody Biomechanical Model)

IMM: Individual Muscle-unit Moment values calculated during post processing

MCF: Individual Muscle-unit Cable force Calculated during post processing

TMCF: Total Muscle Cable force (calculated for individual Muscle group per Table 2)

AHM: Hip flexion/extension moments acquired from Anybody bio mechanical model

HCM: Moments created by Hamstring actuator cable force

QCM: Moments created by Quadriceps actuator cable force

THCF: Hamstring actuator Cable force (sum of all hamstring muscle-unit forces)

TQCF: Quadriceps actuator Cable force (sum of all Quadriceps muscle-unit forces)

NHFr: Net hip cable force calculated after post processing

# Chapter 1
# Introduction

## 1.1 Research Impetus

Knee is one of the most commonly injured joint in the human body (Chew et al, 2007) and an article published by the American association of orthopedic surgeons (AAOS, 2014) suggests that most of them are associated with the ligaments of the knee joint. Among them, the most prevalent form of noncontact knee injury is associated with the rupture of anterior cruciate ligament (ACL) (Flynn et al, 2005) and highly prevalent in sports involving large / rapid landing impact loads, such as basketball and skiing (Yeow et al, 2009). Anterior cruciate ligament (ACL) is a serious and a costly affair (Flynn et al, 2005) and it is estimated that annually about 80,000 to 250,000 anterior cruciate ligament (ACL) injuries occur (mostly to young amateur athletes) in North America (Griffin et al, 2006), resulting up to about 2 billion dollars in treatment costs (Hewett et al, 2007).

Anterior cruciate ligament (ACL) occupies a vital role in providing stability to the knee joint while performing daily living activities and an ACL injury has devastating effects on individuals. Treatment options for ACL injuries are limited and dependent on the extent of the injury however, in case of severe damage to the ligament or complete rupture, ACL reconstruction surgery is essential to restore normal functioning of knee joint (Wilson Ross, 2007). ACL reconstruction surgery ranked sixth among most common surgical procedures performed among surgeons (Garrett, 2004). Although reconstruction surgeries are normally successful, several short and long term implications of such an invasive procedure are prevalent. Several retrospective studies have identified the development of post-traumatic joint degenerative diseases after surgical reconstruction of ACL (Griffin et al, 2006) and individuals' risks of being diagnosed with osteoarthritis have been reported to increase 100 times after a knee injury (Hewett et al, 1999; Freedman et al, 1998; Deacon et al, 1997). In addition, several other immeasurable costs, severe discomforts associated with injury, significant emotional and physical burden inflicted upon individuals who sustain ACL injuries remain unwarranted (Griffin et al, 2008). These direct and indirect consequences of ACL injury has become a premise for several novel research studies that focus in understanding the mechanics of ACL injury, development of preventive measures/techniques and ascertaining the effectiveness of such a prevention program.

One of the prominent preventive measures is to restrain the knee joint by bracing. However this technique is generally adopted in the rehabilitation process post ACL injury. In addition, since their inception in the later part of 1970's, knee brace effectiveness has been major focus of research

(Griffin et al, 2006). Although, biomechanical evidence on the effect of prophylactic knee brace on ACL injury remains unequivocal (Najibi and Albright, 2005), the true efficacy of prophylactic knee braces in preventing ACL disruptions during dynamic movement scenarios that occur in non-contact sports such as basketball remains an unanswered question (Najibi and Albright, 2005). Section 3.3 discusses more about current research undertakings that were involved in evaluating braces.

In conclusion, there is an emerging opportunity to explore several avenues and create a procedure to study the effectiveness of prophylactic braces in reducing ACL strain during dynamic activities. This thesis examines a complex research undertaking that combines both in-vivo/in-vitro techniques to develop an integrated procedure in order to understand the effectiveness of prophylactic knee brace in reducing ACL strain, during a single leg jump landing in an athlete who was determined to be at high risk of ACL injury.

## 1.2 Research Scope and Objectives

This research initiative has been devised into two major stages of study. During the initial phase, the primary objective of this research was to develop a methodology that included a combination of in-vivo / in-vitro techniques to identify effectiveness of a prophylactic knee brace in reducing ACL strain during a single leg jump landing, similar to landing after a basketball lay-up. In addition to this primary objective, during secondary phase of this research a comprehensive case study was conducted utilizing the improvised methodology that was developed during the primary phase, in order to identify effectiveness of a prophylactic knee brace (manufactured by Össur Inc.), on an athlete who was assessed to be at high risk of ACL injury among ten volunteer amateur athletes.

This comprehensive study was pre-established to include multiple steps and at the commencement of the study, single leg jump landing activity was assessed using a high speed motion capturing technique. Subsequently kinematic and ground reaction forces collected during the impact phase of a drop-landing activity performed by this high-risk athlete were subsequently input into a biomechanical model to estimate individual muscle forces surrounding the Knee joint. These estimated muscle forces were then utilized to drive a hybrid surrogate cadaveric knee model instrumented to measure the ACL strain. Finally, ACL strain was assessed during simulation of jump landing activity on a dynamic knee simulator with and without a functional knee brace mounted on the cadaver knee specimen.

## 1.3 Thesis Organization

The second chapter in thesis reviews anatomy of a human knee while explaining various anatomical nomenclatures related to the human body, followed by a brief introduction to the architecture, anatomical characteristics of a human knee. In addition, the chapter also describes the musculo-ligament structures around knee joint finally providing a succinct description of anterior cruciate ligament (ACL).

The third chapter provides a comprehensive review of the research studies that are relevant for this thesis. Primarily the chapter begins with review on the ACL injuries and its impact on human lives, followed by review of studies related to injury mechanism and experimental procedures adopted by researchers. Finally the chapter evaluates several studies that have been employed to understand effectiveness of knee braces on reduction/prevention of noncontact ACL injuries.

The fourth chapter explains about equipment's that were utilized for performing the presented research study. Primarily the chapter explains about the purpose, several unique design attributes and functioning of equipment including Lachman tester, Muscle hardness tester and the dynamic knee simulator. The chapter also focuses on several modifications that were performed to the construction and functional attributes of the dynamic knee simulator to increase effectiveness of the equipment.

Fifth chapter of this thesis reviews development of unique technique to test a prophylactic knee brace. It details the methods that have been utilized in the research undertaking and its unique attributes. The chapter concludes with a review of failed attempts and lesson learnt during this phase of research study.

The sixth chapter discusses about a unique case study that was completed while utilizing improved techniques that were discussed in chapter five, in goal of identifying effectiveness of a prophylactic knee brace that was manufactured by Össur Inc.

In the seventh chapter, a comprehensive summary of the results obtained during the individual prophylactic brace case study are presented under several sub topics. In addition in the eight chapter of this thesis, elaborate discussions are presented on the techniques adopted in the research as well as the comparisons with findings of previous studies that emphasize the relevance of current findings reported in chapter seven.

Ninth chapter of this thesis summarizes findings of the research study while the tenth chapter identifies the shortcomings of the adopted technique and recommendations for future research.

# Chapter 2
# Anatomy of Human Knee

## 2.1 Human Anatomical terms

Anatomy refers to "the science of the structure of living organisms" (Medical dictionary, 2013) and the science of structure of human body is known as human anatomy (Wikibooks.org, 2013). Standard anatomical terms have been established to clearly describe human body and relative position of its parts and organs. Accordingly, human body has been divided into three imaginary anatomical planes as indicated in Figure 1.

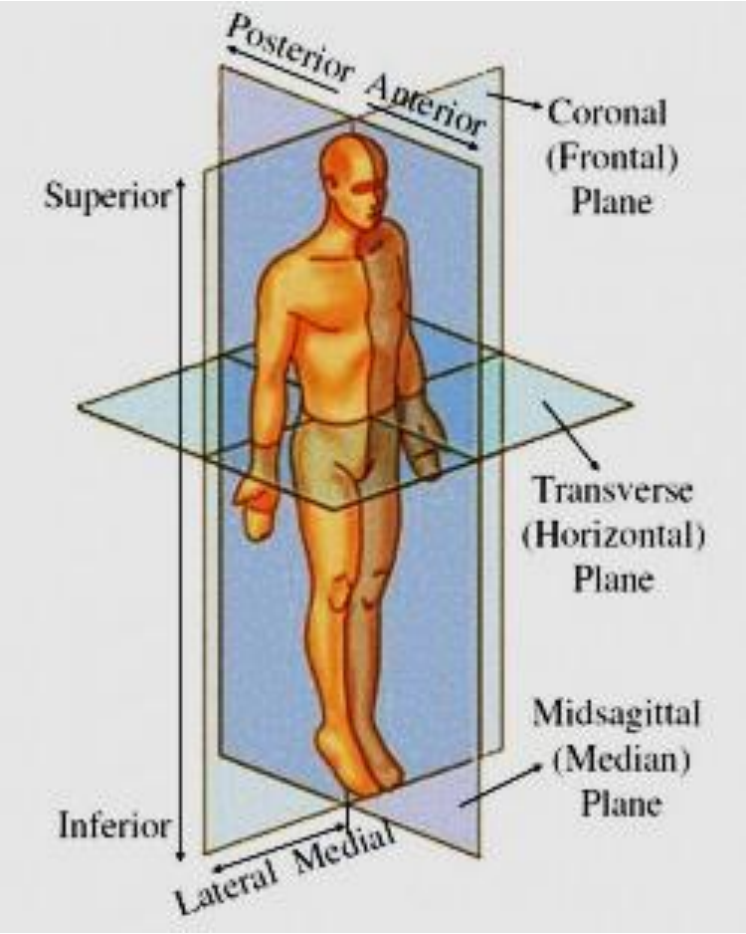


**Figure 1 Anatomical planes and directions**

The Coronary / Frontal plane divide human body into front and back halves also referred to as Anterior and Posterior portions or the front and back sections of the body, while Transverse /

Horizontal plane splits the body into superior and inferior half. The third plane also referred to as Sagittal / Median plane divides the body into right and left sides or as anatomically understood, lateral direction that is pointing away from mid sagittal plane while Medial direction is referred to as pointing towards the mid sagittal plane irrespective of view point of body. Other anatomical terms commonly used to describe organs and tissue in reference to the surface of the body includes the following: (Moore et al, 1999)

- Superficial – refers to structures that are closer to the outer surface of the body
- Deep – refers to structures that are embedded inside the body, closer to the internal region
- Intermediate – refers to structures that are positioned between the deep and superficial layers.
- Dorsal – refers to structures closer to the back of the human body
- Ventral – refers to structures closer to the abdomen region of the body
- Proximal – refers to the point that is closer to a reference structure / location, in comparison to another point that is located away from the reference location
- Distal – refers to the point located away from a reference structure / location, in comparison to another point that is closer to the reference structure.

## 2.2 The Human Knee

Lower extremity region of human body is comprised of the hip, thigh, shin, calf, ankle and the foot. The lower limb comprises of four major bones inclusive of the femur, tibia, fibula and the patella. Femur being the largest weight bearing bone of the connects the knee to the hip joint while the tibia, the second largest weight bearing member and fibula both connect knee to the ankle. Patella is attached to the anterior portion of the tibia via patellar ligament and articulates along anterior surface of the femur and these four bones constitute to form the knee joint. Knee is the largest and most complex of all the joints in the human body and primarily considered as a hinge joint. However, the hinge movement is combination of gliding and rolling with certain degree of rotation along the vertical axis. The knee joint consists of three major articulations that include the lateral and medial articulation between superior plateau of tibia and femoral condyles also known as tibiofemoral joint and intermediate articulation that occur between the patella and the anterior surface of the femur also referred to as the patellofemoral joint (Moore et al, 1999).

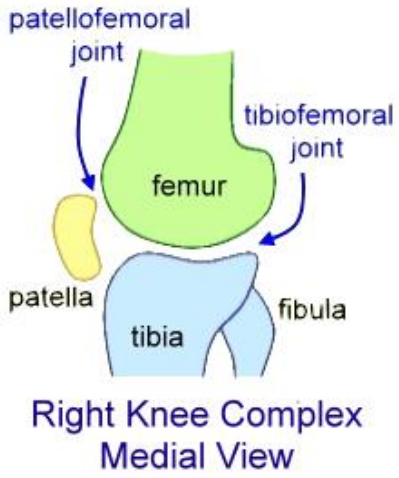


**Figure 2 Articular joints of the Knee**

Mobility and normal functional activities executed with lower limbs involves a variety of complex motions associated with knee joint and various muscle groups are responsible for such intricate movements. Major muscle groups surrounding the knee joint include the anterior muscle group also known as quadriceps which comprises of the rectus femoris, vastus lateralis, vastus medialis and vastus intermdius, the posterior thigh muscle group also known as hamstrings that consists the semitendinosus, semimembranosus and both biceps femoris long, short head muscles and finally the gastrocnemius muscles which include the gastrocnemius lateralisis and gastrocnemius medialisis. Among these muscle groups, hamstring muscle group is primarily responsible for flexion of knee while providing some degree rotation of tibia during flexion whereas the quadriceps muscles group is primarily responsible for extension of knee joint. Gastrocnemius muscles exhibit some degree of assistance for flexion of knee but majorly involved in plantar flexion of the foot. Along with these sets flexion extensor muscles, a number of abductor and adductor muscles that arise from the hip are also responsible for some intricate motions during normal flexion extension as well as to maintain the stability of the knee joint (Sportsinjuryclinic.net, 2013).

The quadriceps muscles are attached along several regions along femur and near the hip joint, distal to the knee while the tendons of each of the four muscles unite proximal to the knee joint forming the quadriceps tendon. This tendon converges beyond the knee joint forming the patellar ligament, while embedding the patella into the tendon tissue. Patella glides over the articulating surface of the femur while acting as a lever point for the quadriceps muscle actuation. All hamstring muscles arise from the posterior region of the hip joint however, semitendinosus and

semimembranosus attach to posterior region of medial tibial condyle while biceps femoris long head and short head tendons attach to head of fibula. The gastrocnemius muscle group arise posterior surface of calcaneus in the foot via calcaneal tendon and attach to superior regions of lateral and medial femoral condyles. In current research, muscle cables are attached to femur and tibia to closely imitate attachment mechanics and replicate the gross effect of the muscle groups on the knee joint (World of Sports science, 2013).

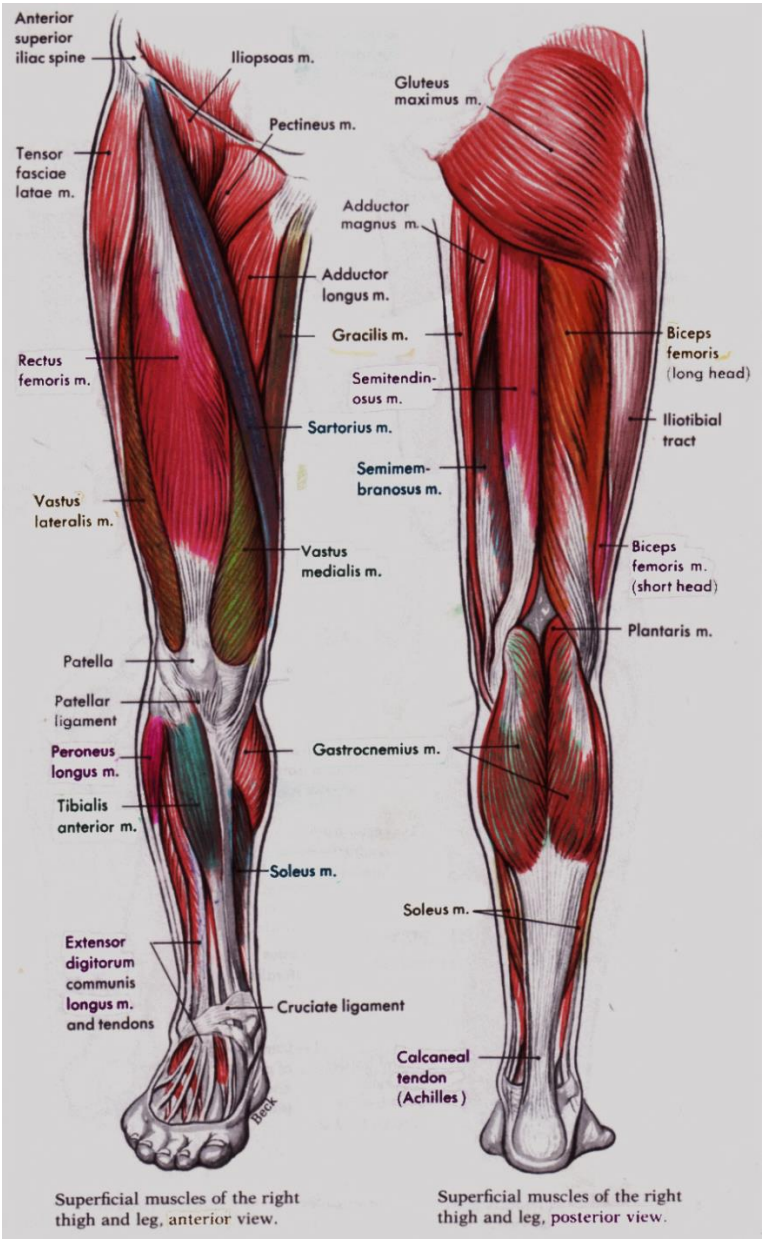


**Figure 3 Muscles of the lower extremity**

## 2.3 Ligaments of Knee

Knee joint is the largest synovial joint in human body, its stability is vital for the weight bearing characteristics it exhibits and this stability is accomplished by surrounding set of muscles, extra-capsular and intra-articular ligaments. Primarily, the joint is encapsulated with a fibrous membrane which is further strengthened by five extracapsular ligaments, inclusive of patellar ligament, fibular collateral ligament, tibial collateral ligament, oblique popliteal ligament and arcuate popliteal ligament. As explained in section 2.2, patellar ligament arises from quadriceps tendon and attach to the tibial tuberosity. Fibular collateral ligament also known as lateral collateral ligament extends inferior to the knee joint from the lateral epicondyle of femur to the lateral fibular head, while the tibial collateral ligament also known as medial collateral ligament extends from medial condyle of femur to superior portion of medial surface of tibia. These lateral and medial condyles provide stability to knee joint by restraining mediolateral translation of tibia with respect to femur. Oblique popliteal and arcuate popliteal ligaments are located in posterior region of knee joint attaching posterior regions of fibrous capsule along femur to posterior regions of tibia and fibular head respectively. Although these extracapsular ligaments are vital to the stability of the knee joint, ligaments within the knee joint capsule also known as intra-articular ligaments are major restraints for femoral tibial translation (Moore et al, 1999).

Intra-articular ligaments include the anterior and posterior cruciate ligaments as well as meniscus discs. Menisci are fibrocartilage crescent shaped structures located on the articular surface of tibia. These structures act as shock absorbers and form a cup shaped cavity to retain the femoral articular surface thereby restraining translation of knee joint. The cruciate ligaments of knee attach to femur and tibia while crisscrossing within articular capsule of knee joint. They arise external to the synovial joint cavity in the intercondylar regions of tibia and attach to medial and lateral condyles of femur. These cruciate ligaments provide substantial stability to knee joint by restraining translation of tibia with respect to femur and maintain normal movement between the articulating surfaces of the knee joint. Among the two cruciate ligaments, posterior cruciate ligament (PCL) is comparatively stronger and attaches from posterior intercondylar region of tibia to the anterior region of medial condyle of femur. PCL is mainly associated in preventing posterior translation of the tibia with respect to femur coupled with preventing hyper flexion of the knee (Moore et al, 1999).

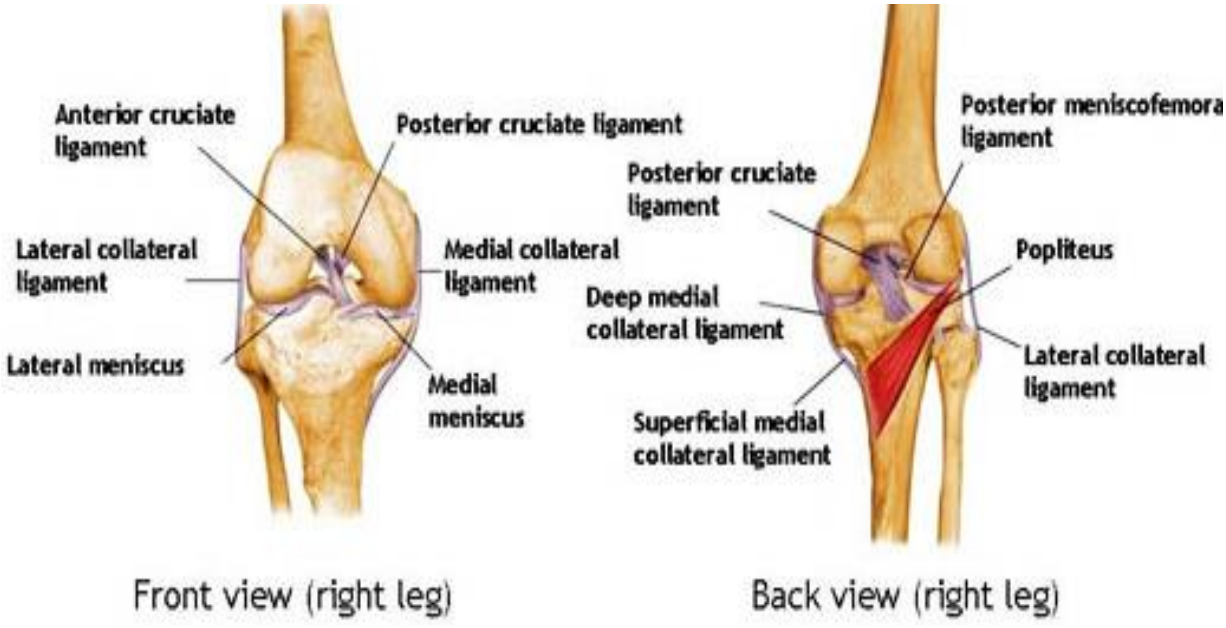


**Figure 4 Ligaments of the Knee**

## 2.4 Anterior Cruciate ligament

Anterior cruciate ligament (ACL) is a band-like structure of dense connective tissue that arises from anterior intercondylar region of tibia posterior to attachment point of medial meniscus disc and extends superiorly, posterior to joint laterally and terminates medial region of lateral epicondyle of femur. ACL is irregular in shape and its cross sectional area increases as it progresses from femur to tibia (Duthon et al, 2006). The ligament attaches to the femur through a collection of individual fascicles and is smaller in comparison to the tibial attachment which is wider and stronger and some fibers attach to anterior or posterior horn of lateral meniscus.

Based on individual functional attributes, (Girgis et al, 1975) ACL is divided into two major groups of fiber bundles namely Anteromedial bundle (AMB) and posterolateral bundle (PLB), in addition Hollis et al (1991) showed that AMB increased in length and tightened as the knee flexes while PLB shortens and slacked. This points out that these bundles (AMB and PLB) are not isometric in flexion and extension of knee and exhibit different patterns or variation in length changes during passive knee flexion and extension. Microscopically ACL is comprised of multiple fascicles of varying diameters made of several sub fascicular fibril bundle units. These individual fibril bundle units are formed by several Type 1 collagen fibrils which are primarily oriented parallel to longitudinal axis of the ligament. In addition these collagen fibrils reinforced with extracellular

matrix that is made of ground substance and water thereby creating a composite structure. Furthermore Duthon et al (2006) had also observed that ACL microstructure is nonlinearly organized such that the fibrils along external peripheral region are arranged in helical wave patterns and this unique microstructure contributes for fibril recruitment thus acting as shock absorbers while load is applied. Water and ground substance in the composite structure contributes for viscoelastic property of the ligament (Chandrashekar N 2005).

Several nerve fibers / mechanoreceptors that display proprioceptive function are embedded among fascicles of ACL and changes in knee postures or deformation in ligament produce signal influencing muscle motor activity around the knee joint through a phenomenon called "ACL reflex" as indicated by Duthon et al (2006). Vascularization occurs to ACL through a branch of blood vessels that arise through intercondylar notch from Middle genicular artery, however proximal part of ACL has better blood supply when compared to distal regions, indicating poor healing quality often associated with the ligament.

ACL is primarily involved in preventing anterior translation of tibia with respect to femur, and plays a crucial role in maintaining joint stability and normal movements of knee joint (Griffin et al, 2000). Amis et al (1991) recognized that during an anterior drawer test, AMB experienced tension dominantly at larger flexion angles while PLB was dominant when the knee was extended and this further signified dual roles inherited by ACL bundles or the non-isometric behavior that resisted anterior tibial translation. Furthermore in a separate test, Gabriel et al (2004) observed tension in ACL bundles when rotational torques were applied to tibia, concluding that ACL plays a secondary role in resisting tibial rotation. Although several researches conclude indicating importance of ACL, its functional attributes as mechanical restraint in maintaining knee passive joint stability, a separate study completed by Ambrose et al (2003) indicated importance of mechanoreceptors in ACL. Study concluded that an injured ACL and lack of mechanoreceptors induced joint instability due to diminished somatosensory information that altered neuromuscular function. This affected muscle firing timing, further increasing functional instability of the joint.

ACL is an important ligament in the knee joint and its structural integrity is crucial in maintaining joint stability through varying motions of day to day activity. A deficient ACL either partially ruptured or plastically elongated drastically affects functional aspects of knee resulting in further degenerative changes caused due to unguided femoral motion. In addition, treating ACL injuries is inherently difficult due to limited healing capacity of ligament, complexities involved in

rehabilitation and possibilities of developing osteoarthritis during post reconstruction phase (Freedman et al, 1998 and Deacon et al, 1997).

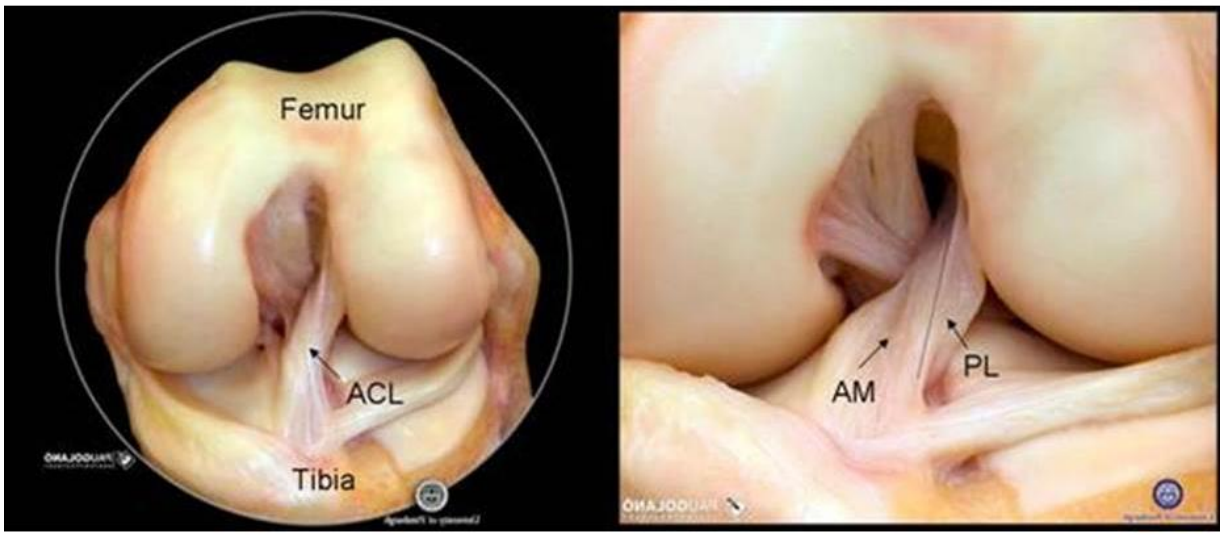


**Figure 5 Anatomy of Anterior Cruciate Ligament (ACL)**

# Chapter 3
# Literature Review

## 3.1 Introduction

In recent times several research initiatives are undertaken to examine techniques of preventing and rehabilitation of ACL injuries which includes understanding basic biomechanical aspects involved in occurrence of injury. In this chapter of the thesis, a comprehensive literature review has been compiled and presented that form a conclusive foundation for current research study.

## 3.2 ACL Injury

Discussion presented in section 2.4 of the thesis highlight important anatomical and structural attributes of ACL and its subsequent relevance in maintaining stability of knee joint. Theories examining ACL injury mechanism (Yu et al, 2007) indicate that preliminary function of ACL is to resist anterior translation of tibia (ATT) with respect to femur. In addition the study also concluded that large strain values induced due to excessive translation, excessive internal rotation of tibia and or valgus collapse of the knee coupled with external tibial rotation all contributed to injuries in the ligament. Injuries to ACL have detrimental effects on knee joint as the joint stability is greatly reduced and its functional abilities are adversely affected. Up to 50% of all sport injuries are believed to be injuries associated with the Knee (de Loës et al, 2000) while 64% of these are related to ACL injuries (Rishiraj et al 2009). Boden et al (2005), Krosshaug et al (2007) found that 72% of the observed ACL injuries occurred due to non-contact mechanism, generally occurring while landing from a jump and moreover it is widely accepted that movements that commonly result in knee injury are planting and cutting, straight jump landings and rapid one-step stops (Lamontage et al, 2009, Mihata et al, 2006). Ebstrup et al (2000), Krosshaug et al (2007) suggested that during these landing maneuvers, the anterior cruciate ligament (ACL) tightens during extreme extension resulting in large magnitudes of strain causing ACL injuries. They also concluded that during internal rotation of a valgus loaded knee or external rotation of a varus loaded knee can cause similar results however, exact injury mechanism is still unclear (Krosshaug et al, 2007).

Past research studies have identified a number of intrinsic and extrinsic factors that increase risk of injury to ACL among individuals. Intrinsic factors include the morphology of ACL, internal structural variations/deficiencies and Anatomical factors such as smaller intercondylar notch width

that results in impingement of ACL (Chandrashekar N, 2005), Q angle or the angle of axial alignment between the femur and tibial segments, degree of valgus tilt of the knee, degree of foot pronation, hormonal and neuromuscular variations amongst individuals and attributes relating to body mass index and proportions (Griffin et al, 2006). While extrinsic factors include the environment that is in interaction during execution of associated activities, biomechanical factors that are inherent to the activity and nature or risks associated with dynamic activity in daily living. The above highlighted intrinsic factors although are important to be explored and understood in order to mitigate risks associated with ACL injury, it is more difficult to be modified in comparison to extrinsic factors (Griffin et al, 2006). Although some control can be exercised over the extrinsic factors associated with ACL injury, research community has not reached precise understanding of the injury and the effect of each of the above factor have not been totally quantified.

ACL injury has detrimental effects and it is generally followed by failure or tear in other ligaments and menisci, patients experience abnormal joint movement and knee instability, followed by further structural disintegration of the joint and early onset of osteoarthritis (Beynnon et al 2005). Studies indicate that risks of being diagnosed with osteoarthritis increases by 100 times after a knee injury (Hewett et al, 1999; Freedman et al, 1998; Deacon et al, 1997).Reconstruction of ACL is imminent under complete failure of the ligament and is required in order to regain normal knee function and to maintain a normal healthy life style however, it does not prevent onset of arthritis. It is estimated that over 200,000 ACL injuries occur in USA and about 100,000 ACL reconstruction surgeries are performed annually (Griffin et al, 2006), nevertheless ultimate outcome of ACL reconstruction surgery are still unknown and true value of the procedure is yet to be quantified (Beynnon et al, 2005). Additionally after reconstruction of ACL and acute rehabilitation, most athletes faced 33% in reduction in performance levels Carey (2006) and Roos et al (1995) observed that 30% of ACL injured Swedish soccer players were active post injury to ACL in comparison to 80% of uninjured individuals. Hence several research studies have been focused in developing ACL injury prevention strategies which include neuromuscular training, strengthening and plyometric training of agonistic muscles and stabilizing knee using braces. (Rishiraj et al 2012, Hewett et al, 1999)

In a separate study report published online by American Association of Orthopedic Surgeons, (AAOS) Dr. Kevin G. Shea et al states “We do not have the highest quality research designs showing us that prevention programs can reduce Knee or ACL injuries” and researchers are in pursuit of this

eternal quest. On another hand considering bracing as a possible preventive measure, past studies provide some evidence that commercially available knee braces stabilize the knee joint and provide some assistance to individuals who have sustained ACL injury during rehabilitation (Théoret et al., 2006; Lu et al., 2006). However in contrary, Birmingham et al (2008) stated that functional knee braces are not different than neoprene sleeves in stabilizing the knee after ACL injury and the effectiveness of knee braces in protecting reconstructed or deficient ACL remains unknown.

## 3.3 Knee Brace Effectiveness Studies

Evidence suggests that braces enhance knee stability after ACL reconstruction only during activities of daily living (Wright and Fetzer, 2007). Historically knee braces have been employed by the sports medicine community as a treatment to stabilize knee with ACL disruption or to protect a knee with ACL graft during rehabilitation and or to prevent knee ligament injuries during sport. Braces are primarily designed with an objective of allowing normal joint kinematics while inhibiting undesired tibial displacement and rotation with respect to the femur, which might otherwise detrimentally strain a healing ligament or graft or produce intra-articular injury due to ligament tear. A study conducted in 1979 over a group of athletes using a brace named "Anderson Knee Stabler" declared that braces prevented ligamentous injury to knee and also guessed that braces also helped prevent anterior tibial translation (ATT) as well as prevented valgus stress to the knee (Najibi S, 2005). Although this was first study that revolutionized use of knee braces in sports, it was completed within a short amount of time with small number of individuals and did not completely prove that the braces assisted in preventing ligamentous injuries. Since then, numerous studies have been undertaken to understand the effect of knee braces in injury prevention to the knee.

### 3.3.1 In-Vivo Studies

Several in-vivo studies have been performed to assess effectiveness of knee braces in eliminating or resisting ATT and internal tibial rotation. In a study conducted by Fleming et al (2000) fifteen individuals were instrumented with DVRT on the ACL through arthroscopic surgery. In addition, these subjects were positioned on a special fixture that was designed to apply shear forces directed in anterior-posterior direction, internal-external torques, and varus-valgus moments to the tibia independently. These loading conditions were completed twice, once with compressive load equivalent to body weight of subject and subsequently without any compressive load applied on the subject's leg. They conclusively reported that when an anterior tibial load of 130 N was applied to the

tibia, bracing condition reduced strain in the ACL both in weight bearing and non-weight bearing conditions.

Direct measurement of ACL strain with and without knee braces under a variety of knee loading scenarios was performed in vivo by Beynnon et al (1997). In this in-vivo study, DVRT was installed through arthroscopic surgery on five subjects and three different tests were performed. Tests that were conducted included anterior posterior loading similar to Lachman testing performed under weight bearing and non-weight bearing conditions and internal external torques applied under non-weight bearing condition through use of a special torque boot device. During the tests, anterior posterior loads were applied on to the tibia using a special fixture arrangement. They concluded that bracing the knee significantly reduced ACL strain values for anterior tibial forces up to the maximum of 140 N. In addition, they also reported that bracing significantly reduced ACL strain values during internal and external tibial torques up to the maximum torque of 6 Nm. Both these in-vivo studies were conducted in static/quasi-static conditions contrary to real high risk dynamic activities like single leg landings. In addition, (Laughlin et al, 2011) shear loads experienced by knee during such dynamic activities were close to 500 N at least four times than what was applied in both these studies.

Beynnon et al (2003) further completed another in-vivo study evaluating subjects with chronic ACL tears under braced and unbraced conditions while shear loads (in anterior posterior direction) were applied to the knee joint to create ATT. This study focused on understanding brace behavior in inhibiting ATT during weight bearing condition followed by ATT during transition into non-weight bearing condition and finally during non-weight bearing condition. They utilized electromagnetic sensors (Flock of Birds, Ascension Technologies, Colchester, Vermont) to measure ATT of knee and used a VKLD (Vermont Knee Laxity Device) to apply loads as shown in Figure 6. They identified that bracing reduced ATT during weight bearing and non-weight bearing conditions whereas it did not reduce abnormal ATT during while transitioning between aforementioned two conditions. This important finding indicates that braces might not be effective in reducing abnormal ATT occurring due to internal loads and when muscle contraction takes place. This study was commissioned on ACL deficient individuals and once again quasi static conditions of loading conditions experienced by subjects in VKLD does not replicate a single leg jump landing activity. In addition, the effect of dynamic muscle forces and the forces created by hip moments that affect the knee during such a high risk activity such as jump landing would be different to ones experience by test subjects in VKLD (Cassidy et al, 2013, Hashemi et al, 2007).

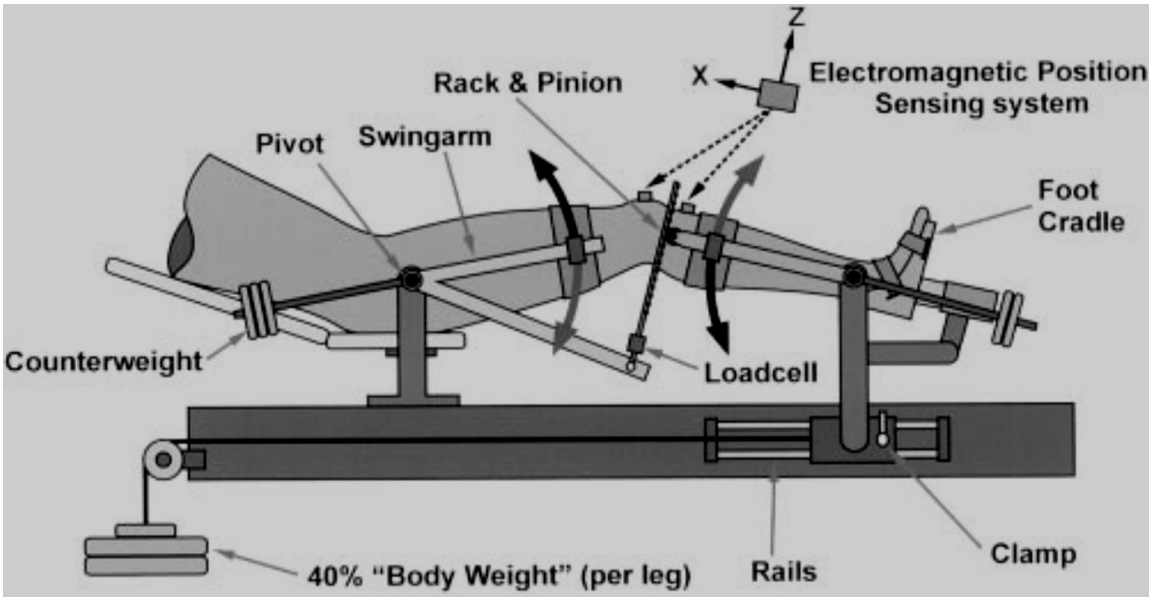


**Figure 6 Vermont Knee Laxity Device (VKLD) set up during study by Beynnon et al (2003)**

In another significant in-vivo study (Mohseni et al, 2009) examined fifteen healthy volunteers using an arthrometer at various knee flexion angles as shown in Figure 7. These arthrometry tests were completed while comparing each loading activity under braced and unbraced conditions. They observed that knee brace reduced ATT (anterior tibial translation) close to about 50% when an anterior tibial load of 150 N was applied at 30 degrees knee flexion indicating the stabilizing effect of the brace. However at flexion angles of 60 and 90 degrees brace's ability to reduce ATT (anterior tibial translation) fell to less that 10% and researchers attributed later findings as limitation of study.

Yeow et al (2010) adopted motion analysis technique to record and compare kinematic and kinetic data variations between braced and unbraced conditions, while ten healthy individuals performed single-leg landing from a 0.6m high platform. An anterior sloped brace was employed during the testing phase and motion analysis was performed using reflective markers with motion capturing system (Vicon MX, Oxford Metrics, UK) and a synchronized Kistler force plate arrangement. ATT (anterior tibial translation) was calculated as difference between coordinates of anatomical landmarks on tibia and femur while ATR (axial tibial rotation) was estimated by computing Euler angle variations between tibia and femur. They observed that anterior sloped brace design increased mechanical stiffness at the knee joint thereby exhibiting reduction in ATT (anterior tibial translation) and ATR (axial tibial rotation) of knee.

**Figure 7 Arthrometry test set up during study completed by Mohseni et al (2009)**

In another motion analysis study conducted by Ramsey et al (2001), they instrumented four ACL deficient individuals with Hoffman bone pins on femur and tibia along with reflective markers. Motion capturing procedure was completed while individuals performed one legged horizontal jumps, landing on their ACL deficient limb. Simultaneously during motion analysis, EMG (Electromyography) data was also collected from electrodes mounted on four major muscle groups. They reported no consistent reductions in ATT between braced and un-braced conditions and concluded that joint stability was not affected by mechanical stabilizing attribute of the brace and perhaps due to the change in the muscle firing pattern due to alteration in proprioceptive feedback in response to application of knee brace.

In a separate in vivo test conducted by Wojtys et al (1996), five individuals with ACL deficient knee were recruited and knee stress test was performed utilizing a special device. The device was designed such that it measure anterior tibial translation but did not restrict free movement of tibia. Muscle activity was recorded simultaneously for thee major groups using EMG, while anterior tibial translation stress test was conducted. Six different braces were tested on individuals and a 30-pound step force was applied on to tibia while tibial translation was recorded using potentiometers. They reported that most braces decreased ATT between values of 28.8% to 39.1% without contraction of stabilizing muscles surrounding the knee. In addition, ATT decreased further to values

between 69.8% and 84.5% due to combined effects of muscle contraction and mechanical stability induced by bracing. As indicated by investigator of this study, it was conducted at a force much lower when compared to ones experienced at complete higher levels daily living activities and further investigation would be necessary to completely understand the effectiveness of braces in preventing ACL injuries.

Researchers have also tried to understand the effectiveness of knee brace by studying muscular activity using electromyography technique (EMG) and then correlate those findings to brace effectiveness. In an in vivo study completed by Osternig et al (1993), six healthy recreational runners were instrumented with electromyography electrodes (EMG) on 9 lower extremity muscles and studied while running on an electric treadmill. In addition, hip knee and ankle joint kinematics were tracked using Selspot automatic tracking system (Selspot Inc. Troy, MI). Test scenarios included braced and unbraced conditions and running at different paces with and without a weighted vest. The study concluded that muscle activities levels significantly changed by application of a brace but does not provide sufficient evidence for brace's effectiveness in protecting ligaments.

In summary literature review presented above highlight several in-vivo techniques that have been adopted by research community to answer the primary question on efficacy of braces. Direct measurement of ACL strain by instrumenting ligaments on live human participants creates ethical concerns and not feasible. Hence researchers have adopted to conduct motion analysis utilizing reflective markers and high speed motion capturing systems with force plates. (Alexander et al, 2000) Inaccuracies arising from skin marker movements are imminent when surface markers are used along with opto-electronic system and in addition, Yeow et al (2010) stated that ATT and ATR values can vary substantially and entirely dependent on the techniques adopted to conduct motion analysis and the type of motion being analyzed. As an alternative to use of surface markers, researchers have opted to use Hoffman bone pins, which are another invasive technique and pose ethical concerns. Furthermore most of these studies are conducted at lower force levels and or applied at static flexion angles, further research in to studying dynamic motions at force levels experienced during daily normal activities is necessary to understand bracing effects. In conclusion, it is evident that each in-vivo technique has its limitation and the mystery surrounding true efficacy of brace in preventing ligament injury remains unanswered (Rishiraj et al 2009, Najibi and Albright 2005).

### 3.3.2 Prospective and Retrospective Studies

Researchers have also tried to correlate and distinguish rate of injuries among braced and unbraced athletes employing prospective and retrospective techniques of evaluation. Sitler et al (1990) completed a two year prospective, randomized study evaluating athletes through seasons of intramural tackle football at a military academy. In this particular study, a total of 21,570 athlete-exposures to the game were assessed with 705 subjects served under controlled conditions performing without brace while 691 individuals conducted wearing prophylactic knee braces during the study period. Subsequent data analysis indicated that higher number of knee injuries occurred in the control group that did not wear a knee brace in comparison to the group that wore knee brace. During the season injury rate among controlled group was derived to be 3.40 injuries per 1000 athlete exposure in comparison to 1.50 injuries in braced group. However, this statistical significance in reduction of frequency of injury due to application of brace was dependent on player position and raised further questions of brace usage versus severity of activity. Furthermore, since the number of ACL injuries observed during the study was very low, (1.1% of subjects observed) statistical analysis was not completed and true efficacy of knee brace preventing ACL remains unanswered.

Risberg et al (1999) conducted a separate prospective study to evaluate knee brace effectiveness after ACL reconstruction surgery. Two separate groups of individuals with ACL injury were examined under the study, the first group included individuals who wore knee braces for 12 weeks post-surgery while the second group of individuals were rehabilitated without use of a brace. Several attributes of knee joint were analyzed and compared between groups, which included knee laxity test, range of motion analysis and functional capabilities analysis of knee using Cincinnati knee score technique. In addition they utilized computer tomography to measure thigh atrophy, employed a varying degree of analog scale to determine pain experienced by subjects during rehabilitation and also an isokinetic test to evaluate muscle strength of the patients. Data was recorded prior to surgery and post-surgery at intervals of six weeks, three months, six months, one year and two years. Risberg et al (1999) found that bracing did not affect any of the examined attributes post-surgery except for functional attributes analyzed using Cincinnati score test at three month follow-up. They concluded that bracing individuals may provide some assistance at early stages of rehabilitation post-surgery during graft healing and recovery. In addition, data collected during the study did not show any indication in reduction of injury to other ligaments or the meniscus post-surgery while using brace,

drawing a need for further scientific evaluation into effectiveness of knee braces in preventing ACL injuries (Osternig et al, 1993) while utilizing innovative techniques

In a retrospective investigation, Tegner et al (1991) compiled knee injury data analyzing response of 600 Swedish ice hockey players to a predetermined questionnaire. The results indicated that a significantly high number of Swedish hockey players sustained injury to the knee however the retrospective nature of study limited the amount of analysis that could be derived from the response and effectiveness of the brace in preventing knee injuries was never identified in the study.

### 3.3.3 In-vitro Studies

Researchers have utilized surrogate knee and cadaver models to evaluate the effect of knee braces on knee stability and ACL strain. In an investigation conducted by Paulos et al (1991), they utilized a mechanical surrogate knee model representing the lower extremity of an individual to evaluate effect of knee brace during lateral impact. The mechanical surrogate model utilized for study comprised of tibial and femoral segments, contralateral limb with weighted torso with a functional hip joint mechanism and ankle segments as shown in Figure 8 and the tibial femoral joint incorporated Teflon coated steel cables aligned with compression springs and load cell representing the tension of ACL and MCL. Although this model was validated to human cadaveric data to replicate dynamic response to valgus load, its authenticity to represent in-vivo human model is questionable and signifies biggest limitation of the study. Six different braces were tested mounted on the surrogate model and compared to unbraced condition while lateral impact was delivered by a special designed weighted shuttle on rails. The tension of the ligament was measured as a function of joint opening, additionally although the study revealed few critical aspects implying that braces protected the knee joint, such as distributing impact away from the knee joint, reducing peak ligament strain and also delay in initiation of ligament tension, study does not focus on knee injuries arising due to biomechanical factors contributing for non-contact injury. The study and model does not account physiological aspects and variances in capsule-ligament structure of a real knee and dynamic muscle forces that occupy major role during dynamic activities (Cassidy et al, 2013, Hashemi et al, 2007).

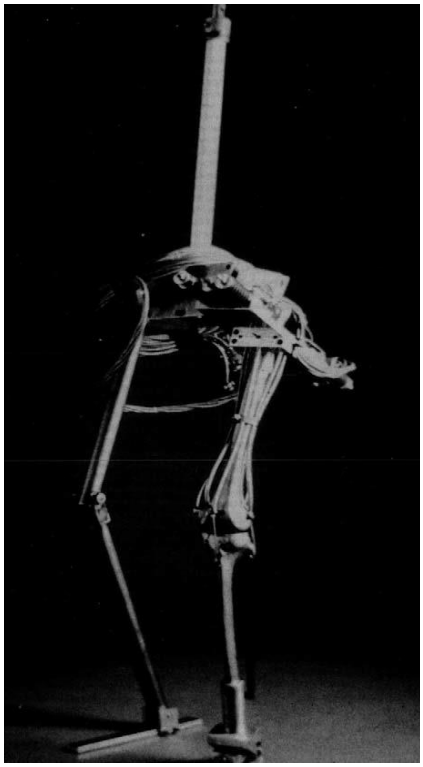

**Figure 8 Mechanical Surrogate Knee model set-up studied by Paulos et al (1991)**

Erickson et al (1993) used a hybrid cadaver-surrogate knee model to evaluate effectiveness of knee brace in protecting ACL and MCL under a lateral impact load. In this in-vitro study, a cadaveric limb instrumented with HEST (Hall Effect Strain Transducer) on MCL, ACL was moulded with foam material to form external shape of a human leg and lateral impact was delivered under a controlled testing apparatus set-up as shown in Figure 9. The cadaver limb was tested in braced condition with and without an intact ACL and the ligament strains were recorded at 0º and 30º knee flexion. Although in this study use of cadaveric limb model accommodates for variances in knee capsule-ligament structure, effect of active and dynamic muscle forces on the knee joint are not taken into consideration. Moreover, muscle force or static load of 15 to 25 kg are applied to the cadaver limb model to maintain flexion angle while realistic muscle forces could be substantially higher (Cassidy et al, 2013 Laughlin W et al, 2011). The study concluded that knee brace did not offer protection to the ACL during lateral impact study. This study although inconclusive paved way as a foundation for an innovative technique where in a surrogate soft tissue is moulded around a cadaver limb to form a composite structure that can be used as the basic frame work for testing knee braces under dynamic activities.

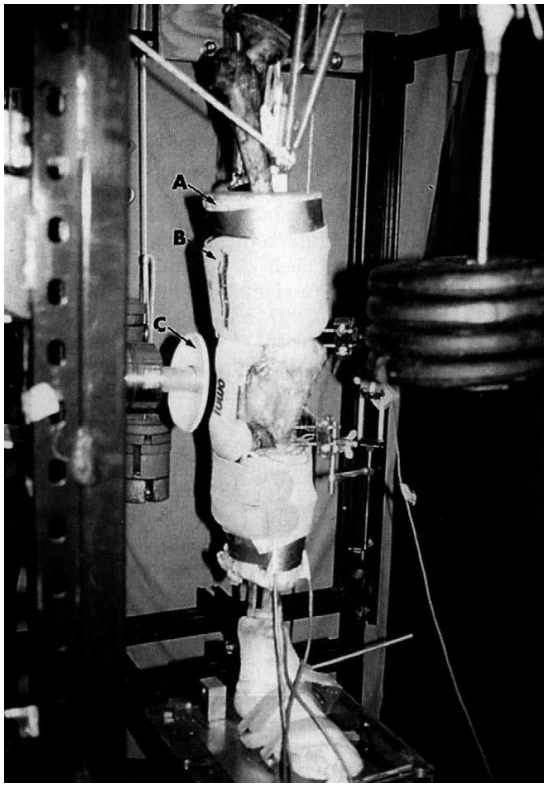


**Figure 9 Hybrid Surrogate Knee Model set up during lateral impact study completed by Erickson et al (1993)**

Hinterwimmer et al, (2004) conducted an in vitro study on effect of mono-centric knee brace observing strain on ligaments surrounding the knee. They used a cadaver knee specimen mounted on special devise as shown in Figure 10 and measured strain on medial collateral and lateral collateral ligaments in both braced and unbraced conditions after the ACL was severed. Although they noticed significant reduction in strains both in MCL and LCL after bracing, it has to be noted that this study was completed on an ACL deficient knee and static muscle force was applied on the joint by hanging weights to tendon attachment sites. This approach does not represent actual dynamic scenario where knee will experience extensive dynamic muscle forces and moreover the brace was fixed on to the cadaver knee specimen using metal clamps not in way that would represent features of a true muscle-brace interface observed while braces are mounted on humans.

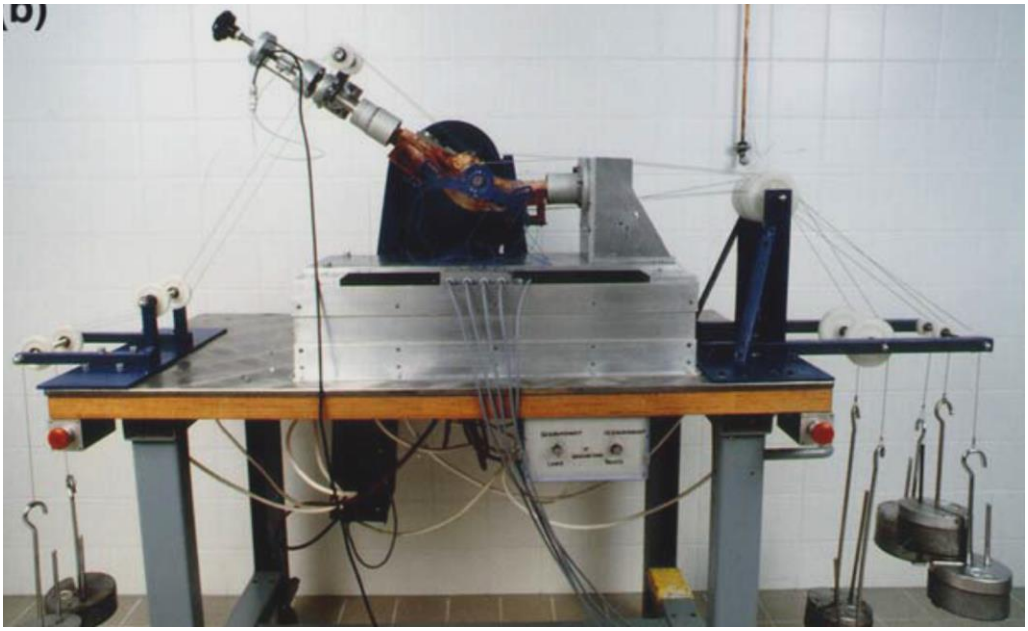

**Figure 10 Experimental set up to study effectiveness of mono centric knee brace completed by Hinterwimmer et al (2004)**

Liu et al (1994) completed a brace effectiveness study using a mechanical surrogate knee model that was made of a metal bars aligned with low friction bearing assembly representing an ACL deficient knee joint. The mechanical joint was moulded with rigid foam to represent soft tissue covering the joint and surrogate knee was set at a static flexion angle of 20˚ and ten different braces were tested while anterior load was applied to translate the tibial component. They established that braces did not provide much restrain to anterior tibial translation when high loads were applied. This study was completed in a static condition in non-weight bearing conditions and moreover author identifies that this testing scenario does not exactly represent conditions experienced by human knee. Model does not account for the physiological variances and effects of capsulo-ligamentous structure surrounding the knee and moreover active dynamic muscle forces that affect the real human knee during strenuous activities were not simulated (Cassidy et al, 2013, Hashemi et al, 2007). The test appears to have tried to isolate the brace design that would be effective in providing some stability to an ACL deficient knee and it fails to provide evidence on braces' effectiveness in protecting ligament during high risk dynamic activities like jump landing.

In-vitro approaches reviewed here do not produce valid output and typical test setup utilizing purely cadaveric tissues do not incorporate the contribution of individual muscle groups and the dynamic loads that cross the knee joint during dynamic activities. And neither of the studies provides

concrete conclusive understanding about effects of knee braces on ACL during high-risk dynamic activities at physiologically realistic load levels. In summary, the efficacy of prophylactic knee braces in preventing ACL disruptions during dynamic movement scenarios that during a non-contact sports injury like in case of landing from a basketball remains an unanswered question (Najibi and Albright 2005). To date no study has been performed in evaluating the knee braces for their prophylactic use in non-injured athletes (Rishiraj et al., 2009) and a prominent reason for this would be that there currently exists no method for testing the effectiveness of these braces in healthy knees. There is an apparent need for developing a unique method by combining in-vivo and in-vitro techniques while elite athletes perform high risk dynamic motion such as jump landing during a basketball maneuver, in order to understand functionality and effectiveness of knee brace in preventing ACL strain.

# Chapter 4
# Test Equipment

## 4.1 Introduction

This section of the thesis encompasses detailed description of design motives, operational features and significant details of equipment that were developed to perform this research. Three major pieces of equipment discussed in this section of thesis, which includes the Lachman tester, Muscle Hardness Tester and Dynamic Simulator. The Lachman tester was employed during the study to determine the zero strain point of the ACL also known as the inflection point, which correspond to the starting point of the strain on ACL due to applied load. In order to mount a custom fit knee brace on the cadaver knee specimen during testing, it was imperative to create a synthetic surface interface between brace and cadaver knee specimen, which would closely replicate surface interface observed while bracing a human leg. In order to achieve this goal, a custom muscle hardness testing device also known as "Muscle Hardness tester" was manufactured to measure stiffness of a muscle under maximum voluntary contraction as well as the stiffness of synthetic interface. Finally the Dynamic Knee simulator was used to simulate the jump landing activity on surrogate cadaver model instrumented with micro strain gauge as explained in (Cassidy et al, 2012), in order to determine effectiveness of brace in preventing ATT (anterior tibial translation).

## 4.2 Lachman Tester

### 4.2.1 Introduction

In a historical note Paessler et al (1992) indicates "existence of a detailed description of testing laxity of knee joint as early as 1875" however, John W. Lachman MD the Chairman and Professor of Orthopedic Surgery at Temple University Philadelphia PA is credited for his work of proposing a simple clinical test to identify ACL instability by manually translating tibia with reference to femur. Since then medical practitioners use this technique to identify ACL instability / trauma effectively. In the proposed research study, this translating technique was utilized to identify inflection point / zero strain position of ACL.

### 4.2.2 Design

Human joints exhibit certain degree of laxity and in order to identify magnitude of actual strain in ACL, as explained by Fleming et al (1994) it is imperative to identify the zero strain position of ACL or inflection point. Hence in this research study Lachman test was performed to determine zero strain reference point for cadaver knee specimen and every time strain measurement device was inserted on to ACL of the cadaver knee the inflection point was identified and the ACL strains were measured with reference to it. To perform this test, customized equipment was manufactured as shown in Figure 11.

This equipment comprised of two linear guide and carriage assembly (McMaster Carr catalogue number 6709K16) bolted on a ½" thick aluminum plate at 90 degrees to each other, as shown in Figure 11. They contained femur and tibial segments of the cadaver knee on two separate aluminum 'V' blocks that were machined and mounted appropriately, such that the distance between femoral and tibial clamping areas were within two cm from the joint line as recommended by Hurley et al (2004) and as shown in Figure 11. 'V' block that was employed to contain femur was mounted such that the long axis of bone remained 30 degrees to the axis of linear guide, while tibia remained perpendicular to axis of linear guide as shown in Figure 11. Equipment was designed such that femur was secure on 'V' block while the carriage assembly would translate freely on linear guide, parallel to long axis of tibia. This was necessary to accommodate for variations in tibial femoral surface architecture within joint capsule that would have otherwise inhibited complete tibial translation. Both bones were clamped on to respective 'V' blocks with a custom fabricated "clamp plate" as shown in Figure 11.

A stepper motor (Model 23A-6102A manufactured of Elwood Getty's) was mounted on to a stationary bracket as shown in Figure 11 and attached to the carriage assembly that held the tibia. This stepper motor was used to create translation of the tibia with respect to femur, while a linear transducer mounted firmly along with the stepper motor and attached to tibia carriage assembly measured the displacement of translation. The motor was connected to a stepper driver (MH10 Oregon Micro Systems Inc.) while both motor and transducer were connected to a LabVIEW data acquisition system (National Instruments LabVIEW, Austin TX, USA).

### 4.2.3 Operation of Lachman tester

The principle concept of operation involved a stepper motor that translated the tibia with respect to femur of the cadaver knee, while a linear transducer (LVDT) mounted on the equipment and differential variable reluctance transducer (DVRT Microstrain Inc. Burlington, VT) instrumented on ACL of cadaver knee (as shown in Figure 58), measured translation and strain respectively. A customized program was developed using LabVIEW software interface to operate the stepper motor thereby translating the saddle that contained the Cadaver knee specimen as shown in Figure 13, back and forth to a preset set distance through an established number of iterations. In addition, simultaneously the software also collected displacement data from linear transducer (LVDT) and DVRT and stored it in an excel file. The output of the Lachman tester was the DVRT voltage and LVDT Displacement plot as shown in Figure 12. Observing the graph, it is evident that uneven pattern of voltage distribution at the start of displacement indicates relaxed portion of ACL while the consistent hysteresis curve as the displacement increases signifies stretched potion of ACL. The point where voltage converges between two portions of curve was estimated to be the zero strain position of ACL or inflection point.

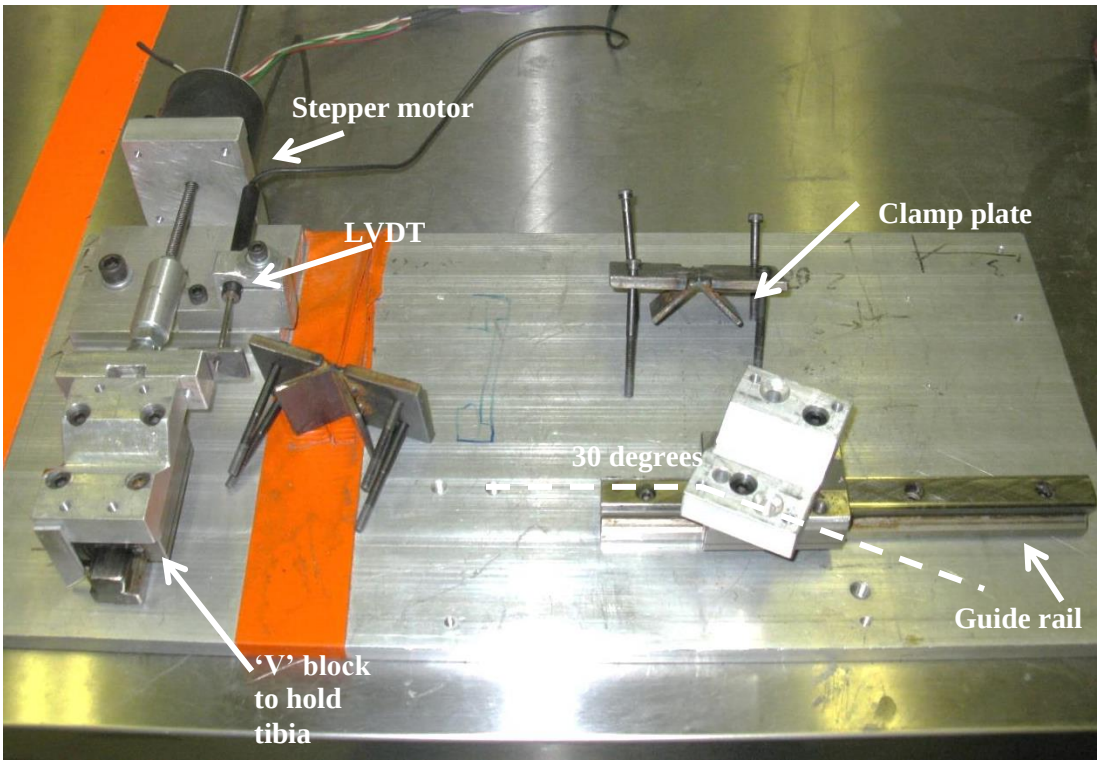


**Figure 11 Lachman Testing apparatus various design aspects and construction**

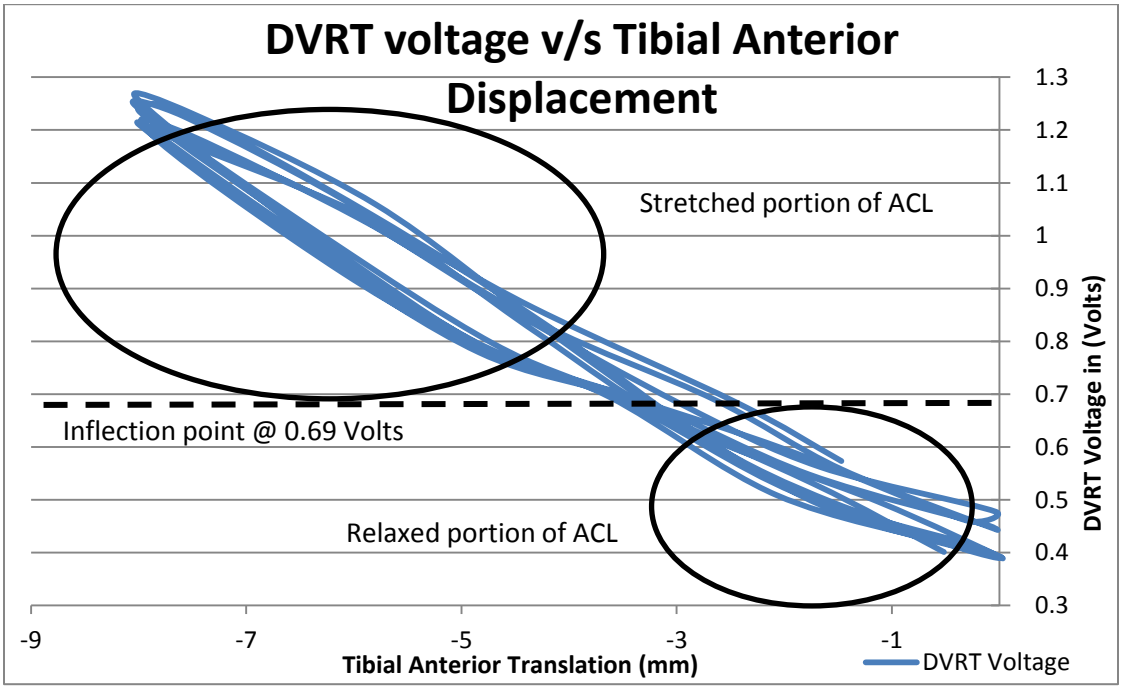


**Figure 12 Lachman tester output data graphed, DVRT voltage data plotted against LVDT displacement values**

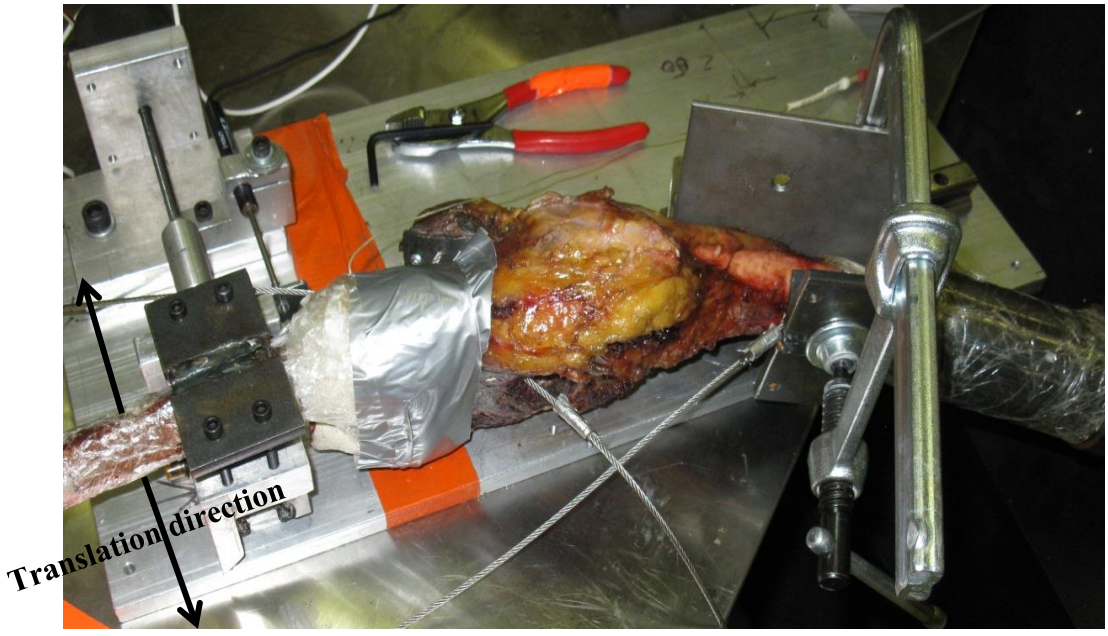


**Figure 13 Cadaver knee specimen mounted on Lachman Tester to determine inflection point, also indicating direction of tibial translation**

### 4.2.4 Modifications of Lachman tester

Initial design of Lachman tester was to hold knee specimen on a parallel plane during translation testing and Lachman tester was successfully utilized to determine inflexion point during equipment test phase and during methodology development phase (first phase) of the research study. However during the second phase of study (actual testing of the knee brace), the procured cadaver knee specimen possessed valgus deformity and was significantly larger in size. These valgus deformities resulted in residual strain on ACL while being clamped on to Lachman tester and hence it was difficult to obtain the inflexion point or zero strain point. Hence, additional changes were performed on the femur carriage assembly to accommodate for valgus deformities. Modification performed included manufacturing a custom welded sheet metal bracket as shown in Figure 14 and repositioning femur carriage guide by ½" inch from its original location as shown in Figure 14. This provided equipment with additional versatility to test cadaver knees with valgus deformities in either direction of frontal plane.


**Figure 14 Modifications completed on Lachman Tester**

In addition, the stepper motor (Model 23A-6102A manufactured of Elwood Getty's) that was employed to translate cadaver knee specimen had capacity of exerting 40 Lbf. and such low force application did not successfully translate larger cadaver knee specimen that was being utilized during second phase of research study. Eventually the Lachman tester was upgraded with a stepper motor (Model 23A-6108A manufactured of Elwood Getty's) capable of exerting 100 Lbf.

## 4.3 Muscle hardness tester

### 4.3.1 Introduction

Several techniques of measuring muscle stiffness have been investigated in biomechanical field of study and most common style of testers available in the market work on principle similar to that of a commercial Durometer. However employing a Durometer to measure stiffness of foam material was difficult and not repetitive. Hence in order to satisfy such specific need of measuring porous foam material and to accommodate for current research financial constraints, it was necessary to develop a cost effective testing apparatus. This section of the thesis describes a custom muscle hardness tester that was fabricated as a fourth year mechanical engineering student project at University of Waterloo, based on principles described by Horikawa et al (1993).

### 4.3.2 Design features of Muscle hardness tester

In order to measure stiffness of a muscle under voluntary contraction, a customized handheld tester was manufactured based on working principles as described by Horikawa et al (1993). Preliminary design and detailed drawings were completed as a fourth year mechanical engineering project. The design of tester included two major components namely “inner piston” made of two inch diameter nylon shaft, which was located and guided in a “piston bore” made of standard aluminum tubing. The piston bore was capped on the top end with a round aluminum disc “Piston cap” and clamped with three screws as shown in Figure 15.

A load cell (force gauge in drawing) Omegadyne Inc. LC202-500 s/n 237679 was attached on to a nylon shaft “External piston” and assembled on to inner piston as shown in Figure 15. In addition, a Linear Variable Displacement Transducer LVDT (Omega Engineering Inc. Stamford, CT, LP804-2 1030) was positioned in a locating hole on the piston cap as shown in assembly drawing, Figure 15 and fastened on to the inner piston at a strategic location. The load cell was utilized to measure force applied on the inner piston, while LVDT measured the corresponding displacement due to compression of muscle tissue. These data values were captured by LabVIEW data acquisition system through the use of a customized LabVIEW program. Slope of the curve formed by plotting applied load against displacement of inner piston provided and estimate of equivalent muscle stiffness in Lb/mm units and further converted to units in N/mm.

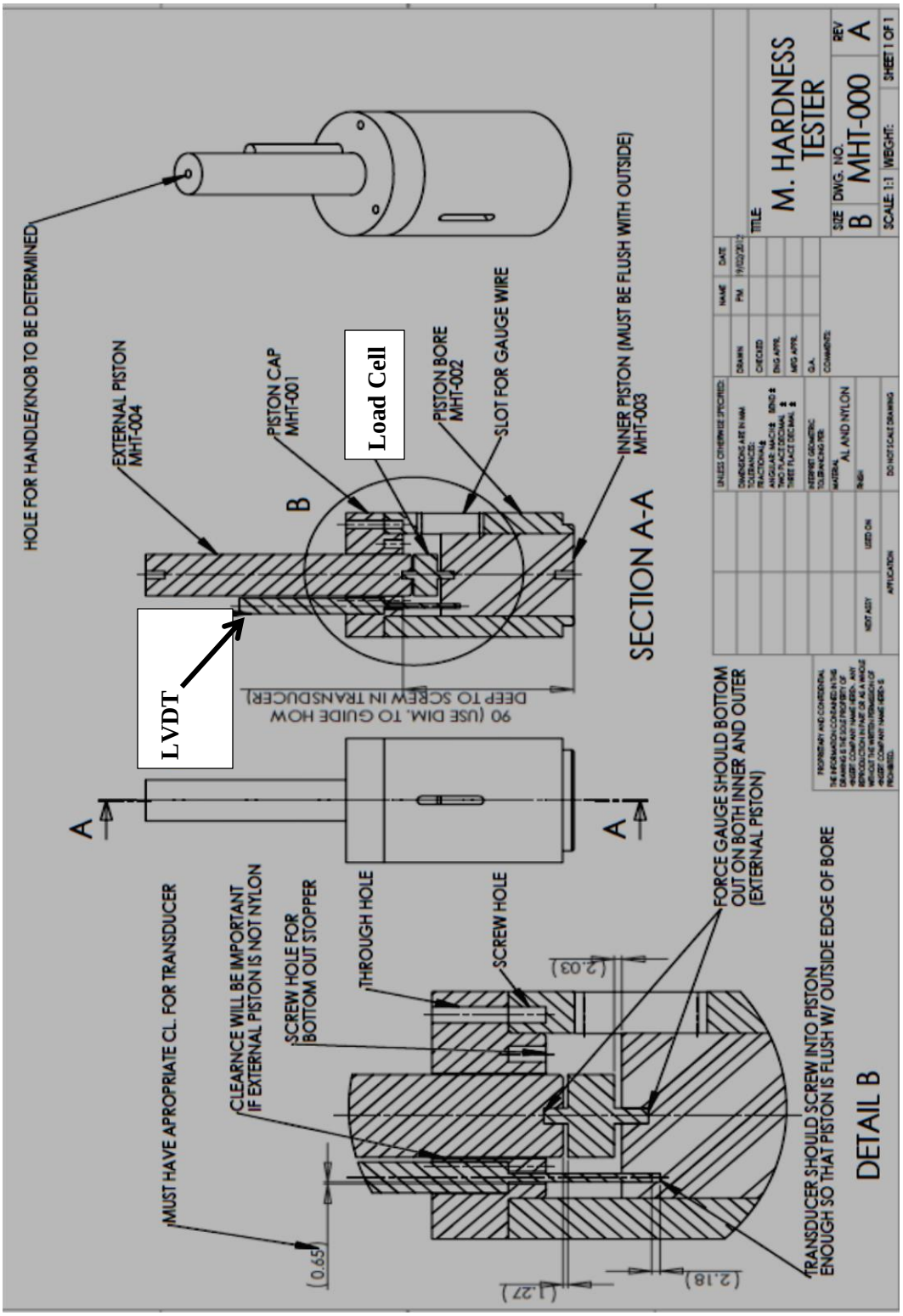


**Figure 15 Muscle hardness tester assembly drawing and relevant parts of device**

### 4.3.3 Operation of the Muscle hardness tester

The compressive stiffness of thigh muscles under voluntary contraction was measured on a live person during flexion/extension of the leg while an external force was applied to the limb to restrict motion. The tester was placed on the subject's leg as shown in Figure 16 and a customized LabVIEW program was initiated to commence operation of the equipment. Upon initiation, the load and displacement sensors were reset to zero and subject instructed to perform flexion extension motions. Once the subject began MVC (maximum voluntary contraction) of thigh muscle due to external resistance, the software was initiated to collect and a gently force was applied manually on to handle area of external piston as shown in Figure 16. Immediately after the load was released, data collection was stopped and automatically saved by the software into an excel format. Subsequently, several areas on subject's thigh region were randomly measured utilizing similar technique and plotted using an excel scatter graph tool as shown in Figure 17.

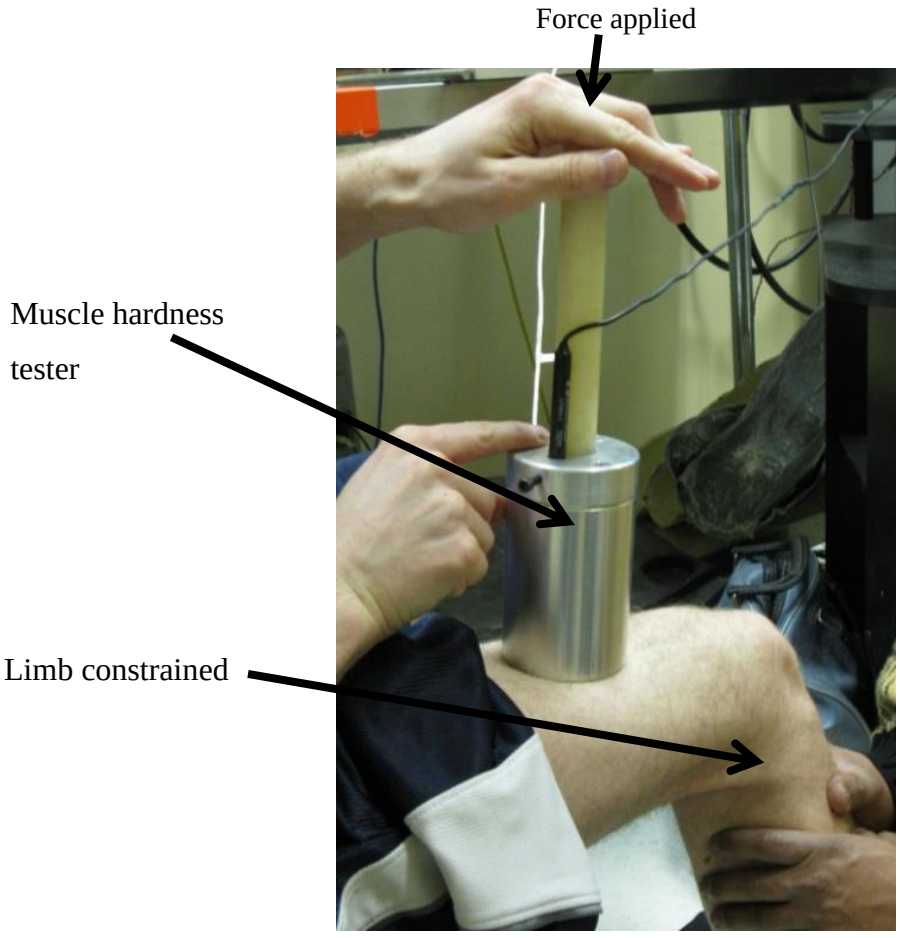


**Figure 16 Muscle hardness tester under operation**

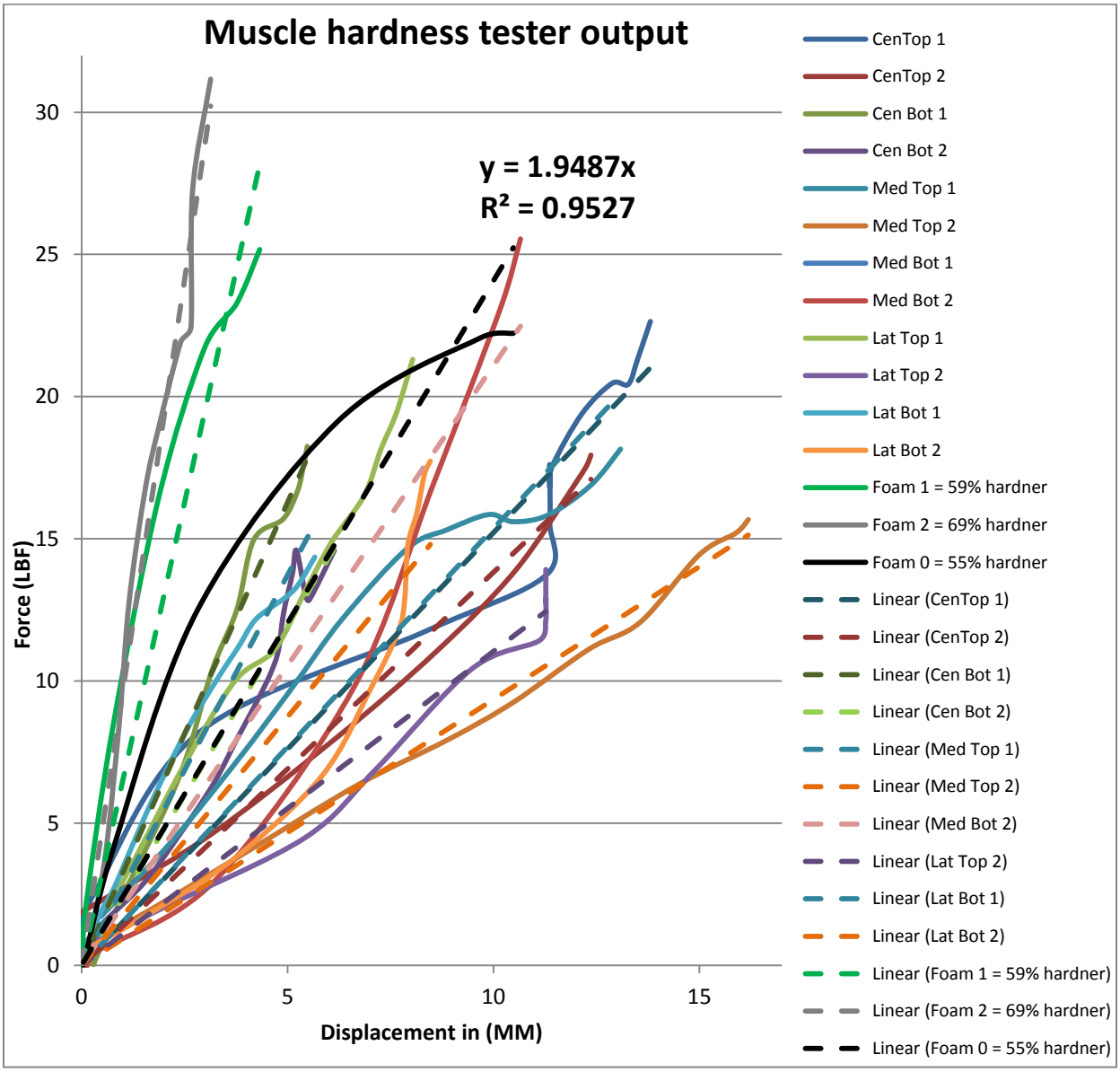


**Figure 17 Muscle hardness tester output plot of Force v/s Displacement and slope**

Finally average of the measured stiffness values (19.3 N/mm) was considered as the baseline parameter for selecting the substitute foam material, which would be used to create the artificial surface interface between brace and the cadaver specimen. Furthermore, varying hardness of foam materials were mixed in different proportions to create test samples and subsequently measured using hardness tester. Finally, it was discovered that foam material mixed with 55% ratio of hardening agent reproduced stiffness value of 17.56 N/mm and closely replicated the average muscle stiffness value and hence was selected to be used in the research study.

## 4.4 Dynamic Knee Simulator

### 4.4.1 Introduction

Dynamic knee simulator utilized for this research is innovative test equipment developed at the University of Waterloo and mainly designed to understand neuromuscular and biomechanical effects on ACL injuries. This machine was designed to reproduce kinematic and kinetics effects induced due to muscle activations surrounding the knee joint. Several electromechanical systems are utilized functioning as a close looped control system while replicating sagittal plane motion of human knee joint and complete design and development of the simulator is explained in (Cassidy K, 2009).

### 4.4.2 Construction

Dynamic Knee simulator incorporates two linear belt actuators constructed such that they provided vertical and horizontal planar motion to replicate hip and ankle motions along the sagittal plane. As shown in Figure 18 the vertical linear belt actuator driven by servo motors (AKM73P-ANC2R-00 manufactured by DANAHER motion) contains a swivel joint reproducing motion of hip joint while horizontal linear belt actuator driven by a similar motor containing a 3D load cell (model PY8595, serial 3190171-081009109 manufactured by BERTEC Corporation), mounted under a fixture set-up replicates ankle joint as shown in Figure 18. These linear belt actuators are controlled in a position control mode and encoder counts representing velocities at each time step was programmed into individual actuators to replicate knee motion. In addition, four servo motors (Model AKM44J – BKCNC-00 Manufactured by KOLLMORGEN) connected to linear screw actuators (Model RSA32 BN02 SK4 LMICLV Manufactured by TOLOMATIC. USA) are positioned at strategic location on the knee simulator as shown in Figure 18. In addition hip moments acting on the knee joint are replicated by a servo motor with a push pull cable as shown in. These servo motors are controlled in force control mode and hence each brake cable attached to individual motor actuator system is connected in line with a load cell (Omegadyne Inc. Model: LC203-2K, s/n 240594) and output from this load cell is used as feedback for close loop system. These servo motors were connected to cadaver knee specimen through a system of brake cables and pulleys to replicate main muscles around knee inclusive of Quadriceps, Hamstring and Gastrocnemius muscle as shown in Figure 18. A 3D load cell (model PY8595, serial 3190171-081009109 manufactured by BERTEC Corporation) placed directly under the ankle joint link as shown in Figure 18 is utilized to measure the ground reaction force values observed during simulation of Cadaver knee specimen. Furthermore, a twin axis

angle goniometer (SG 150 Twin axis angle goniometer - b3657 manufactured by Biometrics ltd) was utilized to measure the knee flexion extension angles between femur and tibia during the simulation activity. The knee simulator is controlled using controller (DMC 4060 manufactured by Galil motion control USA) and during simulation, data from load cell was set to be collected at 1000 HZ using National Instruments DAQ (model USB-6229, part no: 195840A -01 manufactured by National Instruments USA).

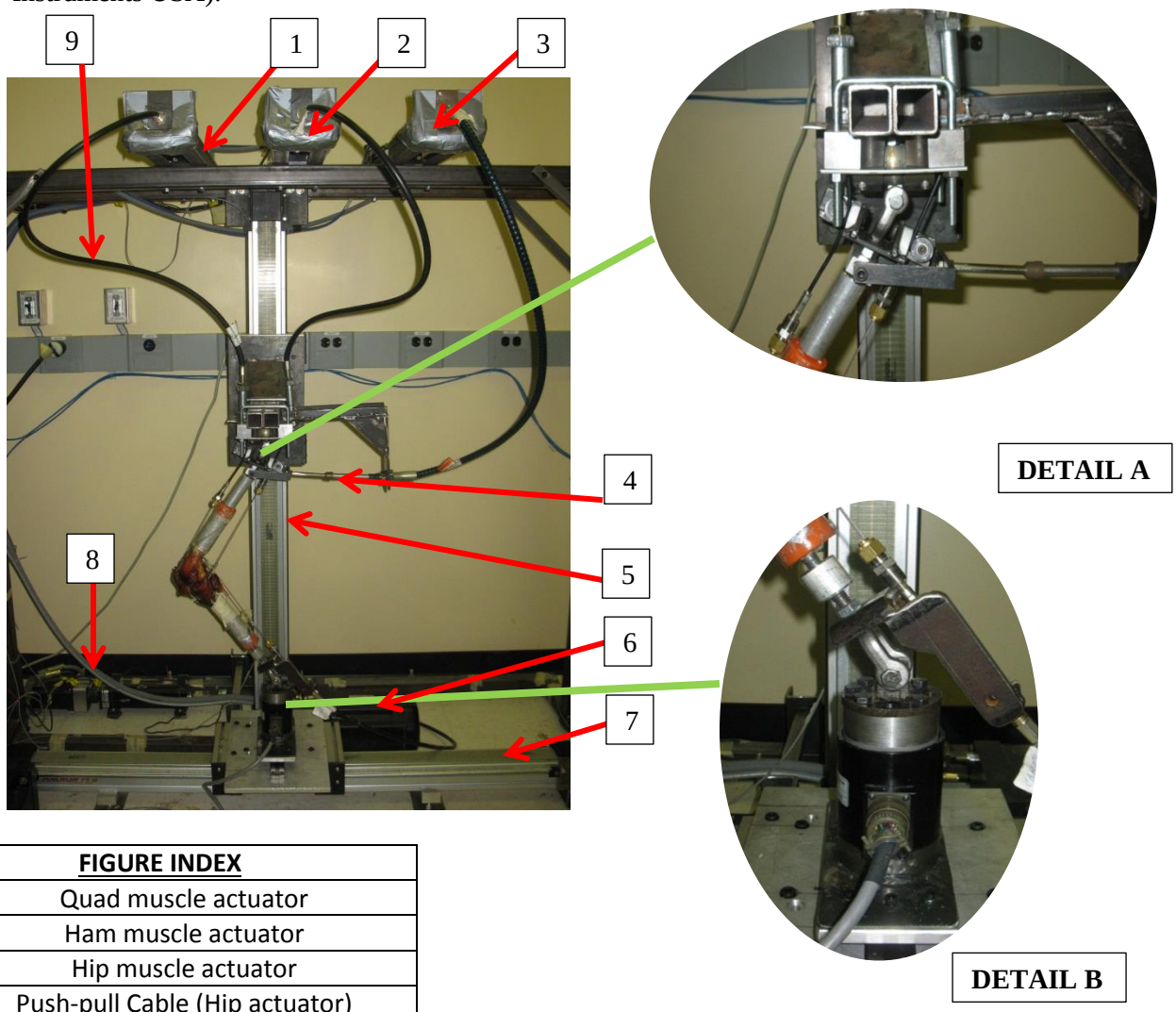


| FIGURE INDEX | |
|---|---|
| 1 | Quad muscle actuator |
| 2 | Ham muscle actuator |
| 3 | Hip muscle actuator |
| 4 | Push-pull Cable (Hip actuator) |
| 5 | Vertical belt actuator (E axis) |
| 6 | Vertical actuator servo motor |
| 7 | Horizontal belt actuator (F axis) |
| 8 | Gastrocnemius muscle actuator |
| 9 | Pull – Pull /Brake cable for Muscle actuators |

**Figure 18 Features of Dynamic Knee simulator (detail A) Hip joint, (detail B) Ankle joint**

### 4.4.3 Program Modifications

Dynamic knee simulator was developed to satisfy research condition of simulating single leg jump landing motions on cadaver knees. However due to the customized nature of equipment, programming and operating it were cumbersome and inconsistent. In addition, manual coding/user input was necessary to move actuators during set-up events. Consequently, the equipment was often prone to uncontrolled motions due to programming/manual coding errors thereby exhibiting safety hazard in some instances to the researcher. Hence a separate LabVIEW program was developed to streamline user inputs and equipment operation such that a standardized GUI was created for operating galil controller and manual programming of the equipment was totally eliminated during simulation.

Horizontal and vertical axes (E and F belt actuators) of the knee simulator were not sequenced and position relative each other was not established. Hence at each instance of machine set-up (prior to simulation), distance between each axes were physically measured and set by jogging individual axes in manual mode. This technique inherited several inaccuracies into test procedure and posed severe safety hazards due to input errors during manual coding. As a remedy, additional limit switches (homing limit switches) were installed to individual (E and F axes) axes at predetermined distances with reference to an absolute zero position along individual axis. This absolute zero position was established by jogging individual axis to a location wherein ankle joint center land mark (link) on horizontal axis and hip joint center (swivel link) of vertical axis aligned up with each other.

In addition, a specific homing routine was developed for the equipment to establish and register the absolute zero position every time the machine was powered into service. This encompassed moving actuators in a pattern to sense and locate homing limit switch on respective axes. Once limit switch was located along each axis, the position was registered with a predetermined encoder count that corresponded to distance of individual limit switch from the pre-established absolute zero position on individual axes. This method enabled programming location of hip and ankle joint centers accurately during simulation.

### 4.4.4 Hardware Modifications

Although dynamic knee simulator was a novel idea incorporating several electromechanical components and was extensively capable of reproducing high speed dynamic motions and forces, several limitations persisted in the original design and required hardware modifications. Additional cross braces were added to the main equipment frame and both vertical and horizontal axis were anchored to the main frame with custom brackets as shown in Figure 21 and re aligned to be perpendicular to each other. In addition, equipment was stabilized and leveled to the floor by adding several leveling screws as shown in Figure 19 and this reduced mechanical noise due to vibrations.

Two additional support blocks were manufactured and mounted below the horizontal axis of the equipment as shown in Figure 19 in order to prevent the horizontal axis from bucking due to forces exerted by the vertical axis.

**Figure 19 Leveling feet added to the actuator frame to stabilize the equipment**

Muscle cables were initially designed such that they were anchored on the frame of the vertical axis and did not tilt to keep force line of action consistent as the knee flexed and extended. Hence roller bearing were added to the hip actuator assembly and muscle actuator cables were wrapped around the pulleys as shown in Figure 25 and this ensured that muscle line of action remained consistent throughout the various flexion/extension angles of the knee.

Ankle actuator was originally designed such that the 3D load cell was fastened to the horizontal axis and was constrained in Medio-lateral direction. This constraint added additional strain on the cadaver knee when the tibia or femur on cadaver knee specimen had severe valgus deformities due to alignment issues between E and F axes. Hence ball bearing linear guide rails were added underneath the 3D load cell as shown in Figure 21. This permitted natural movement of cadaver knee specimen along Medio-lateral direction and accommodated for valgus deformities of specimen.

Originally vertical axis consisted of a custom machined bracket and ball socket arrangement creating the hip joint shown in Figure 25. However, since extensive clearances were incorporated in the bracket design, it resulted in backlash while hip muscle actuator created flexion/extension moments on to knee joint. This caused lag in the system while hip actuators changed from exerting flexion moments to extension moments during trial. To eliminate this issue, a hinge style bearing mechanism was designed to keep hip axis constrained to sagittal plane and securely mounted on the vertical axis frame with four 3/8" screws as shown in Figure 20.

Hamstring actuator was repositioned on machine main frame as shown in Figure 20 and the actuator cable was attached to specimen through an opening adjacently above the hip cable. This was needed to provide additional space for cable attachment hardware

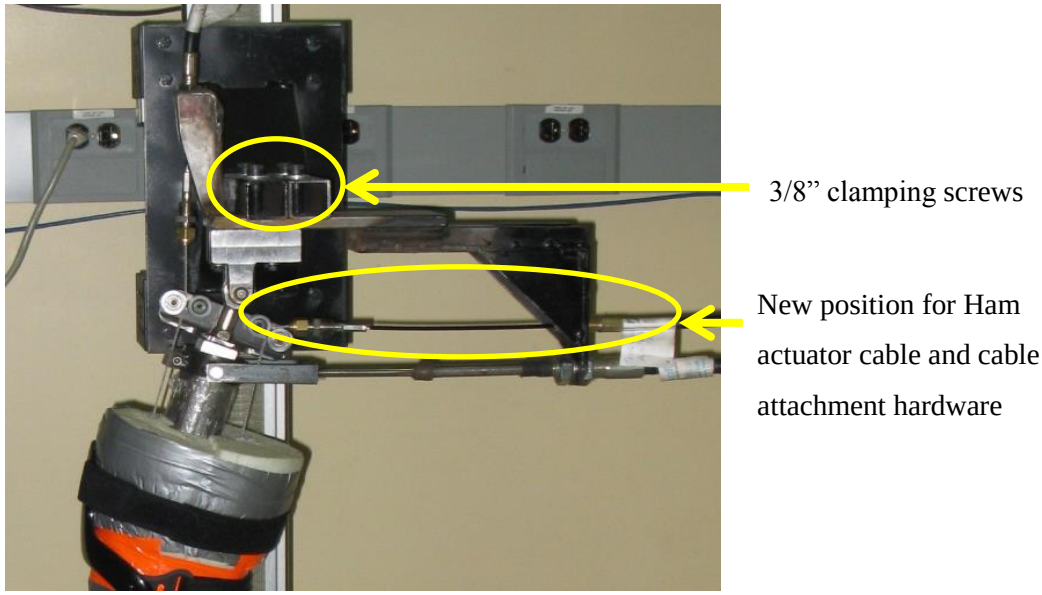


**Figure 20 Additional hardware modification performed on to actuator to eliminate backlash in hip joint**

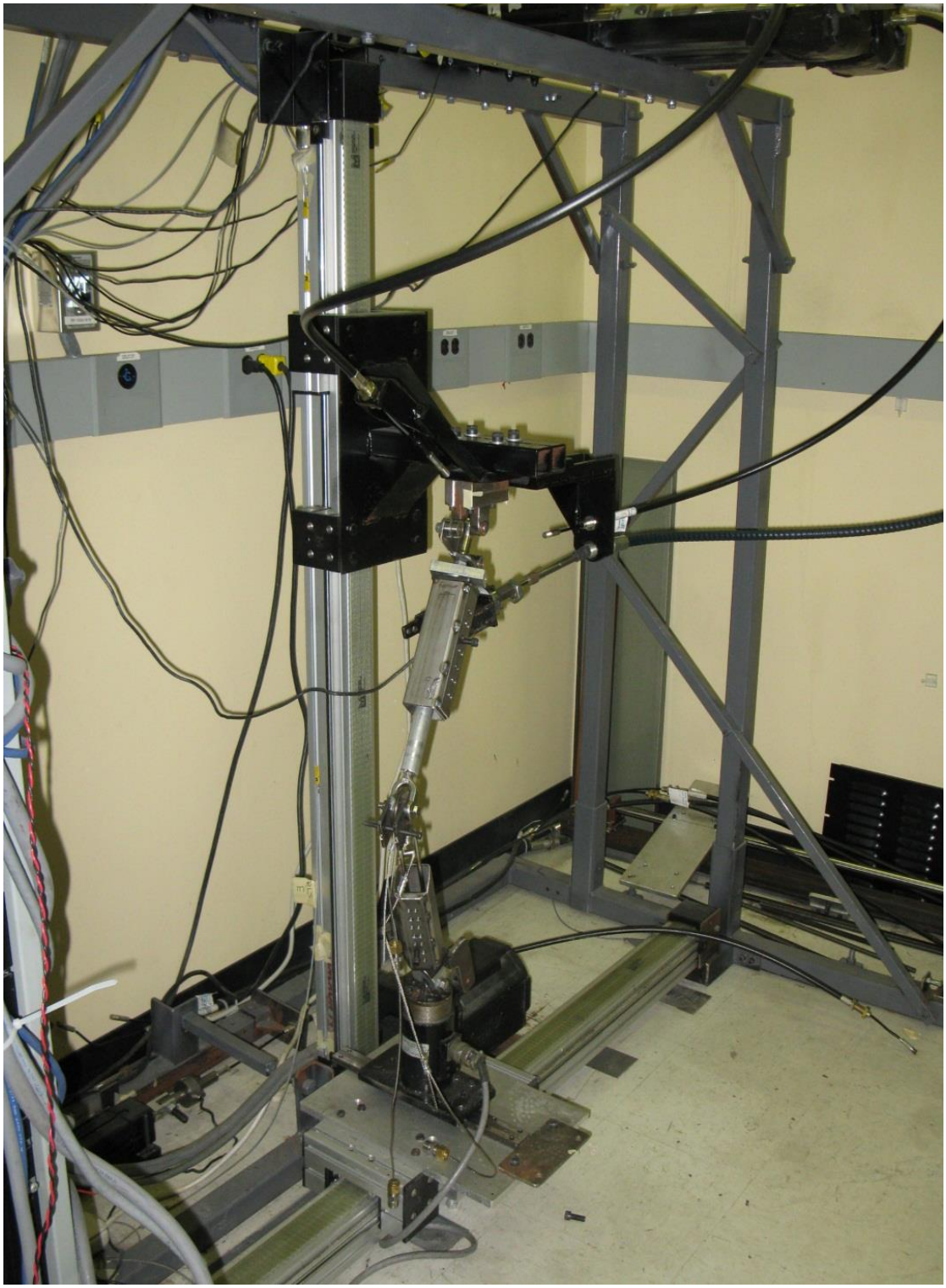

**Figure 21 Mechanical knee model mounted on Dynamic Knee simulator**

# Chapter 5
# Phase 1 Knee Brace Testing Procedure Development

## 5.1 Introduction

This chapter elaborates an innovative technique developed based on research methodology validated and utilized by Erickson et al (1993). During this initial phase of research, a technique to evaluate prophylactic brace was developed utilizing a hybrid surrogate specimen that was mounted on the Dynamic Knee Simulator (developed by Cassidy K, 2009) and a dynamic (In vivo) motion was simulated on the machine. Furthermore, this combination technique of using motion captured data to simulate the dynamic knee simulator and study ACL strain was published to validate methodology in the research community (Cassidy et al, 2013).

## 5.2 Motion Capture

Innovative aspect of this research involves a combination of In Vivo/In Vitro procedures utilized to determine ACL strain in a Knee during jump landing. Hence, In Vivo kinetic and kinematic data were collected by 3D motion capture technique using an Optotrax high speed motion capture system (Certus Optotrak, Northern Digital Inc., Waterloo, ON). In this technique a set of strategically positioned high speed cameras tracked infrared markers that were positioned on bony landmarks of subject's body, thereby obtaining real time 3D co-ordinate information with respect to a global co-ordinate system. In addition, a force plate (OR6-7-1000, AMTI, Watertown, MA) was synchronized to camera set-up and used to collect ground reaction force data (GRF). Position of force plate was derived from 3D corner location data (force plate corner) with relevance to the global co-ordinate system for ease of computation, Global co-ordinate system (GCS) was set-up at corner of force plate as shown in Figure 22. The normal set-up of the GCS in the motion capture lab was in a conventional orientation with + Z axis oriented vertically away from ground. Hence, the text file that was used by software to determine and initiate the GCS was modified to establish ISB convention, with + Y axis oriented vertically away from ground as shown in Figure 22.

A female volunteer weighing 61 kg and 1.62 m tall was instructed to jump as high as possible and land on her dominant leg (right leg). The participant was asked perform this single jump landing at her convenient pace and style but was specified to retain her body balance after landing on her dominant leg. Subject was instrumented with clustered infrared markers as shown in Figure 23, while

strategic bony landmarks on torso, leg were digitized with reference to these infrared clusters and Table 1 lists all relevant bony landmarks used during motion capture. As a priory, for scaling biomechanical model and calibration purposes, a "stand-up trial" was recorded while participant was standing motionless on the force plate. After performing few tryouts of single leg jump landing, participant performed multiple single leg jump landings.

**Table 1 List of clustered infrared markers and digitized bony landmarks used for motion capture**

| **Body Segment** | **Marker set used** | **Digitized bony landmark** | **Abbreviated in C3D file** |
|---|---|---|---|
| Right Thigh | Cluster marker on thigh | Lateral femoral condyle | LC |
| | | Medial femoral condyle | MC |
| | | Greater trochanter | GT |
| Right Shank | Cluster marker on anterior shank | Lateral malleoli | LM |
| | | Medial malleoli | MM |
| Thorax | Lower back cluster marker<br>Upper back cluster marker | Right anterior superior iliac spine | RASIS |
| | | Left anterior superior iliac spine | LASIS |
| | | Right posterior superior iliac spine | RPSIS |
| | | Left posterior superior iliac spine | LPSIS |
| | | 10 segment of thorax spine | T10 |
| | | 7 segment of cervical spine | C7 |
| | | Right Acromion | RA |
| | | Left Acromion | LA |
| | | Sternal notch | SS |
| | | Xyphoid process | XP |
| Right Foot | Individual marker placed on Head of Metatarsal 1 | | MT1 |
| | Individual marker placed on Head of Metatarsal 5 | | MT5 |
| | Individual marker placed on Head of Phalanx Metatarsal 1 | | TOE |

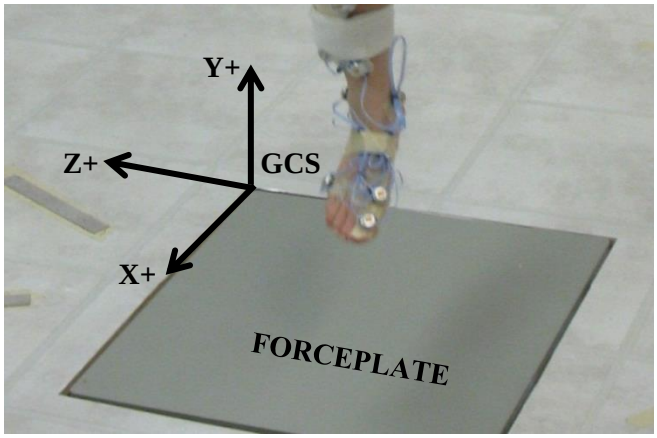


**Figure 22 Location and orientation of GCS with respect to force plate**

**Figure 23 Athlete instrumented with infrared markers during motion capture**

## 5.3 Editing C3D data file

During high speed motion capture, full body kinematic data (Marker Data) was collected at 100 Hz while force plate data was collected at 1000 Hz. The data was collected in C3D file format however certain relevant force plate calibration were not included in the originally exported C3D file. Hence each data file was further edited using a C3D editor to add relevant force plate information such as the corner locations, force plate scaling factor, force plate origin location and orientation and the force plate calibration matrix values obtained from the force plate user manual.

## 5.4 Bio Mechanical Model

### 5.4.1 Anybody® Modeling

Several studies have indicated the influence of agonistic and antagonistic muscle forces on ACL (Li et al, 1999). In this knee brace study, a bio mechanical model developed by Anybody® Technologies Inc. Aalborg, Denmark was utilized to estimate muscle force among four major muscle groups. Anybody® modelling software utilizes a muscle min/max criterion optimization algorithm to solve muscle recruitment problem in order to estimate individual muscle force (Damsgaard et al, 2006). A lower extremity gait model was extracted from Anybody® model repository, which utilized kinematic and kinetic data in C3D format for inverse dynamic analysis. This biomechanical model was developed on a text based input and utilizes a special declarative, object oriented programing language called anyscript. The downloaded folder consisted of several files and supporting programs that were further interlinked through several layers of model structure. These subprograms were initiated through a main program file called "`GaitLowerExtremity.main.any`" and the edited C3D motion captured data was introduced into biomechanical model. Several single leg landing trials were included along with a stand-up trial for calibration purposes. In addition, anthropometric details of subject including mass, height, thigh, shank, foot lengths, trunk height and the pelvis width were measured and input into the software. A comprehensive copy of the important sub programs and modified Anybody® codes are included in Appendix 1 under several sub sections.

By incorporating these modifications into the file, markers listed in Table 1 were introduced into biomechanical model. Subsequently, marker co-ordinates on individual body segment were adjusted in order to scale virtual model and also to ensure that the C3D marker location and driver location coincided as shown in Figure 24. A copy of the co-ordinate information and modified codes are included in Appendix 1 Section 1. The Bio mechanical model downloaded from repository

included body model of a male subject and since the study included motion capture data of a female, female body model was included and initiated by modifying codes as shown in Appendix 1 Section 2. Based on subject's height, weight and reviewing anthropometric data published in Chaffin et al (2006) it was concluded that the subject belonged to a $50^{th}$ percentile female category of US women. Hence the program was further modified to include scaling laws to fit archetypical body size of a $50^{th}$ percentile woman.

The model utilizes an optimization algorithm to scale body segments parameters utilizing marker positions that were associated with bony landmarks. Optimization of selected body segment parameters were subsequently enabled or disabled by modifying codes as shown in Appendix Section 3. In addition to this, certain body segments that were not instrumented with infrared markers (such as left leg, arms) during motion capture were removed from the biomechanical model by altering codes as listed in Appendix 1 Section 4. Anybody® modeling software utilizes a set of markers to drive individual body segment and during motion capturing markers were not utilized to track the neck and head of the athlete, additional drivers were added to the main program file to drive the neck and body segments of the biomechanical model in co-ordination to the trunk markers. Modified trunk driver codes are listed in Appendix 1 Section 5. In addition to the aforementioned modifications to the code, convergence accuracy for both kinematic and inverse dynamics solvers were adjusted and software solving iterations were tweaked in the main program file by modifying values of variable "`nStep`" to obtain output muscle force data at 10 milliseconds time intervals.

### 5.4.2 Extracting muscle forces

Once Anybody® kinematic solver completed kinematic analysis, inverse dynamics analysis was initiated and solved resulting in estimation of force in 168 different muscle units. However since the scope of current study is limited to analyzing sagittal plane biomechanics of knee during single leg jump landing, muscle forces for three major flexor extensor sets of muscles crossing the knee capsule and flexion-extensor hip moments were extracted and utilized for simulation. Primarily complete set of muscle force data was extracted using plotting tools in Anybody® software and the extracted data was copied in a text format into an excel for further processing.

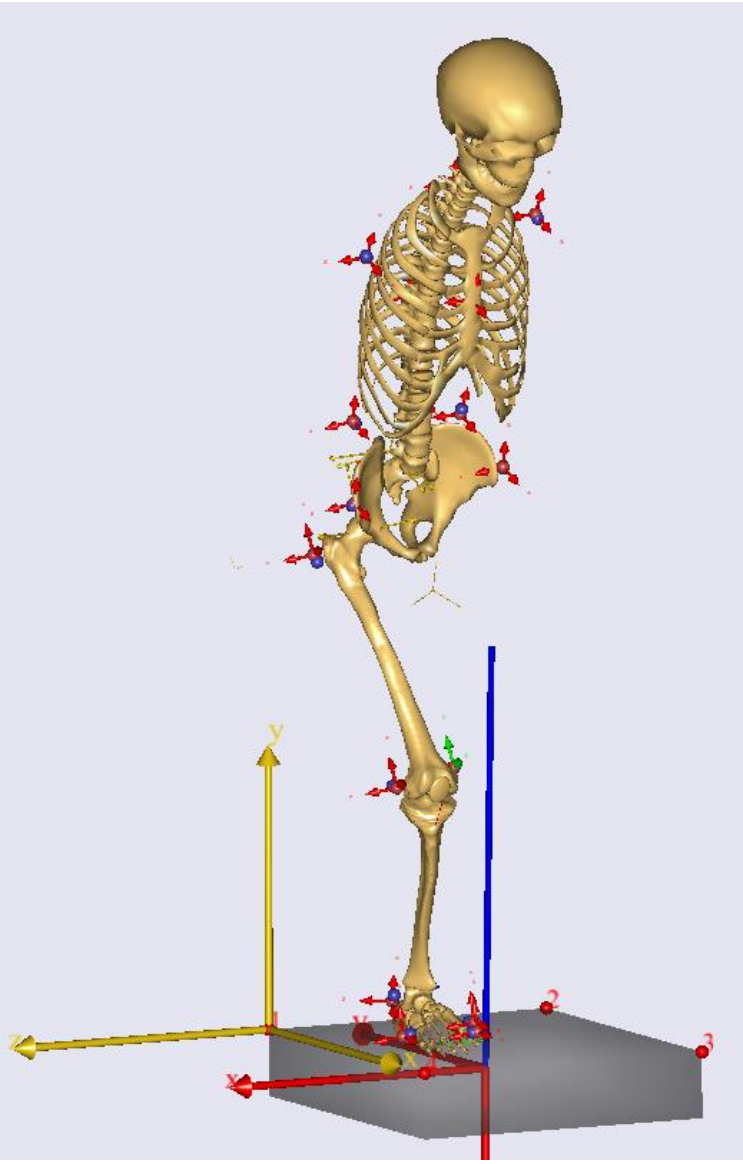


**Figure 24 Biomechanical model with all input marker locations after kinematic analysis**

### 5.4.3 Grouping muscle forces

Although Anybody® output muscle force data included forces of large number of muscle units, only three muscle groups crossing the knee joint (as listed in Table 2) and hip flexion/extension moments were utilized for the research study. In addition, respective muscle unit's forces that were extracted from biomechanical model were summed together under respective muscle group, whereas hip flexion and extension moments were derived directly from Anybody® software.

**Table 2 Various muscle groups and constituting muscle unit members**

| Muscle groups | Individual muscle units |
|---|---|
| Hamstring | Bicep femoris longhead<br>Bicep femoris shorthead<br>Semimembranosus<br>Semitendinosus |
| Quadriceps | Rectus femoris<br>Vastus lateralis<br>Vastus medialis<br>Vastus intermedius |
| Gastrocnemius | Gastrocnemius lateralisis<br>Gastrocnemius medialisis |

Multiple steps were involved in grouping and summing forces of individual muscle units. Primarily, moment arms for individual muscle groups were acquired from OpenSim 3.2 biomechanical software (developed by Stanford University). Utilizing plotting tools in the software, moment arm values of three muscle groups listed in Table 2 were plotted and acquired for knee flexion angles ranging from 0 to 90 degrees. These moment arm and conforming knee flexion angle values were input into a Mat Lab program to obtain coefficients that corresponded to the order/degree of polynomial for the input data curve. In addition after inverse dynamics analysis was completed (in Anybody® biomechanical software), knee flexion angle for each time step was acquired for the jump landing activity. Furthermore utilizing previously obtained coefficient values (from Mat Lab program), new muscle moment arms (NMM) for individual muscle unit were calculated for each time step by using a curve fitting function in Matlab. Finally Individual muscle unit forces (IMF), derived from Anybody® software were multiplied with newly calculated moment arm values (NMM) thereby resulting in Individual muscle moments (IMM) acting at the knee joint.

Lastly these calculated individual moment values (IMM, acting at knee joint) were transformed into forces acting along respective cable forces (MCF) attached to cadaver knee specimen using Equation 1. In order to do this, actual moment arms of cables (ACM) attached to the cadaver knee were calculated by utilizing tendon excursion technique (Delp et al, 1994). Consequently, the Cadaver knee was suspended in a fixture set-up as shown in Figure 26. A Linear Variable displacement Transducer (LVDT, Omega Engineering Inc. Stamford, CT, LP804-2 1030) was attached with a thin rope to the end of the muscle attachment cable at site of attachment to the cadaver knee as observed in Figure 26. In addition, a twin axis angle goniometer (SG 150 Twin axis angle goniometer - b3657 manufactured by Biometrics ltd) was mounted on the cadaver knee specimen as shown in Figure 26. A specialized LabVIEW program was utilized to collect and output the data from LVDT and angle goniometer (National Instruments, Austin, TX) and as the program was initiated for collection, the knee was flexed and extended from 0º to 90º. The software output the data into an excel file containing displacement of the LVDT which was plotted against the flexion angle recorded by the angle goniometer. The slope of this flexion angle v/s displacement curve was determined from the plotted graph and considered as the estimated moment arm of the cadaver knee muscle attachment cable. Subsequently this process was conducted for all three muscle attachment cables to obtain respective moment arms.

Finally these attained moment arms values were used to divide individual knee muscle moments that were calculated (as explained in previous paragraph). This process was completed for each muscle unit at each time step and finally summed together into groups (as categorized in Table 2) using Equation 2, resulting in forces applied along respective actuator cables (TMCF) on the knee simulator. Construction of cable guides at the hip joint of knee simulator as shown in Figure 25 resulted in additional moments created by cable forces. Hence to account for these additional moments, net cable force for hip actuator was calculated by using Equation 3.

$$\boldsymbol{MCF} = \frac{((\boldsymbol{IMF}) \; x \; (\boldsymbol{NMM}))}{(\boldsymbol{ACM})}$$

Where,

MCF = Individual muscle unit cable force

IMF = Individual muscle unit force derived from Anybody® Modelling software

NMM =New moment arm for each muscle corresponding to jump landing activity knee angle

ACM = Actual cadaver muscle actuator cable moment arm

**Equation 1 Used for Calculating individual muscle unit cable force**

$$\boldsymbol{TMCF} = \sum \boldsymbol{MCF}$$

Where Σ refers to summation of individual muscle unit cable force to create total cable force (TCMF) representing muscle actuator force for muscle groups listed in Table 2.

**Equation 2 Used for calculating total muscle actuator force on knee simulator**

$$\boldsymbol{NHFr} = \frac{(((\boldsymbol{AHM}) - (\boldsymbol{HCM})) + (\boldsymbol{QCM}))}{\boldsymbol{0.080}}$$

Where NHFr = Net hip cable force (Calculated)

AHM = Hip flexion/extension moments acquired from Anybody® bio mechanical model

HCM = Moments created by Hamstring actuator cable force = (THCF*0.042 meters)

QCM = Moments created by Quadriceps actuator cable force = (TQCF*0.042 meters)

0.080 = Distance of hip actuator cable from hip joint on the knee simulator in meters

**Equation 3: Used to calculate net hip cable forces**

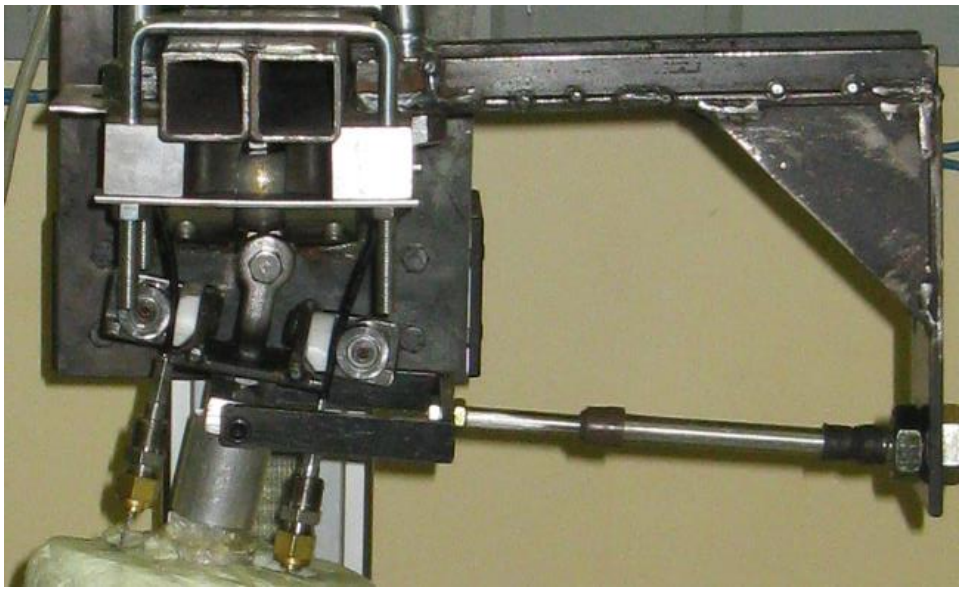

**Figure 25 Muscle cable guide attachment configuration at hip joint site on Dynamic Knee simulator**

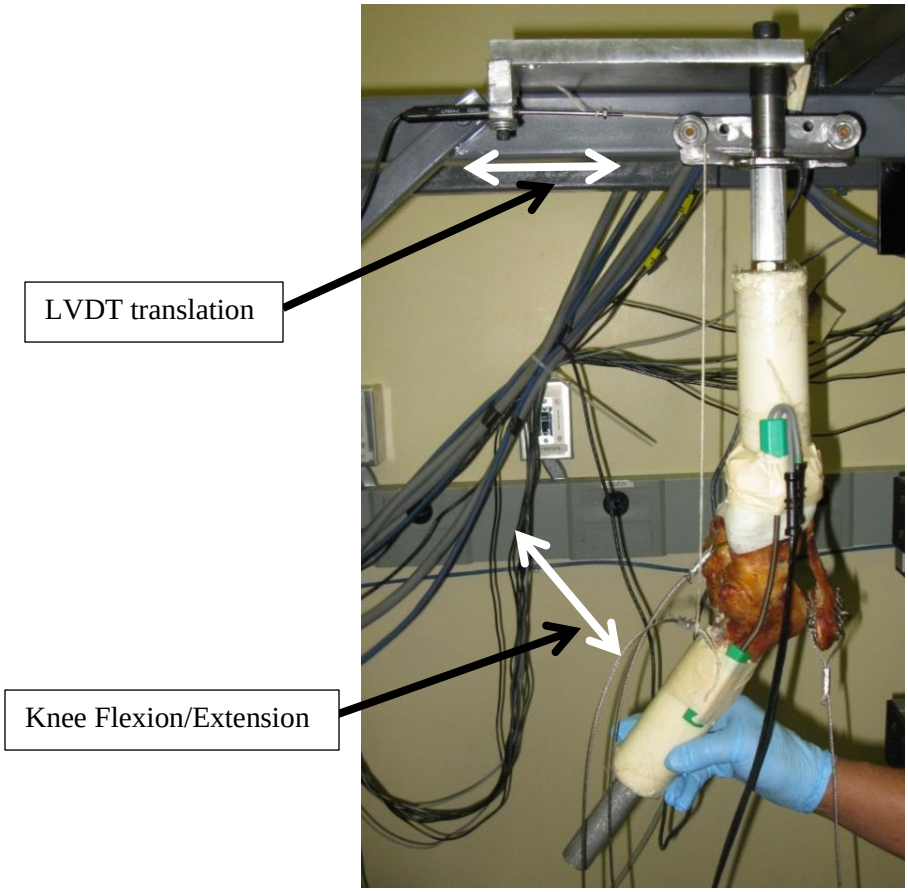


**Figure 26 Cadaver knee specimen set up to obtain muscle attachment cable moment arms using tendon excursion technique**

### 5.4.4 Converting Muscle forces to Encoder counts

The muscle actuator cable forces calculated were in Newton and the knee simulator required inputs in encoder counts. As explained by Sabharwal P (2011) in his thesis work (table 4.4 of page 66) on the knee simulator, the load cell on muscle actuators were configured such that 10 volts output of load cell resulted in 2047 encoder counts of the muscle actuator system. However this configuration of load cell signal amplification resulted in limiting the force exerted by muscle actuators to 400 Lbf. at 10 volts output. Hence, load cells were recalibrated and respective amplifiers were adjusted such that relationship between voltage output of load cell and the actuator encoder counts corresponded such that every 1.02 encoder count resulted in 1 Lbf. force in actuator and utilizing these empirical relations, muscle forces were converted into encoder counts through Equation 4 where 0.224808 is newton to pound conversion factor.

$$(\boldsymbol{Actuator\ cable\ force}\ (\boldsymbol{N}) \times 0.224808) \times (-1.02\ (\boldsymbol{encoder\ counts}))$$

**Equation 4 Conversion from cable forces to encoder counts**

Finally, the time step at the point where subject's foot touched the force plate (during landing) "point of landing" or initial foot contact was identified from (observing the rise in GRF data) GRF data that was downloaded as Anybody® output. And the muscle force / encoder count data for time steps 100 milliseconds prior to the "point of landing" and 200 milliseconds after it were selected to form an array of encoder count values. Since the resulting encoder count array indicated patterns of un realistic and abrupt changes in force magnitudes within short intervals of time, they were curve fit to a $12^{th}$ degree polynomial creating a new array of encoder counts and these values were listed under individual muscle headers as shown in Figure 28. These new array values were saved in an excel format and subsequently input into a program to activate the dynamic knee simulator

### 5.4.5 Extracting joint position data

Position of hip and ankle joint were acquired from Anybody® output marker data. In this study, lateral malleoli marker position data was used for ankle joint of the actuator and greater trochanter marker position data was used for hip joint of the actuator. However, since Anybody® output the marker data in reference to number of time steps, menu options were adjusted as explained in Anybody® software manual to obtain marker data plotted against relevant time intervals as shown in Figure 27 and this way it was possible to ensure that both muscle force data and marker data corresponded to common time series. Furthermore, these selected marker data were copied in text format and converted into encoder counts as explained by Sabharwal P (2011) and finally transformed into velocities for every 10 millisecond time step.

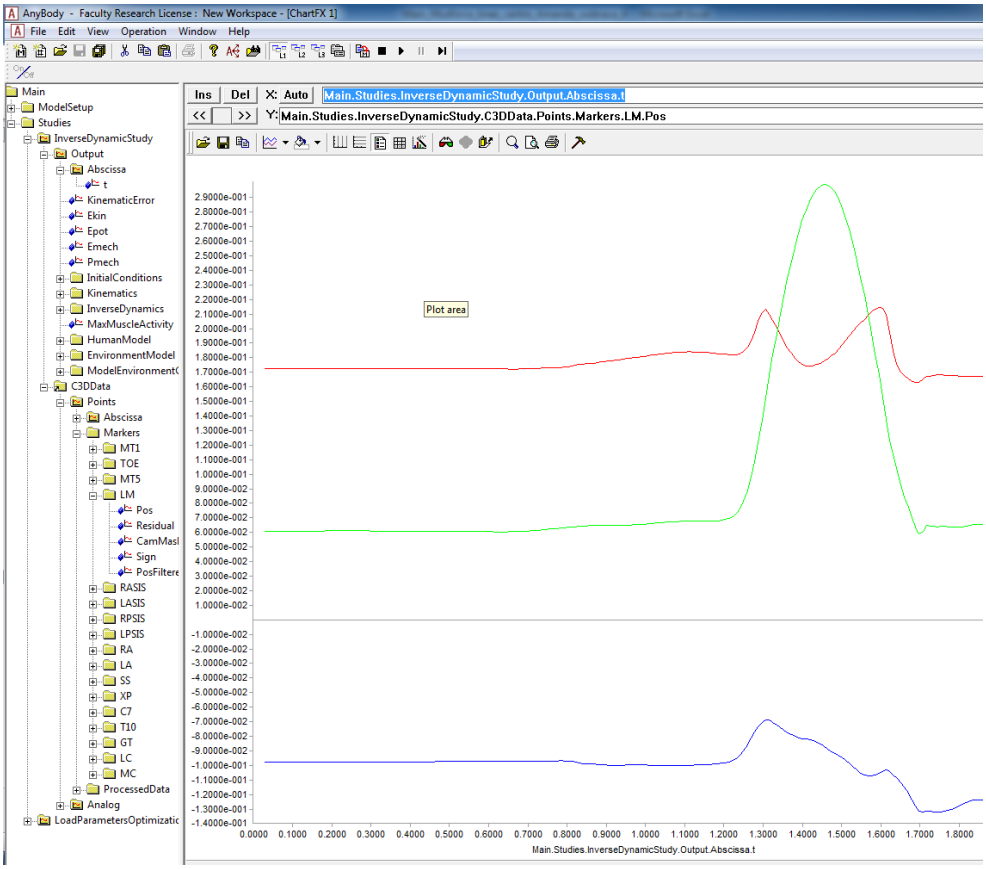


**Figure 27 Marker data (X,Y and Z co-ordinate values) plotted against time using plotting tools of Anybody® software**

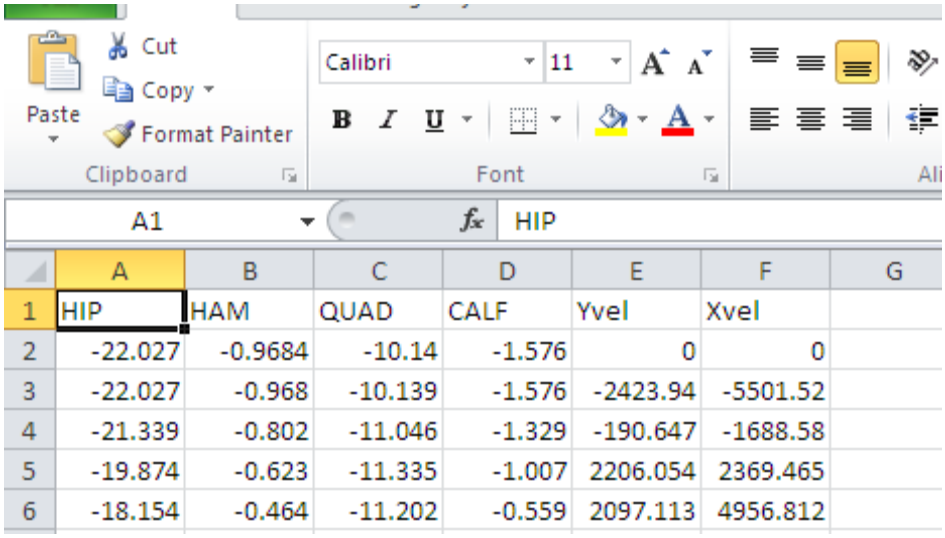


| | A | B | C | D | E | F | G |
|---|---|---|---|---|---|---|---|
| 1 | HIP | HAM | QUAD | CALF | Yvel | Xvel | |
| 2 | -22.027 | -0.9684 | -10.14 | -1.576 | 0 | 0 | |
| 3 | -22.027 | -0.968 | -10.139 | -1.576 | -2423.94 | -5501.52 | |
| 4 | -21.339 | -0.802 | -11.046 | -1.329 | -190.647 | -1688.58 | |
| 5 | -19.874 | -0.623 | -11.335 | -1.007 | 2206.054 | 2369.465 | |
| 6 | -18.154 | -0.464 | -11.202 | -0.559 | 2097.113 | 4956.812 | |

**Figure 28 Array format with appropriate headers input into Dynamic Knee simulator**

## 5.5 Preparation of Test Specimen

Preparation of test specimen was crucial for this research study and the primary goal was to produce a hybrid surrogate model with polymer outer shell possessing surface stiffness equivalent to a stiffened muscle under voluntary contraction (MVC). Which when molded encapsulates the cadaver knee. This hybrid surrogate limb was matched to external shape and size of the cadaver leg specimen while having flexion extension mobility matching a human limb. The outer shell facilitated proper mounting of the prophylactic knee brace and molded to maintain orientation of the cadaver knee.

Several steps were involved in producing such intricate hybrid specimen and this section of report explains individual stages of its development.

### 5.5.1 Preparation of negative mould / "Tape mould"

Erickson et al (1993) proposed a methodology of replicating soft tissue utilizing a foam material and in this study similar technique was adopted to develop the hybrid surrogate model. A fresh frozen cadaver knee specimen harvested from a 23 year old male, 183 cm tall and weighing 96 Kg was retrieved from an organ donation repository. In order to cast the external foam surrogate shell encapsulating the cadaver knee, a negative mould "tape mould" of the cadaver knee was prepared. However since the cadaver knee specimen was deformed while initial freezing and muscle mass had concentrated along posterior end, in order to obtain a consistent shape and to correct deformities on external surfaces, the cadaver knee was thawed out for eight hours such that only the external surface of the cadaver knee was soft and flexible. In this condition external muscle tissue was reshaped by hand and retained into position using a clear tape thereby returning cadaver knee into a normal shape of human leg. And finally the cadaver knee was carefully refrozen to maintain remodeled shape as shown in Figure 29.

Once again the cadaver knee was retrieved from the freezer and while in frozen condition, inter medullar canals of femur and tibia were carefully drilled to a 1 ½" depth, soft tissue and organic content were removed. Two threaded rods of diameter and thread size of ½" NC were inserted carefully into the cleaned out canals as shown in Figure 30. To ensure that threaded rods were completely secured in bone, four wood screws (size 4 x 1) were drilled into bone perpendicular to axis of canal such that they indented into threaded rod.

**Figure 29 Cadaver knee specimen that was reshaped to correct deformities**

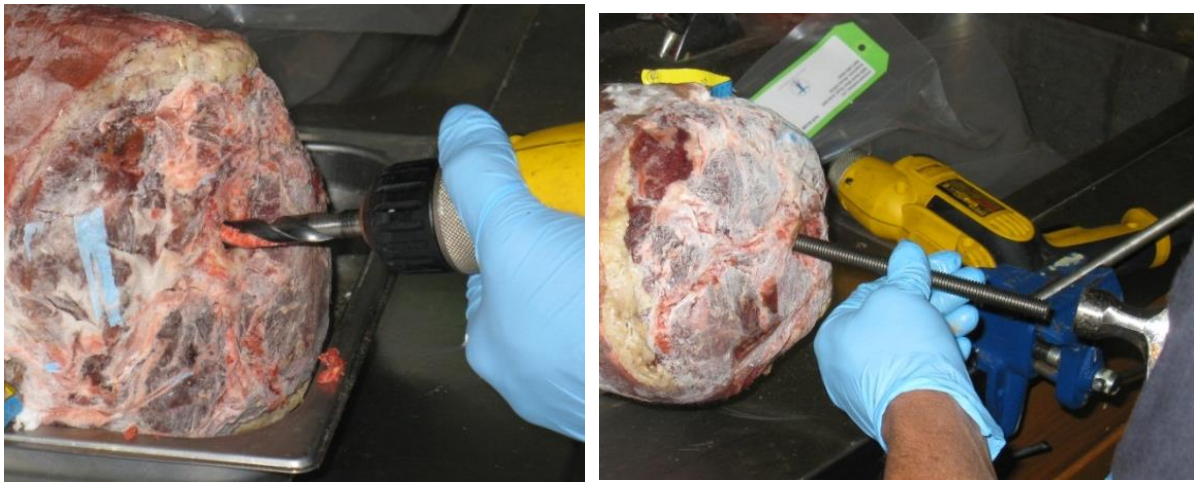

**Figure 30 Drilling and insertion of threaded rod into medullar canals during preparation**

Once the threaded rods were inserted securely, two ½" thick rectangular aluminum blocks known as "locator blocks" of dimensions (1 ½" x 1") were fabricated with threaded holes in center as shown in Figure 31. A high strength thread locker liquid (Loctite 263 thread locker) was applied on to threaded rod and locator blocks were fastened as shown in Figure 32. They were fastened securely and ensured to have bottomed on to bones and remained integral part of cadaver knee. In addition, two polycarbonate (PC) sheets of ½" thickness were cut to appropriate outside dimensions so that it covered both distal end cross sectional areas of the cadaver knee. Two rectangular openings were then machined in the center of these PC sheets to suit locator block dimensions as shown in Figure 33. These PC sheets also known as "endplates" were aligned with aluminum locator blocks in goal of maintaining location and orientation of cadaver knee in negative mould while casting foam outer shell. Endplates were positioned and aligned with locator blocks at each distal end of cadaver knee as shown in Figure 33 and two holes of diameter 0.200 inches known as "locator holes" were marked and drilled on each of these endplates. These holes were positioned such that they lined up along external surface of cadaver endplates as shown in Figure 33 and were strategically positioned to ensure that the endplates located and oriented in one unique direction at each distal end.

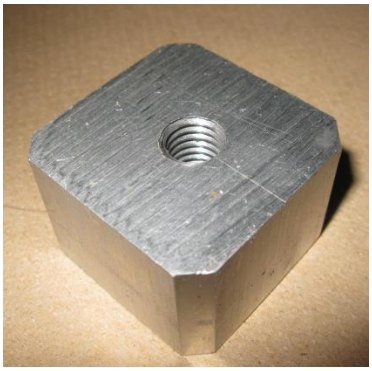

**Figure 31 Locator Block for aligning Cadaver Knee to Tape Mould during foam moulding**

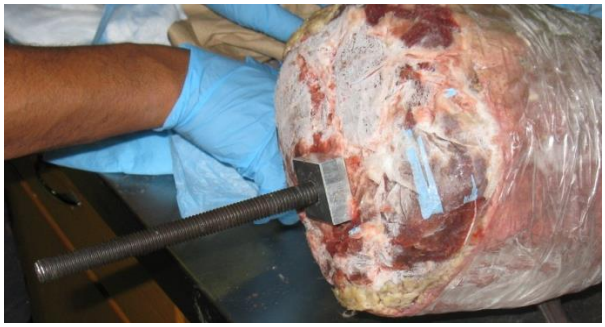

**Figure 32 Locator blocks mounted on distal ends of un dissected cadaver knee**

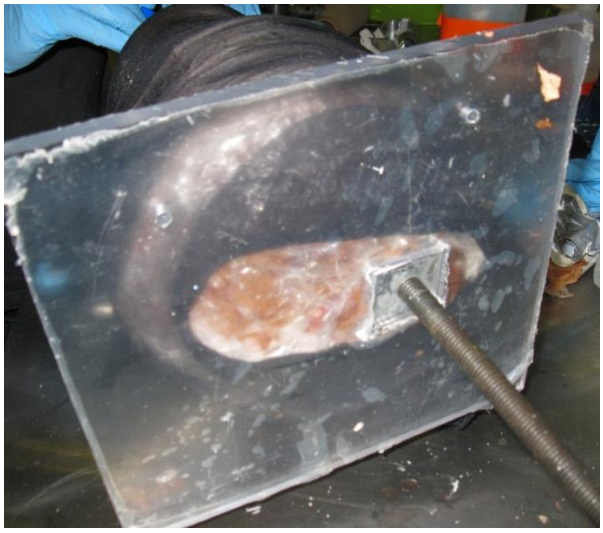

**Figure 33 End plates aligned to locator blocks on distal ends of cadaver knee specimen**

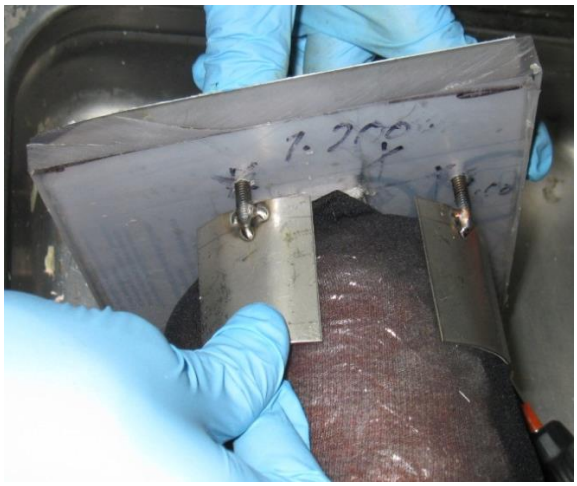

**Figure 34 Locator posts inserted into end plates during preparation of tape mould**

Four 3/16" diameter pins known as "locator posts" were custom fabricated and inserted into the locator holes of endplates such that they projected on to external surface cadaver knee as shown in Figure 34. Locator posts were designed to become an integral part of negative mould, while endplate and aluminum locator block assembly remained as integral part of cadaver knee. A women's nylon stocking was applied on to cadaver knee to prevent casting tape sticking on to cadaver knee surface. In addition, patellar and condyles positions were sketched on the nylon stocking using a permanent marker to create prominent landmarks that would create imprint on to the "tape mould" there by

providing visual aids for aligning the dissected knee to same orientation as the original un dissected knee (in “tape mould”) during foam shell casting.

The distal ends of cadaver knee were initially wrapped one inch casting tape (Scotchcast Plus by 3M) such that it formed a base layer for securing locator posts in negative mould known as “tape mould” as shown in Figure 35. Once the one inch base layer of cast tape was hard, end plates were inserted on locator blocks and locator posts were aligned into holes of end plates as shown in Figure 34. These locator posts were glued on to the one inch cast tape base layer with Loctite super glue and instantly additional two layers of four inch wide polymer casting tape (Scotchcast Plus by 3M) were wrapped around cadaver knee encapsulating the locator posts securely between layers of cast tape, resulting in it becoming an integral part of negative mould known as “Tape mould”.

**Figure 35 Creation of negative mould (“tape mould”) in shape of cadaver knee for future foam casting**

Once tape mould was semi rigid and capable of retaining its shape, the end plates were disengaged from locator posts and tape mould was marked and cut open on posterior side of the knee as shown in Figure 35. Immediately, the cadaver knee was removed from the tape mould and another layer of casting tape was wrapped around the mould such that split seam was closed back thereby retaining original shape of tape mould. When the tape mould was hard, it was sent for preparation of a custom knee brace. This procedure was strategically adopted to obtain an ideal structure and surface

interface for testing the custom fit knee brace, while the brace remained consistent to external features of test specimen. After the knee brace was manufactured, the tape mould was marked at cut along medio-lateral plane, resulting in two separate halves of tape mould as shown in Figure 36.

**Figure 36 Tape mould cut along medio-lateral plane and prepared for moulding external foam shell on a custom built fixture**

### 5.5.2 Preparation of Cadaver knee

After preparation of negative mould ("tape mould"), frozen cadaver knee was allowed to thaw out and carefully dissected to remove all skin and muscle tissue whilst keeping the joint capsule along with all ligaments, patellar and meniscus remained intact as shown in Figure 37. Fibula was screwed and secured to tibia to ensure that it remained intact throughout experiment. In addition, 1/8" diameter holes were drilled into tibia, femur, and patellar at strategically marked muscle insertion locations and the muscle attachment cable, a 3/32" diameter stainless steel aircraft cable (McMaster Carr catalogue number: 3458T76) was crimped by looping around the bone as shown in Figure 38. These cables were cut to appropriate lengths and crimped at distal end with aluminum crimps as shown in Figure 40. Special custom cable clamps were fabricated by modifying standard hydraulic connectors as shown in Figure 40 and the crimped end of cable was inserted through a ¼" hole on the end cap of the hydraulic connector while two split ferrules made of 4140 steel were assembled into position with the main body of hydraulic connector to hold the cable as shown in Figure 39. These

cable clamps (modified hydraulic connectors) were used to connect cables on cadaver knee to muscle actuators on dynamic knee simulator as shown in Figure 41.

A four inch long metal tube with two inch outer diameter and wall thickness of 0.065" was positioned and covered at distal end of femur while a two part plastic resin (R1 Fast Cast #891, Golden West MFG, Inc. California, USA) was poured to encapsulate the bone thereby providing reinforcement to the threaded rod as shown in Figure 42. In addition, this moulded metal casing also assisted location of femur on 'V' blocks of Lachman tester as explained in Section 4.2.3.

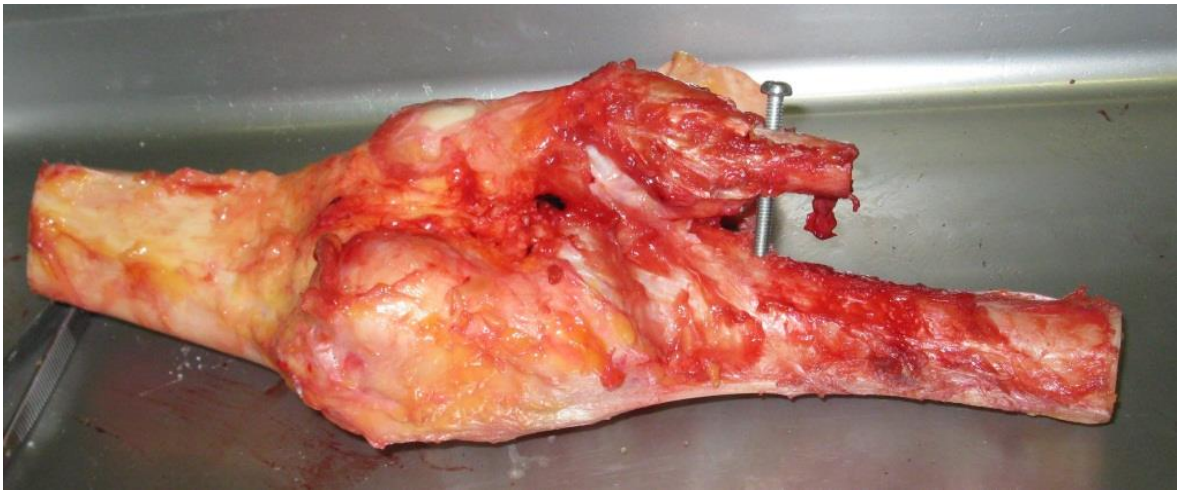

**Figure 37 Cadaver knee specimen dissected and prepared for foam casting**

**Figure 38 Cadaver knee specimen prepared with muscle force cable attachments**

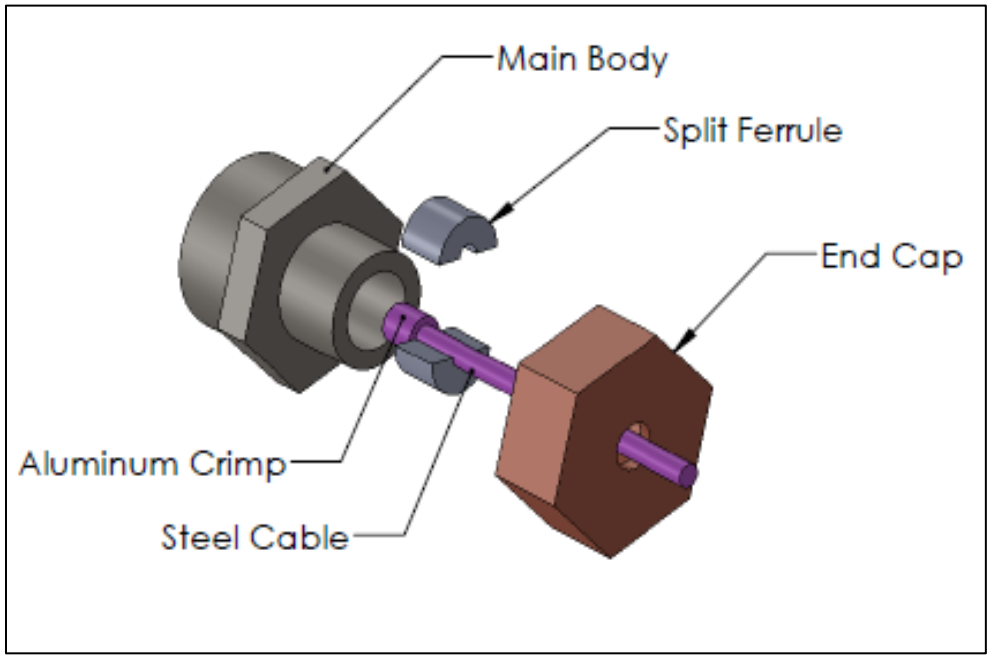


**Figure 39 Exploded view of Cable Clamp Assembly**

**Figure 40 Cable clamp hardware in proper configuration prior to assembly**

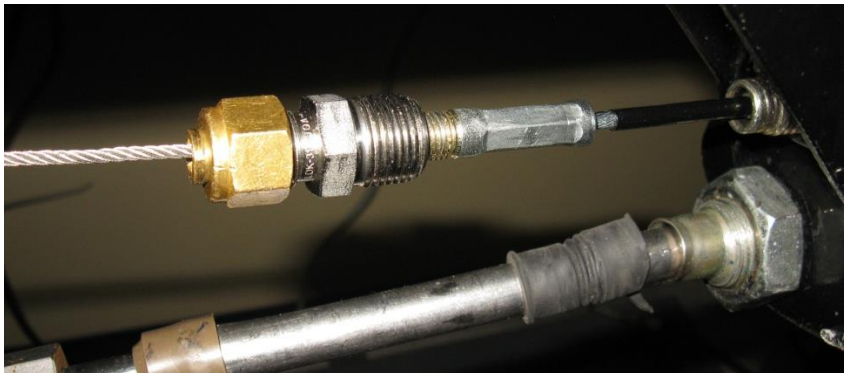

**Figure 41 Cable clamp hardware attached to the muscle actuator cable on knee simulator**

**Figure 42 Metal tube encased on femur of cadaver knee for reinforcement**

### 5.5.3 Casting polymer outer shell

Tape mould was cut along medio-lateral plane and anterior part was set-up on a custom built fixture as shown in Figure 36. Multiple layers of masking and clear tape were applied to internal surface of both halves of tape mould so that it would assist in easy release of moulded polymer shell. As shown in Figure 43, cadaver knee was wrapped with clear plastic tape while enclosing all muscle actuator cables in order to avoid contact with the polymer foam. Three aluminum tubes of 3/8" external diameter and 0.040" wall thickness were cut to appropriate lengths and taped into appropriate positions on cadaver knee as shown in Figure 44. These aluminum tubes were designed to behave as conduits for muscle actuators cable such that constant muscle force line of action is maintained during flexion extension of knee and they remain embedded in polymer outer shell after moulding. Proceeding further, end plates were mounted on locator blocks in respective positions of the cadaver knee and to accommodate the aluminum tubes, three relief holes of diameter 0.400" were drilled as shown in Figure 45. The cadaver knee and end plate assemble was inserted on to locator posts on the tape mould into respective positions and through this process it was possible to acquire proper orientation of cadaver knee in tape mould matching the original orientation of un dissected cadaver knee specimen. Furthermore, in order to allow flexion and extension of test specimen, on posterior side of cadaver knee capsule ½" thick blue rectangular piece of sponge was taped over the cadaver knee. This sponge material was eventually moulded into polymer outer shell shown in Figure 47 and tape was carefully cutoff the cadaver knee, thereby allowing posterior area of joint to compress and conform to shape changes that occurred during natural flexion extension motion of specimen.

**Figure 43 Cadaver knee wrapped with clear tape prior to foam shell moulding**

**Figure 44 Prepared cadaver specimen oriented and located in tape mould along with aluminum tube conduits for muscle actuator cables**

**Figure 45 Aluminum tubes located in holes drilled in end plates while cadaver knee specimen and locator blocks remain aligned to tape mould**

Sunmate foam material was prepared in predetermined proportions, quantity and poured into the prepared tape mould/cadaver knee assembly. As soon as the material was poured as shown in Figure 46, posterior part of tape mould was enclosed and held in place until foam was fully cured. Once cured, moulded specimen was removed from tape mould and cut along medio-lateral plane and cadaver knee was separated from polymer outer shell. Finally as shown in Figure 47 anterior half of outer shell was cut along knee joint line to accommodate for knee flexion extension motion.

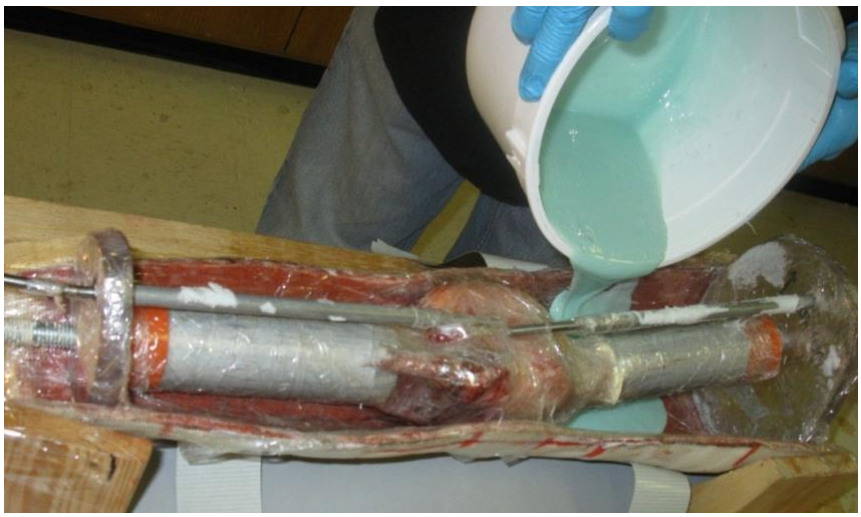

**Figure 46 Sunmate foam being poured into prepared specimen tape mould assembly**


**Figure 47 Hybrid surrogate specimen with foam casing encapsulating cadaver knee specimen**

## 5.6 In-vitro Simulation

Dynamic knee simulator was designed and capable of exerting forces up to 2670 lbf. with Tolomatic linear actuators (Tolomatic Inc. Hamel, MN) to replicate individual muscle forces and as explained in section 4.4.2, output voltage signal from individual load cell of muscle actuators were collected at 1000 HZ using National Instruments data acquisition system and LabVIEW software (National Instruments, Austin Texas). At commencement of the simulation, voltage output of individual load cell was compared with input array to ensure that the actuators were precisely following input muscle profile paths. Additionally PID parameters of individual actuators were adjusted to tune them such that output voltage data matched input array curves. To facilitate such a rudimentary task, a mechanical knee joint as shown in Figure 48 was manufactured and several trial runs were performed with this mechanical knee set-up while adjusting PID parameters of individual actuators. After the machine was tuned and homed to start positions of trial, the prepared cadaver specimen was flexed approximately to 25 degrees and a Differential Variable Reluctance Transducer (DVRT Microstrain Inc. Burlington, VT) was carefully inserted on to distal portion of the anteromedial bundle of ACL as explained by Cassidy et al (2013) and as shown in Figure 58. Then

this specimen instrumented with DVRT was positioned on Lachman tester as shown in Figure 13 in order to determine zero strain point or inflection point of ACL. Following this process, the specimen was located inside the polymer outer shell and wrapped securely using masking tape on the outside as shown in Figure 47. Finally the specimen was mounted on the Dynamic knee simulator using hip and ankle attachment hardware as shown in Figure 49. Subsequently two jump landing simulations trial runs were performed with the cadaver knee specimen and all load cell output data including ACL strain gauge data that was collected during testing was reviewed to ensure that the dynamic knee simulator accurately reproduced the input force array profiles.

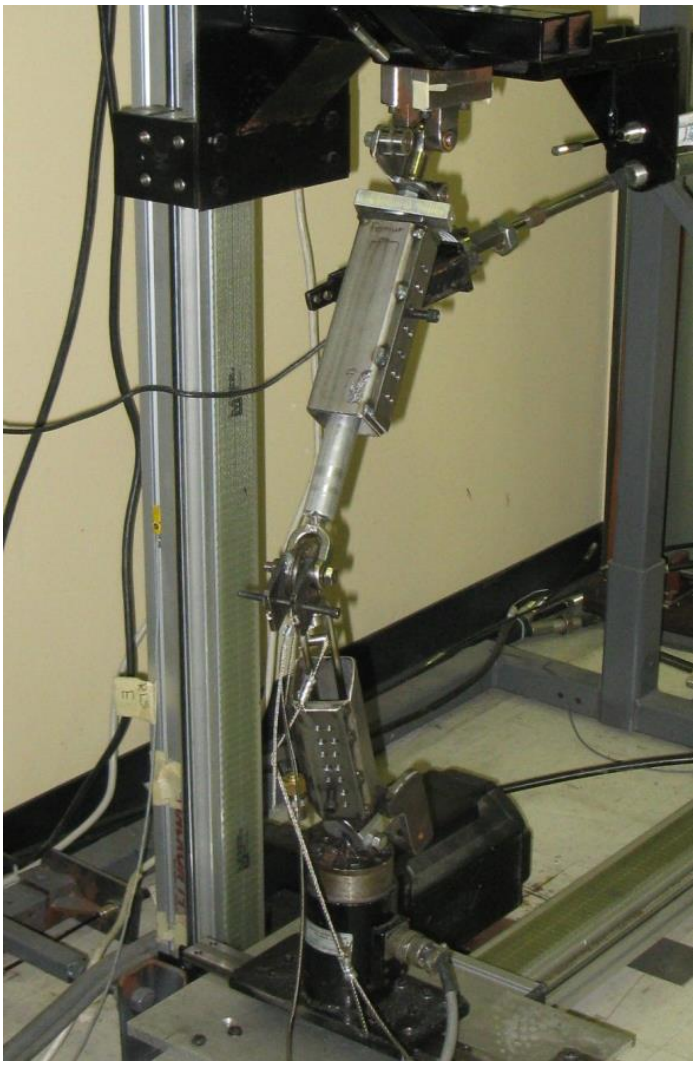

**Figure 48 Mechanical knee model mounted on knee simulator for tuning the equipment prior to actual simulation**

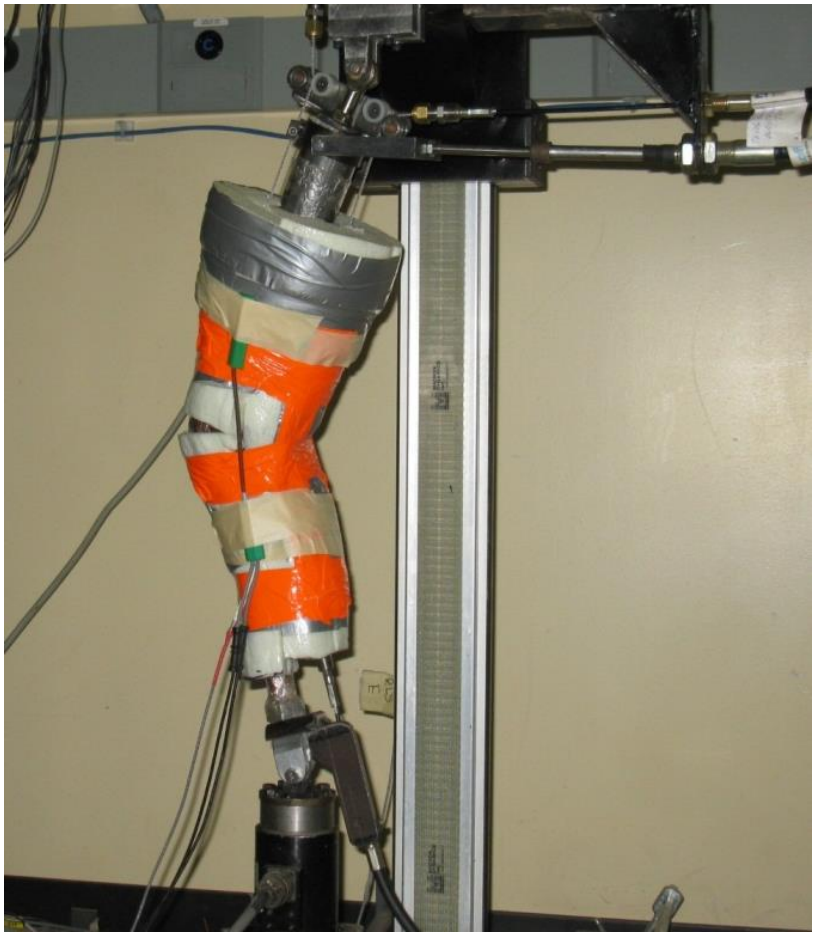

**Figure 49 Hybrid surrogate specimen mounted on dynamic knee simulator for testing**

## 5.7 Lessons Learnt

This section of the report highlights few important lessons that were conceived after the knee testing procedure was developed. Based on these refreshed understandings, the second phase of the research study was further refined by incorporating subtle changes to the testing procedure that was developed and the following litany of items elaborate those changes:

- During testing procedure development, motion capturing of jump landing task was completed with markers only on the thorax region and the right leg, and consequently during creation of biomechanical model, thorax region scaling was inaccurate. Hence, it during the second phase of testing decision was made to utilize markers on hands and acromion region of the shoulder to obtain better scaling of the biomechanical model.

- Ground reaction forces (GRF) are collected by force plates during motion capturing and the orientation of the force plate co-ordinate system dictates alignment and application of GRF forces in the biomechanical model. Additional to this, force plate scaling factor determined the magnitude and direction of application of the forces with respect to the force plate co-ordinate system. However both the force plate co-ordinate system and the scaling factor were manually edited after motion capturing and the scaling factor was entered as a positive value which reversed the application of forces in the biomechanical model. Consequentially this error further affected the muscle forces pattern as forces were directed away from the foot towards the center of the force plate. However, since the primary goal during first phase of study was only to develop a methodology and to validate the use of simulator to replicate a given active muscle force profile, variations in muscle patterns did not pose significant changes to the conclusions obtained from the study. Henceforth during the second phase of study, (case study of actually testing a knee brace) the scaling factor was input as (-0.007630) a negative value and thereby the forces were applied in the proper direction away from the center of the force plate on to the body of the individual, resulting in the biomechanical model producing appropriate muscle force pattern output. As explained in (Cassidy et al, 2013) the dynamic knee simulator replicated the input muscle profile very well and the standardized root mean square (SRMS) error of the output force profile in comparison to the input muscle profile was within 12%. Hence this methodology and equipment was deemed feasible approach to conduct the second phase of the study (case study on a custom fit knee brace).

# Chapter 6
# Phase 2 Prophylactic Knee Brace Case Study

## 6.1 Introduction

This chapter of thesis presents a comprehensive discussion of techniques adopted on the basis of methodology developed (as explained in Chapter 5) in order to evaluate effectiveness of a custom manufactured braced (CTI custom brace manufactured by Össur Inc.)

## 6.2 Selection of high risk subject

Primarily goal of this research was to determine effectiveness of knee brace in reducing ACL strain occurring during dynamic activities such as single leg jump landing. Hence, it was imperative to conduct analysis upon activity performed by an athlete, who was deemed to possess higher potential for injury due to unique landing characteristics (Onate et al, 2005). As a preliminary step, after University ethics committee reviewed and accepted the proposed motion capture activity, ten amateur athletes were recruited based on criterion that "they were to be actively involved in at least one college level sport activity" and the strategy included selecting a potentially high risk athlete among this pool of ten volunteers.

### 6.2.1 Motion capturing

As strategized earlier while setting scope of the study, (as discussed in section 1.2) motion capture was completed on ten amateur athletes performing single leg jump landing activity by stepping off a 45 cm platform on to a force plate as shown in Figure 50. Kinematic analysis was be completed on the motion captured data by Micah Nicholls of Össur Inc. and a high risk subject was selected by comparing various parameters such as ground reaction force during landing, trunk flexion angle, knee abduction angle of all subjects during jump landing activity. These ACL risk identification factors were identified and analyzed based on published literature (Boden et al., 2009; Blackburn and Padua, 2009; and Hewett et al., 2005). Analysis concluded that high risk athlete was a female ice hockey player, weighing 52 Kg and 5 feet 2 inches tall. This individual was measured and a CTI custom fit brace was manufactured by Össur Inc.

In continuation, subject was instrumented with infrared markers as listed in Table 1of section 5.1 and in addition two separate sets of cluster markers that were added to both upper and lower arms

of subject as shown in Figure 51. Additionally motion capturing was conducted as explained in section 5.2 but during this phase of testing RA and LA bony landmarks were digitized with reference to these upper arm cluster markers not the trunk cluster markers as explained in section 5.2. This change was incorporated to ensure that the digitized landmarks belonged to corresponding rigid body segments. In addition during this phase of study, motion capturing was conducted with Optotrak motion capturing system (NDI, Waterloo, ON) and the marker data was collected at 100Hz while the force plate data was collected at 3000 Hz. The subject performed a total of ten "single leg jump landing" by stepping off a 45 cm platform. This included the first five sets that were performed wearing the custom fit knee brace as shown in Figure 50 and subsequent sets without a brace. In addition, the participant was allowed to perform few practice jump landings to ensure that she could adapt to new braced condition. During motion capture of jump landing activity while wearing knee brace, six markers were added on to knee brace as shown in Figure 51.

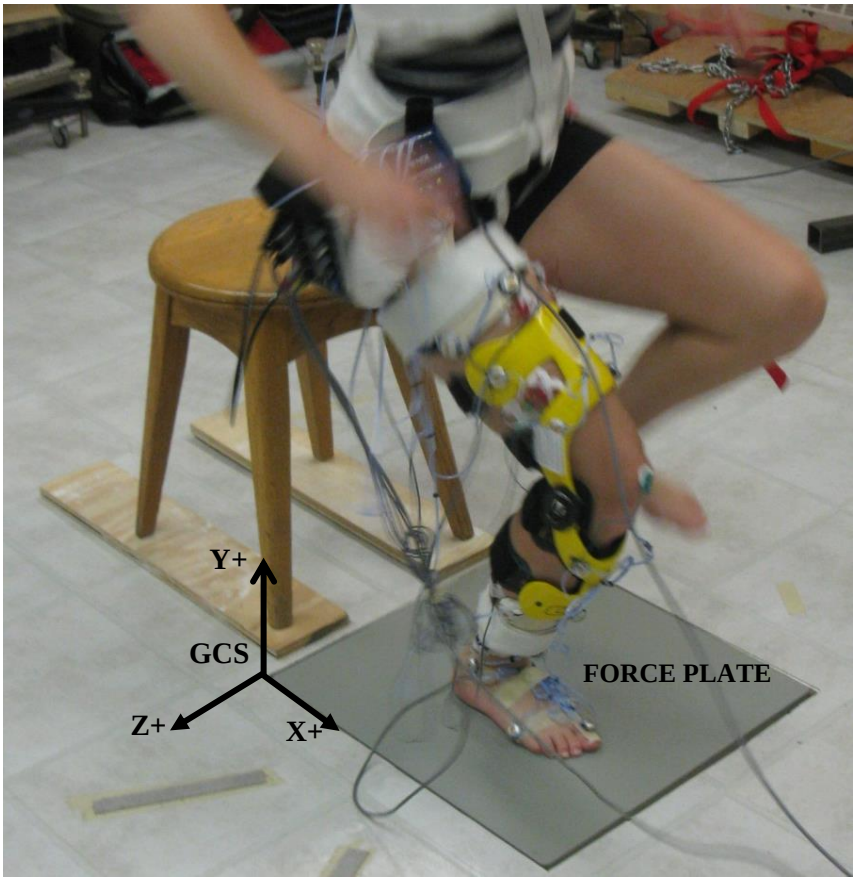


**Figure 50 Orientation of GCS in reference to the force plate and the motion capture set up that was utilized for second phase of research study (brace effectiveness study)**

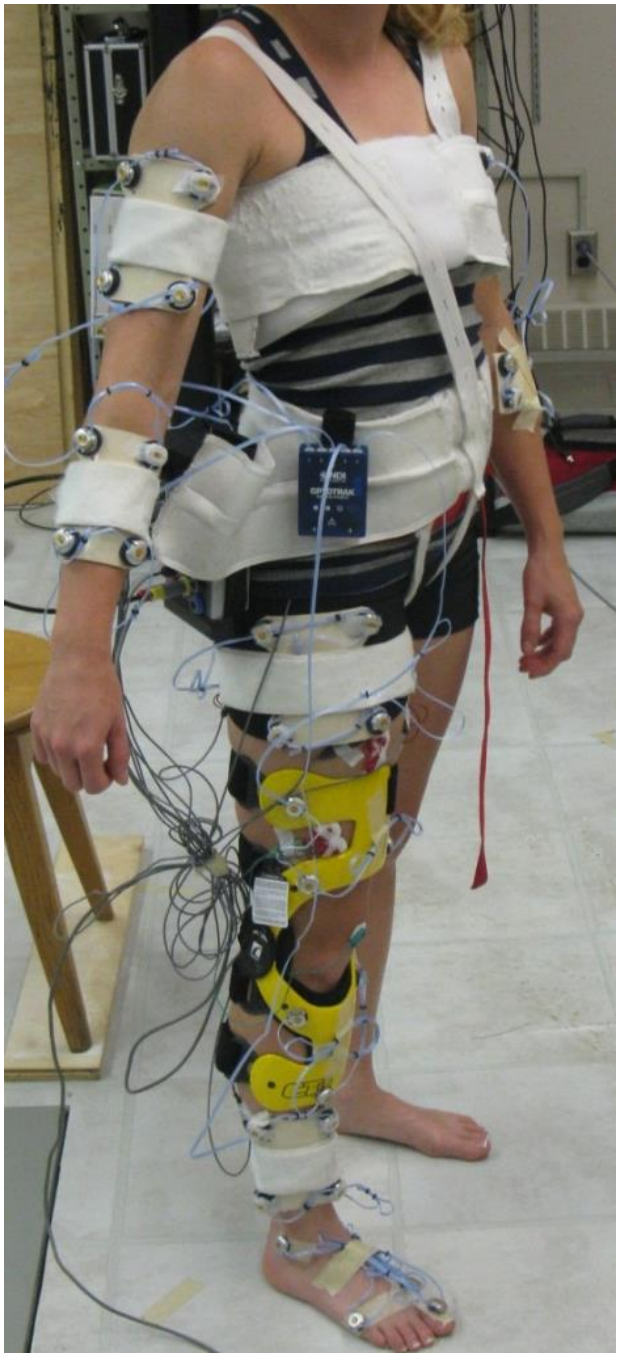

**Figure 51 Motion capture subject instrumented with clustered markers on relevant individual body segments**

## 6.3 Bio Mechanical Modeling

### 6.3.1 Anybody® Modeling

Biomechanical model utilized for first phase of study was further modified to suit high risk subject anthropometric characteristics in order to extract muscle forces, however based on lesson learnt during first phase of research, several changes were incorporated. As a priory, since the high risk subject was deemed to be $15^{th}$ percentile woman (Chaffin et al 2006), codes were modified to include scaling laws pertaining to body parametric of the subject and optimization of trunk height with reference to shoulder markers was enabled. Furthermore, arm segments were included in the biomechanical model and RA & LA markers (Right and Left Acromion respectively) were scaled in reference to scapula co-ordinate system of the model. This was necessary to obtain appropriate scaling of trunk segment and modified codes reflecting these changes are added in Appendix 1 Section 6.

In Anybody® biomechanical software, individual body segments are driven by marker data and during this phase of study, trunk and lower extremities were driven by relevant markers. However as arms, head and neck body segments were not driven by motion captured marker data, additional drivers were added to the main program file and modified driver codes are added in Appendix 1 Section 7. Subsequently, marker locations were adjusted to scale the biomechanical model and the number of iterations of kinematic solver was increased to obtain output data at 2 millisecond interval and the peak magnitude of GRF data output from the software accurately represented the input C3D data. Once inverse dynamics was completed, muscle forces were extracted and moment arms of the cadaver knee specimen was obtained Section 5.4.3. In continuation, muscle force data were converted into relevant knee joint moments and subsequently into grouped cable force while joint position data was calculated at 10 milliseconds as detailed in section 5.4.5.

Finally since the obtained muscle force data and joint position data were output at different frequencies, it was necessary to obtain final cable force data and actuator positions matched at 10 milliseconds and this accomplished in following stages:

- Anybody® output muscle force data had displayed physiologically unrealistic peaks and muscle force variance hence data was filtered using a special function that attained a true optimum cut-off frequency in dual stages, solely based on the frequency of the obtained output as explained by Yu B et al (1999).

- Finally to maintain consistency, both marker data and muscle force data were input into a special interpolating function in Matlab such that the final output was obtained at every $10^{th}$ millisecond interval.

Finally, as explained in Section 5.4.4 all grouped muscle cable force data and joint position data were converted into encoder counts and input into array files for simulation.

## 6.4 Preparation of Test Specimen

Preliminary plans for the second phase of research study (knee brace testing phase) included utilizing test specimen that was prepared during first phase of study (procedure development phase) as explained in section 5.5. Hence, the negative mould that was prepared as detailed in subsection 5.5.1 was utilized to create a custom brace by CTI. However due to high muscle forces observed during high risk athletes jump landing, patella of test specimen fractured during a subsequent testing phase. This was probably due to development of stress concentrations around holes that were drilled to insert muscle actuator cables and or due to deficiencies in bone matter of test specimen. Therefore, in goal of establishing a fail proof methodology for inserting quadriceps muscle actuator cables into patellar tissue of the cadaver specimen, several techniques were developed and tested.

As an initial effort, few wood screws were drilled to rebind fractured portions of the patellar tissue however since the experiment failed, further trial was conducted by looping the muscle attachment cable around patellar tendon and grasping it beneath the patella bone tissue (near the tibial attachment site). Nevertheless, this technique tore the patellar tendon from tibia hence as a successive effort, a polymer mould was prepared to match the patella geometry and an artificial patellar was created by pouring a two part plastic resin (R1 Fast Cast #891, Golden West MFG, Inc. California, USA) into the polymer mould. This artificial patella was subsequently attached on to specimen and tests were performed unsuccessfully. In continuation since these preliminary techniques were unsuccessful, a custom metal bracket was manufactured and attached to the tibia such that cable could attach to the metal bracket and pull on the tibia while quadriceps muscle actuator exerted force. On the other hand the bracket was bulky and not efficient to sustain loads without migrating on the tibial slope, this methodology was deemed unsuccessful. Hence an additional cadaver knee specimen that was harvested from a 23 year old male, 183 cm tall and weighing 96 Kg was procured to create the new test specimen.

The newly obtained cadaver knee specimen was processed to create the negative tape mould, locator elements as explained in subsections 5.5.1, and custom brace was manufactured to match the external shape and features of the cadaver knee. Additionally, the cadaver knee dissected and prepared as described in subsection 5.5.2. As a continuation, in order to find an alternative method of attaching quadriceps muscle cable to cadaver knee, a custom metal brace was manufactured and attached to tibia as shown in Figure 52 and quadriceps muscle attachment cable was inserted into bracket and bracket was attached firmly on to tibia using polymer casting tape as shown in Figure 53. In addition, a 1/8" thick sheet metal shim was fixed on top surface of patellar as shown in Figure 53 while muscle attachment cable was clamped over metal surface as shown in Figure 53 using two additional metal shims.

**Figure 52 Custom metal bracket that was fabricated and positioned on tibia for attaching the quadriceps muscle actuator cable on knee**

As this method was also futile, alternative method was adopted which included two metal shims that were placed on both superior and inferior faces (either sides) of patellar tissue as shown in Figure 54 and Figure 55 and two holes drilled through the metal and patellar tissue assembly as shown in Figure 54. The muscle attachment cable 3/32" stainless steel cable was looped through the drilled holes and crimped. These attached sheet metal shims prevented cable from creating stress concentration in the bone tissue and in addition this cable attachment set-up was tested successfully.

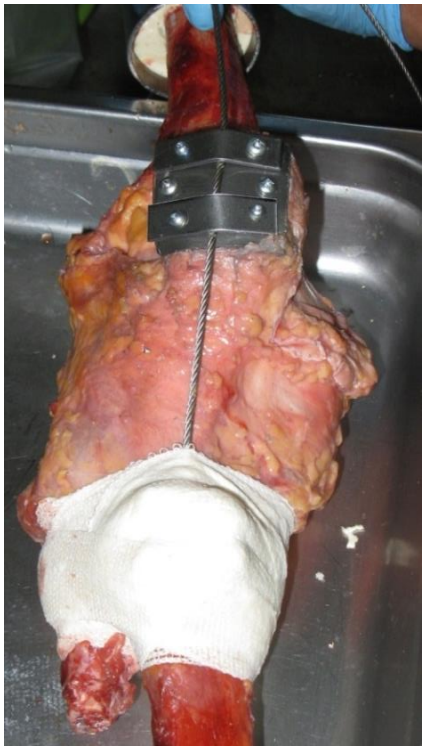

**Figure 53 Quadriceps muscle actuator cable attached to tibia with custom metal bracket and cable held on superior portion of patella using metal shims**

The hamstring muscle actuator cable was attached on to tibia through two 1/8" diameter holes drilled at muscle insertion site on posterior portion of tibia as shown in Figure 57. Holes were drilled at an angle such way that they remained close to being parallel to femur axis as indicated in Figure 56. As indicated in Figure 57 additional layers of casting tape were wrapped around bone for reinforcement and metal shims were placed on anterior portion of tibia beneath cable to avoid creating stress concentrations on the bone due to applied muscle forces and finally the cable was crimped posterior to knee capsule. In continuation, as explained in subsection 5.5.3 the polymer outer shell was moulded over the cadaver knee specimen to assist mounting of a custom knee brace that was manufactured for the cadaver knee. In addition, 1/8" holes were drilled in femur at the Gastrocnemius muscle insertion point and the muscle attachment cable was looped around the bone and crimped as shown in Figure 57. Finally, the cadaver knee specimen was instrumented with DVRT to measure ACL strain as explained in Section 5.6 and shown in Figure 58 and mounted on Lachman tester to determine inflection point. However, it was not possible to determine inflection point for reasons explained in Section 4.2.4, a different approach of calculating ACL strain as relative value to

preset distance of the strain gauge when mounted on ACL. This technique of finding ACL strain as a relative strain has been validated used by Beynnon et al (1992). Finally the instrumented hybrid surrogate cadaver knee specimen was mounted on dynamic knee simulator for testing the custom knee brace.

**Figure 54 Quadriceps muscle actuator cable attached to patella with reinforced metal shims to avoid stress concentration (new technique of attaching quadriceps cable to patella)**

**Figure 55 Metal shims layered on both inferior articulation portion and superior portion of patella to avoid stress concentration around holes drilled in patella and muscle actuator cable inserted through the holes drilled in patella**

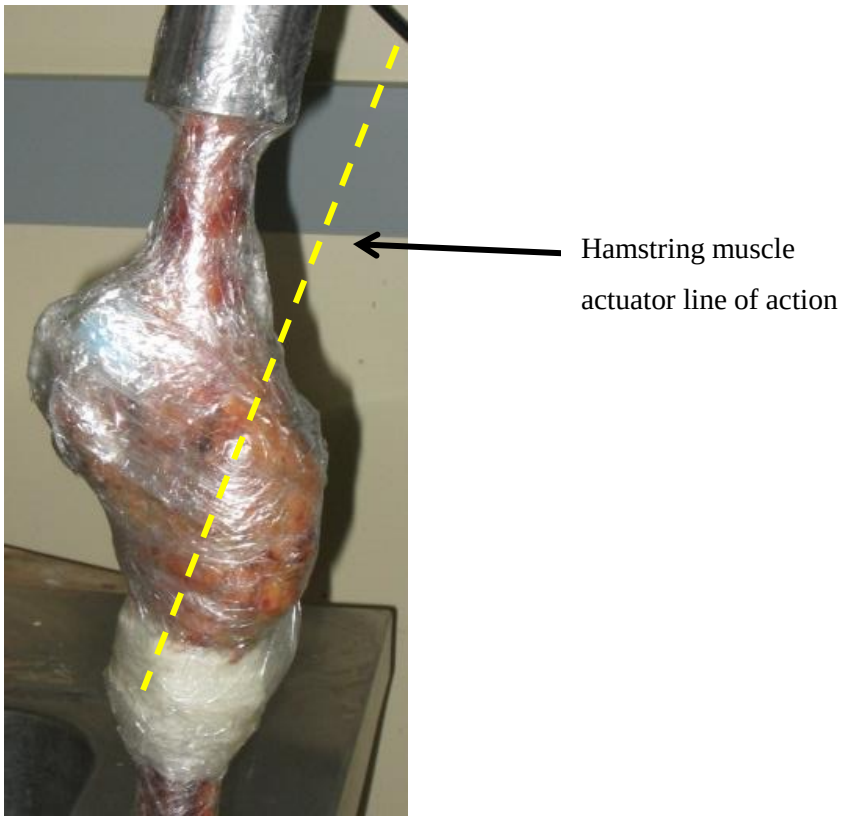


**Figure 56 Hamstring muscle attachment site and resulting hamstring muscle actuator line of action that was retained parallel to axis of femur**

**Figure 57 Hamstring and gastrocnemius muscle attachment sites on cadaver knee specimen**

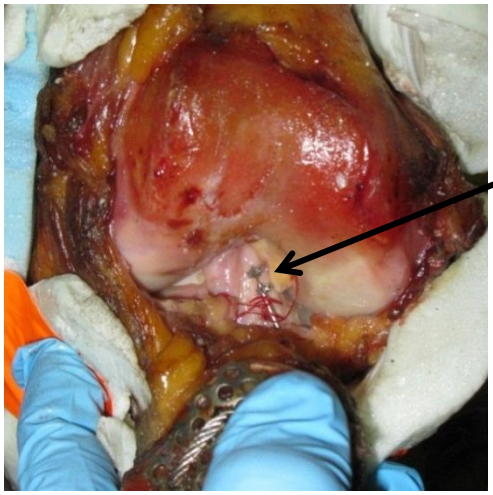


**Figure 58 DVRT mounted on anteromedial band of ACL**

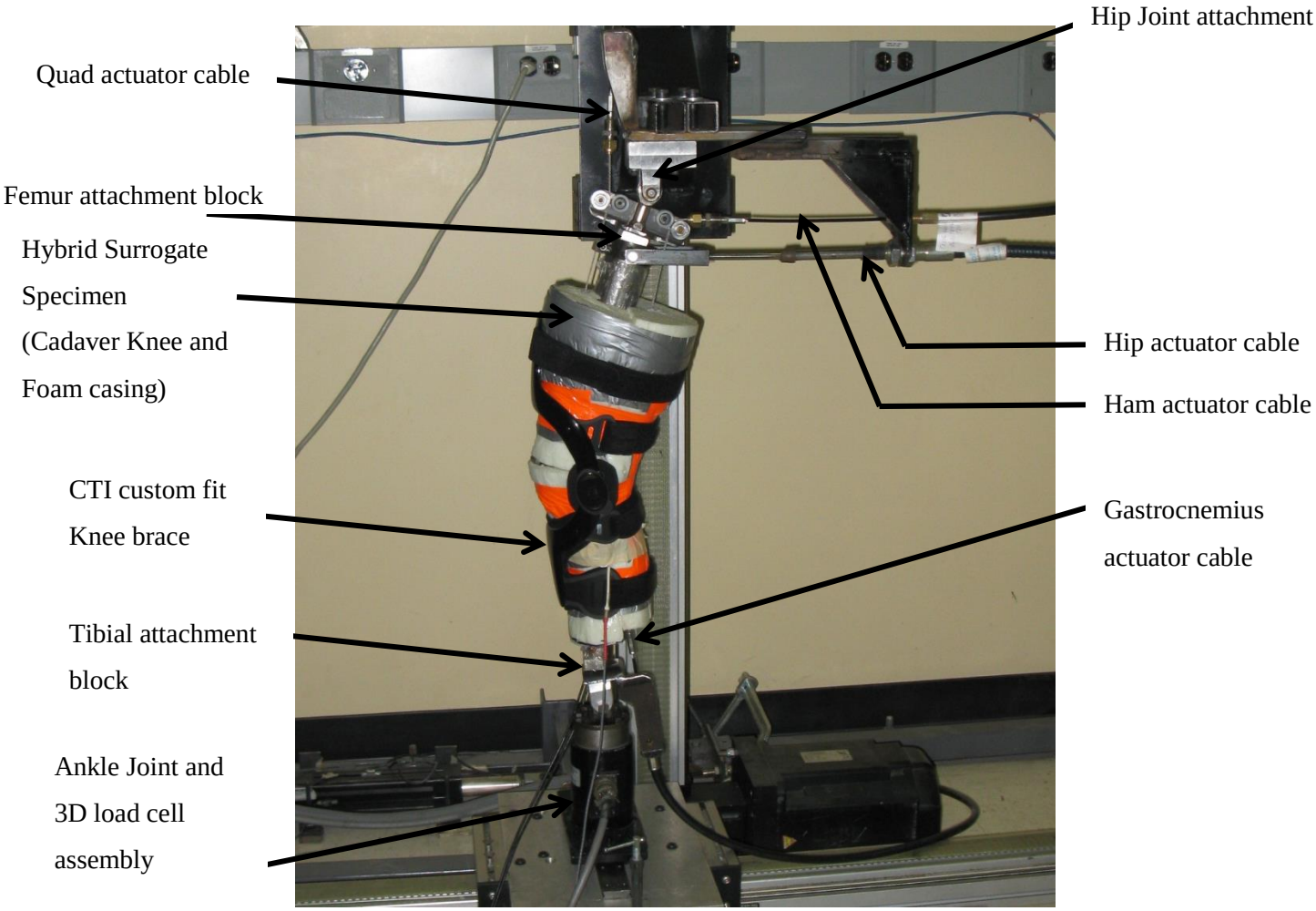


**Figure 59 Surrogate cadaver specimen on dynamic knee simulator with Brace during testing**

## 6.5 In-vitro Simulation

Freshly prepared cadaver specimen, instrumented with DVRT was encapsulated with the (external cast) foam outer shell and wrapped with duct tape as shown in Figure 49. As a priory, the dynamic knee simulator was tuned while adjusting the PID parameters of all relevant actuators to ensure that the simulator could replicate the newly acquired muscle force profiles as explained in Section 5.6, additionally the simulator was homed such that hip and ankle actuators aligned to the trial specific start positions and special custom attachment blocks were mounted on distal ends of the cadaver knee specimen and subsequently mounted on to the knee simulator as shown in Figure 59. Finally all dynamic knee simulator operation sequences were executed and as primarily strategized, four different scenarios of jump landing trials were conducted in listed sequence in five repetitions:

- Jump landing trial without brace on cadaver knee specimen, simulated with muscle force profile of athlete wearing brace.
- Without brace on cadaver knee specimen, with muscle force profile of athlete without brace.
- Simulation with knee brace mounted on cadaver knee specimen, simulated with muscle force profile of athlete without brace.
- With knee brace mounted on cadaver knee specimen, while simulating muscle force profile of athlete wearing brace.

# Chapter 7
# Results

## 7.1 Introduction

Comprehensive analyses of the data collected during different phases of the research are presented in the section. Although this thesis is presented as two separate stages of research study, the results acquired during the case study of evaluating the custom fit prophylactic brace are presented in this chapter under separate subsections.

## 7.2 Phase 2 Prophylactic Knee Brace Case Study

### 7.2.1 In-vitro Simulation inputs compared to Knee Simulator Outputs

During the first phase of the study, investigation was completed by comparing the input and output variables of the Dynamic Knee Simulator and it were observed that the Knee Simulator was capable of replicating the input dynamic profile closely and ACL strain values measured during the jump landing simulation were similar to findings /predictions of researchers in the past (Cassidy et al, 2013). Hence this novel approach was considered an appropriate technique to evaluate the prophylactic brace effectiveness in preventing ACL strain. Subsequently prior to initiation of the case study (phase 2 of the research), actuators were tuned such that they closely matched input muscle profiles as explained in Section 5.6.

### 7.2.2 Muscle forces calculated by Anybody® Biomechanical modelling software

Observing the muscle profiles derived through inverse dynamics using Anybody® biomechanical software following variances in the muscle force profile can be noted.

- Quadriceps muscle begins to activate at the time of initial ground-foot contact (IC) and peaks to gradual to a peak force of 4650 N from 50 milliseconds to 175 milliseconds after IC in the unbraced landing muscle profile. On the contrary during braced landing, quadriceps muscle force increases to close to 2500 N between 20 milliseconds to 60 milliseconds after IC and gradually increasing from there on to peak at 3930 N by the end of the trial (at 200 milliseconds after IC)
- Hamstring muscles indicated a steady rise in activation from IC and peak to 3500 N at point of peak GRF (within 25 milliseconds) in unbraced landing muscle profile. On the

other hand observing the braced landing, hamstring muscle activation begins at IC but creates dual peak force dropping partially at 26 milliseconds interval and rises to peak force of 1930 N at the point of peak GRF. The total Hamstring activation time to peak is about 43 milliseconds after IC.

- Gastrocnemius (Calf) muscle profile appears to be consistently rising from point of IC to a peak of 460 N during unbraced landing while peaking to a force of 390 N during braced landing.
- Hip moments calculated by Anybody® software was converted into cable forces as explained in Section 5.4.4. However, considering that hip moments act a major role in ACL loading and noncontact injury mechanism (Hashemi et al, 2007) net hip moments are displayed followed with a comprehensive discussion in Chapter 8. Observing net hip extensor moments, Figure 60 the peak value of unbraced landing scenario is about 317 Nm while during braced landing Figure 61, it peaks to 254 Nm. The interesting portion is delayed rise of net hip extensor moment in case of braced landing, where the net moments possess a double peak path similar to that observed in hamstring muscles and peaking in both cases at the time point of peak GRF. During unbraced trial the time to peak net hip extensor moments is about 26 milliseconds whereas during braced landing, the time to the final peak value is about 43 milliseconds.
- Looking at the ground reaction force (GRF), it is evident that during unbraced landing the peak GRF is about 2700 N while in case of braced landing condition the peak GRF is 2400 N. The important aspect observed is the time to peak GRF, which in the case of braced landing seems to be delayed and occurring at 43 milliseconds after IC contrary to the case of unbraced landing where the time to peak GRF is about 26 milliseconds.

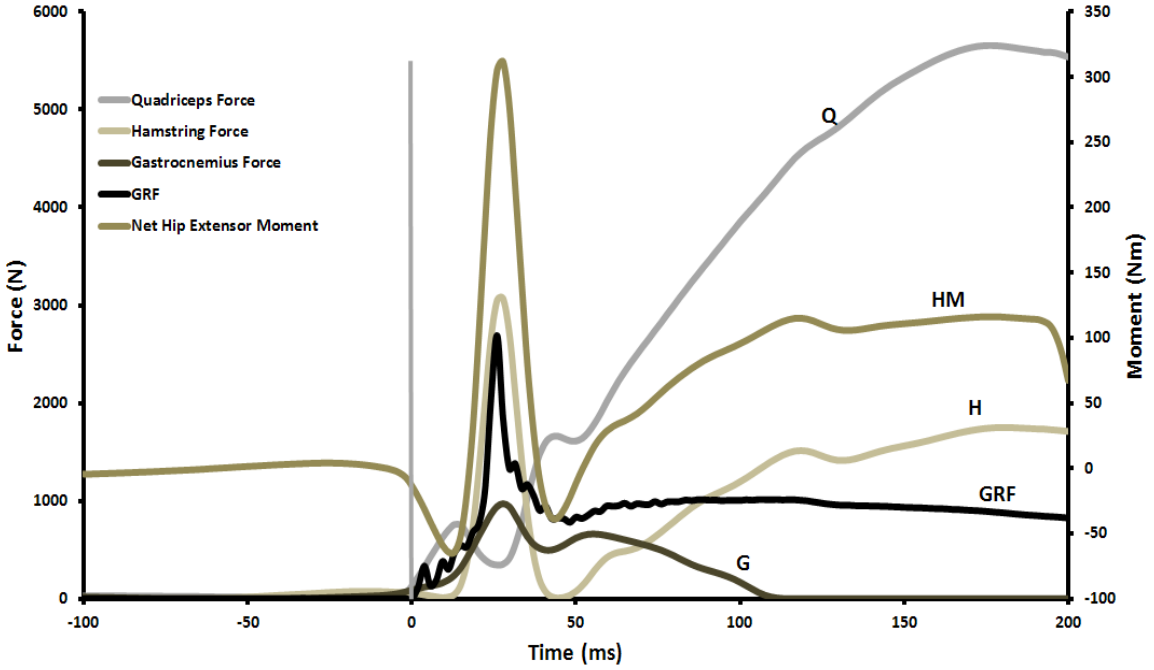


**Figure 60 Muscle force profile output obtained through Anybody® software for Unbraced single leg landing activity (here 0 along "time" axis indicates point of initial foot contact)**

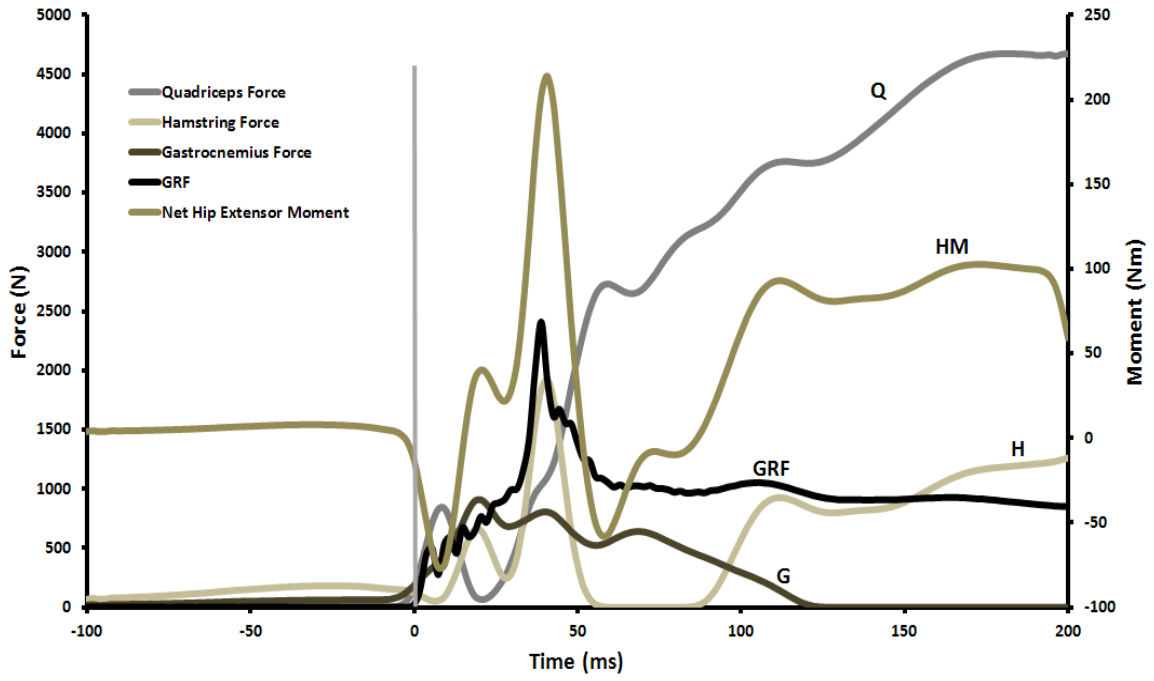


**Figure 61 Muscle profile output obtained through Anybody® software for Braced jump landing activity (here 0 along "time" axis indicates point of initial foot contact)**

- ACL strain data collected during in-vitro simulation are displayed in the Figure 63. In this graph, condition a – d are referring to simulations with muscle forces obtained from braced and unbraced landing motion captures respectively as listed in Table 3. DVRT voltage data was collected using LabVIEW data acquisition software system (National Instruments Lab VIEW, Austin TX, USA.) at 1000 Hz. However, since the inflection point was not found during Lachman testing for this cadaver specimen as explained in Section 4.2.4, it was necessary to adopt a different technique of calculating ACL strain in reference to strain in ACL during insertion of strain gauge (at 25˚ flexion angle). This methodology was validated and used by Beynnon et al (1992) hence DVRT prongs were set at 5 mm distance while inserting on ACL and actual ACL strain was calculated utilizing this preset 5 mm as reference strain value of the ACL. The voltage data collected during trial was converted into strain value and subsequently normalized for each individual trial. Finally average value of five repetitions of each distinct trial was plotted to obtain the graph in Figure 62. Tabulated below in Table 3 are the peak ACL strain values for all trials a – d, (as shown in Figure 62) this reveals that peak ACL strains of close to 20% were observed during simulating unbraced landing conditions and 8% during braced landing simulations. This further signifies that ACL strain reduced significantly by about 11% due to the application of brace by changing the muscle firing pattern and further discussion on this finding along with other results conceived during experiment are presented in Chapter 8.

**Table 3 Average ACL strain values observed during simulation of four distinct scenarios**

| **Condition** | **ACL strain Mean ± SD** |
|---|---|
| (a) Un-braced specimen with braced muscle firing pattern/kinematics | 0.076±0.02 |
| (b) braced specimen with braced muscle firing pattern/kinematics | 0.080±0.03 |
| (c) braced specimen with un-braced muscle firing pattern/kinematics | 0.2±0.015 |
| (d) un-braced specimen with un-braced muscle firing pattern/kinematics | 0.18±0.04 |

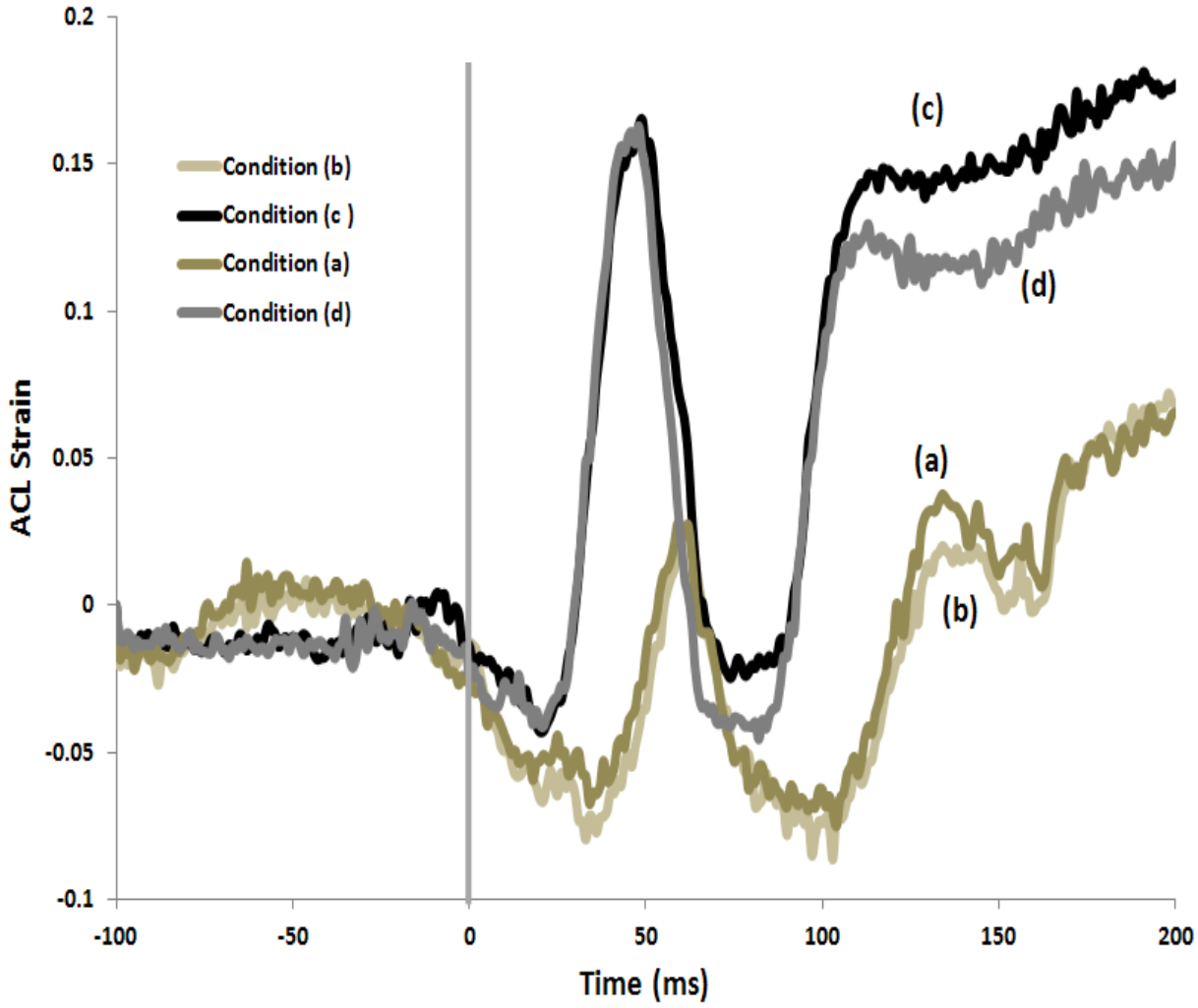


**Figure 62 Average ACL strain values plotted against time, conditions a – b refer to unbraced and braced simulation using braced jump landing muscle profile, while conditions c – d refer to braced and unbraced simulation using unbraced jump landing muscle profile. (Here 0 along "time" axis indicates point of initial foot contact)**

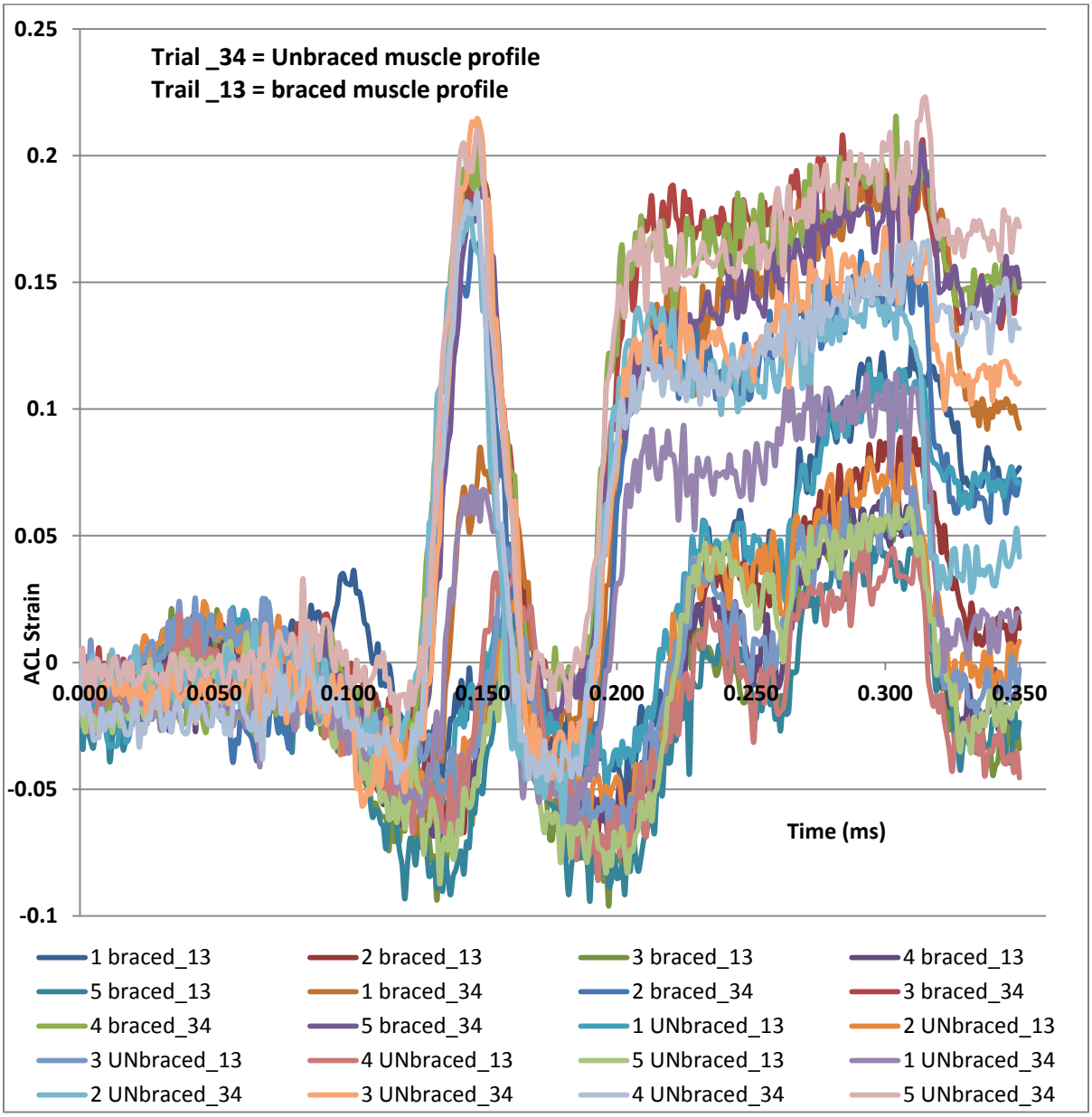


**Figure 63 Raw ACL strain values obtained for four different braced and unbraced condition in five repetitions, as listed in Table 3**

### 7.2.3 Kinematics Analysis

Observing sagittal plane kinematic data acquired during motion capturing, it indicates that knee was flexed to about 18˚ during unbraced landing condition while it was close to 7˚ during unbraced landing at the point of initial ground contact (IC as shown in Figure 64). Similarly as shown in Figure 65, hip was flexed to higher degree in unbraced landing condition contrary to braced landing condition where the hip was more extended and in addition at the time of landing, hip and knee experience greater range of motion during braced condition. Looking at the frontal plane kinematics in Figure 66, it is evident that the knee abduction angle was greater during unbraced landing condition when compared to the braced landing condition. This frontal plane kinematics difference could have attributed to higher ACL strains however under current testing set-up and it is difficult to establish this speculation as the knee simulator was developed only to observe sagittal plane biomechanics.

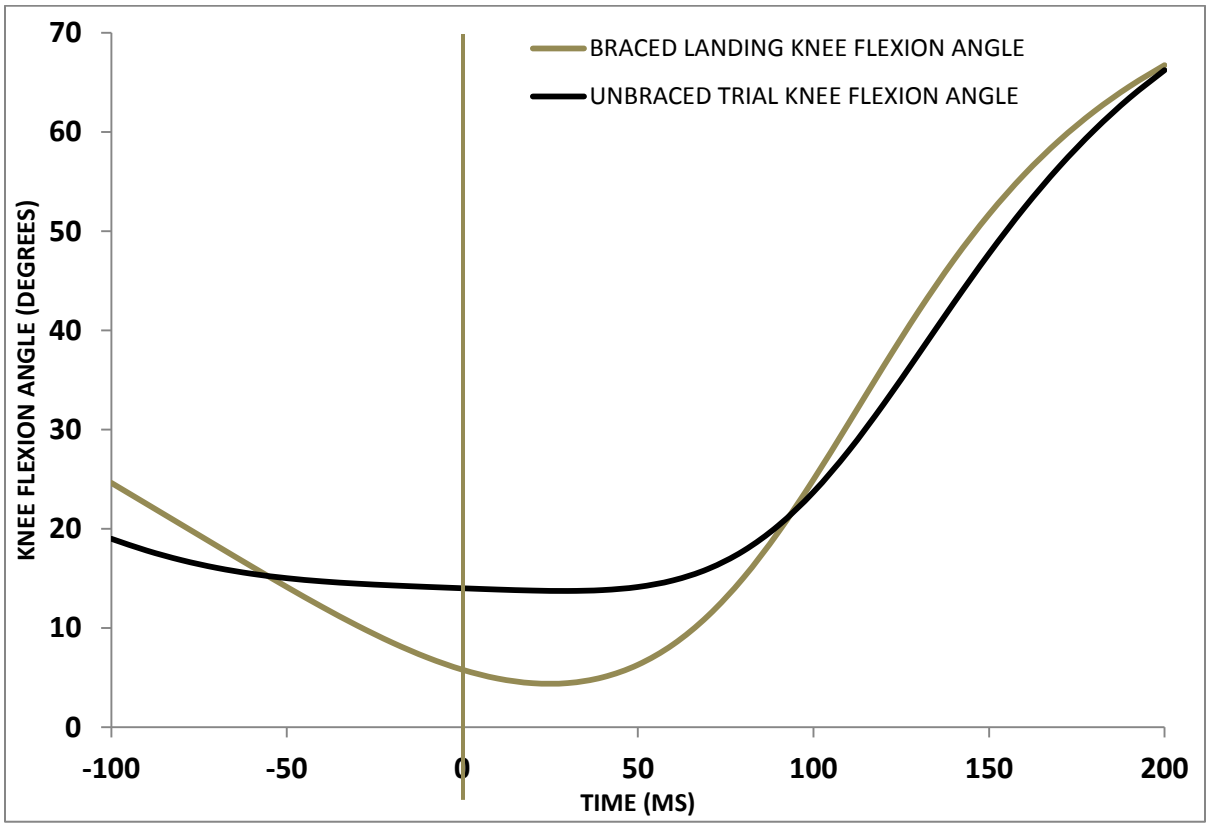


**Figure 64 Knee flexion angle variation during jump landing as observed during motion capture for both braced and unbraced landing condition. (Here 0 along "time" axis indicates point of initial foot contact)**

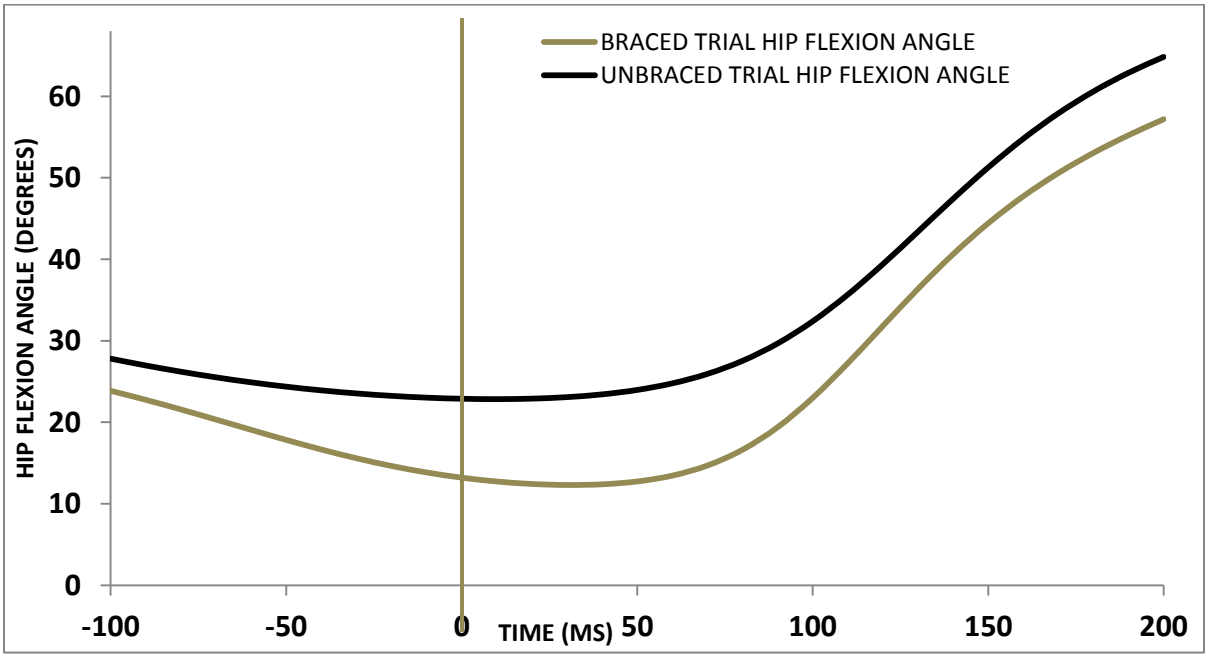


**Figure 65 Hip flexion angle variations observed during motion capture for both braced and unbraced landing condition. (Here 0 on "time" axis indicates point of initial foot contact)**

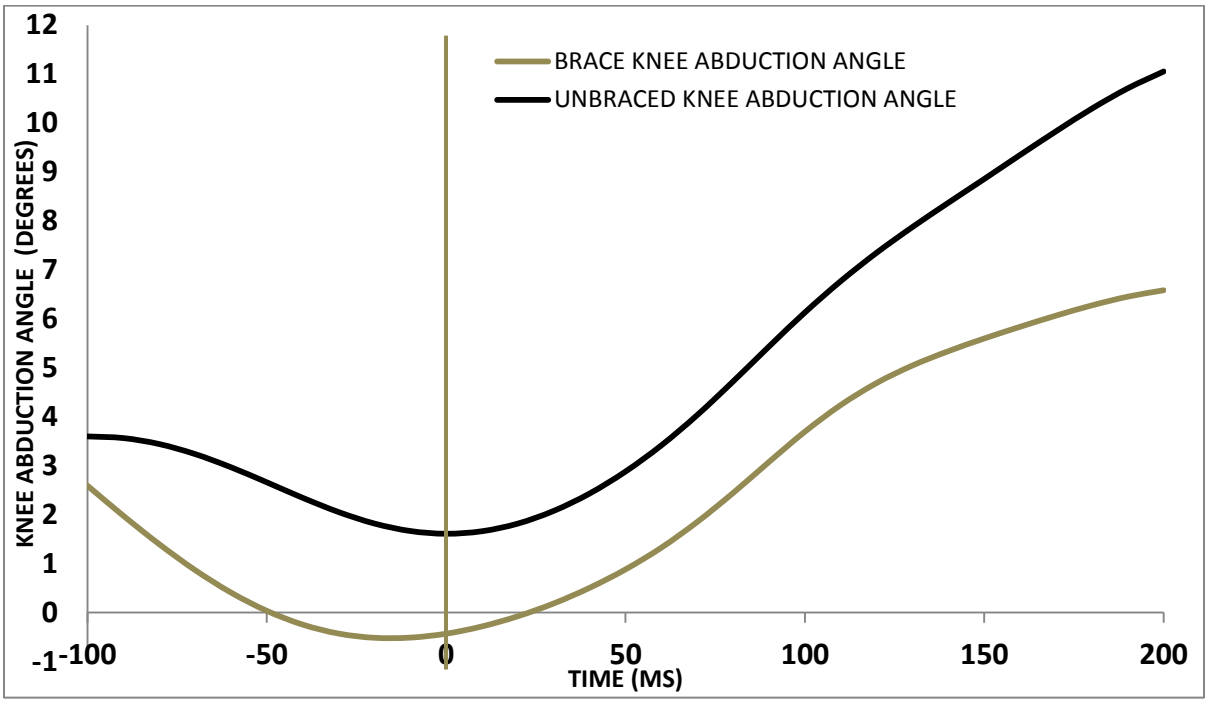


**Figure 66 Knee abduction angle variations observed during motion capture for both landing conditions. (Here 0 on "time" axis indicates point of initial foot contact)**

# Chapter 8
# Discussions

Researchers in the past have adopted several in vivo and in vitro techniques, both in static and quasi-static conditions (Beynnon et al, 1993, Fleming et al, 2000) to resolve mystery surrounding effectiveness of braces but to date no such study exists that resolves this issue in a dynamic scenario (Rishiraj et al, 2009). This consequently created impetus for the current research study that involved a novel idea of combining in vivo and in vitro techniques to identify bracing effects during a dynamic scenario. Furthermore, research indicated that about 72% of ACL injuries occurred due to non-contact mechanism (Boden et al, Krosshaug et al 2007) and generally occurring while performing high risk activity similar to those experienced by athletes in basketball such as landing from a jump (Mihata et al, 2006). Research studies conducted simulating one leg jump landing to understand landing techniques and its significance to ACL injuries have analyzed participants landing from heights between 0.3 to 0.6 m. Furthermore, higher ground reaction forces (GRF) of up to four times the individuals body weight was observed during 0.45 m single leg drop landing (Yeow et al, 2009). Hence, during the second phase of study (during brace effectiveness study) the jump landing activity was conceived such that participant would drop off a 45 cm high platform and perform a single leg landing on to a force platform while maintaining his/her balance. Additionally this technique of landing activity was adopted to maintain consistencies with the study that was used to determine athlete with potential of high risk for ACL injury.

The primary goal of this study was to identify the true effect of brace in preventing ligament injury, which implied that study was to be conducted on activity that was performed by an individual susceptible to ACL injury or has higher potential of injuring the ACL due to abnormal landing patterns (Onate et al, 2005). Consequently a female subject was selected among 10 amateur athletes performing the chosen high risk activity while comparing kinematic and kinetic data acquired during high speed motion capturing as explained in Section 6.2. Osternig et al, (1993) indicated neuromuscular control was altered due to application of prophylactic brace, followed by alteration in kinematics, kinetics behavior of individuals and it was imperative to capture those changes occurring during jump landing activity. Hence it was predetermined that the athlete would perform single leg jump landing activity both under both braced and unbraced conditions.

Muscle forces occupy an important role during dynamic activities and several researchers have attributed to occurrence of ACL injuries to forces exerted by different agonistic and antagonistic muscle groups and torques exerted by hip flexion extension muscles on knee (Cassidy et al, 2013, Hashemi et al, 2007, Li et al, 1999, Taylor et al, 2011). Hence inverse dynamic analysis was performed on the (high risk activity) motion captured data utilizing Anybody® biomechanical modelling software (Anybody® Technologies Inc. Aalborg, Denmark) with an optimization algorithm as explained by Damsgaard et al (2006), (Cassidy et al, 2013), in order to resolve the muscle recruitment issue and obtain muscle firing pattern unique to the input kinematic data. Finally these muscle force data were input into a Dynamic Knee simulator to simulate the jump landing activity on a cadaver knee both in braced and unbraced conditions to examine the ACL strain patterns. Research studies indicate that ACL injuries occurred between 17-50 milliseconds after the initial ground contact (Krosshaug et al, 2007). Hence entire simulation process was focused only on 300 milliseconds out of the complete jump landing activity, which included 100 milliseconds prior to the moment when the participant's feet touched the force plate during landing (start of ground reaction force in the C3D data) till 200 milliseconds thereafter.

Taylor et al (2011) used a novel technique of combining motion capturing with fluoroscopy and magnetic resonance imaging techniques to measure ACL strain during jump landing however, this technique has limitations due to the field of view and moreover, this technique derives an estimate of ACL strain using valid solid models but not the measurement taken directly from ligament. Researchers in past have measured ACL strain directly by implanting strain gauges on ligaments of live human beings (in vivo techniques adopted by Beynnon et al (1993), Fleming et al (2000) however such invasive techniques are risky and pose ethical concerns. Cadaver knee specimens have been used in past by researchers and validated to study ACL loading and to understand injury mechanism (Hashemi et al, 2007, Withrow et al, 2006, Cassidy et al, 2013, Erickson et al, 1993). In these in-vitro studies, ACL on cadaver knee was instrumented with a strain gauge to obtain measurement and this is a close approximation to acquiring strain measurements on a live individual.

In the case study presented here (in this thesis), a hybrid surrogate cadaver model was utilized to complete the in vitro investigation. As devised by Erickson et al (1993), the surrogate model included a foam shell encompassing the cadaver knee which formed an interface for mounting brace during simulation and analysis. In order to maintain consistency and to employ a custom fit brace for

the cadaver knee, the surrogate foam shell was molded and modeled to suit shape and size of the cadaver knee prior to dissection as explained in Section 5.5. By adopting this technique, it was also possible to obtain the hybrid cadaver knee specimen with outer foam shell as hard as a stiffened muscle with the femur and tibia precisely oriented into same anatomical locations of the un-dissected cadaver knee specimen. In addition, muscle cables that were linked to muscle actuators cables of knee simulator were positioned inside that surrogate foam shell such that hybrid surrogate cadaver knee model closely represented flexion extension attributes exerted by a human limb during dynamic activity simulation.

Observing the motion captured and biomechanical output data as explained in Section 7.2, Figure 60 and Figure 61, it is evident that during braced condition the time to peak GRF (ground reaction force) increased from 26 milliseconds to 43 milliseconds indicating attenuating effects of the prophylactic brace. In addition, the GRF during braced landing dropped to 2400 N from 2700 N as observed in unbraced condition, which is about 5 times body weight of the subject. And a study completed by Yeow et al (2009) studying single leg jump landing indicates peak GRF to about 4 times body weight while landing from 0.45 M and the results of current case study indicate an increase by one magnitude which can be due to landing attributes of selected high risk athlete. In addition during the braced jump landing, the quadriceps peak force reduced from 4650 N (unbraced jump landing) to 3930 N while the hamstring muscle force peak value reduced from 3500 N (unbraced condition) to 1930 N and net hip extensor moments reduced from 317 Nm to 254 Nm as explained in Section 7.2.2. In addition, similar to these findings Branch et al (1989) reported reduction in EMG muscle activity in lower extremity due to bracing and likewise in another study, Osternig et al (1993) also indicated 72% in significant reduction in EMG activity among flexor extensor muscles due to application of brace. This reduction/change in muscle firing pattern due to application of brace explains the reduction in GRF and such reductions in Peak value of GRF has been reported by Rishiraj et al (2012).

Observing sagittal plane kinematics in Figure 64 and Figure 65, it can be deduced that during braced landing, the knee and hip were in extended position in comparison to the unbraced landing scenario. However the graph also reveals that at the time of landing, hip and knee experience greater range of motion during braced condition, indicating dissipation of energy resulting in reduction in peak GRF and attenuation of internal joint forces. This is similar to findings revealed by Onate et al (2005) where they observed reduction in peak GRF while individuals performed jump landing with

an increase in their Knee angular displacements and Yu et al (2005) found comparable results of reduction in vertical peak GRF due to active hip and knee flexion motions during IC. Furthermore viewing the plot in Figure 66, bracing condition also affected the frontal plane kinematics. It is very clear that the knee abduction angle reduced to greater extent while athlete performed jump landing with a brace. Krosshaug et al (2007) and Hewett et al (2005) have indicated that valgus loading occurring due to abducted landing is a major factor contributing for ACL injuries among athletes and the reduction in knee abduction observed during current braced jump landing can be an important indicator that the protective effect of bracing during jump landing.

During completion of four unique combinations of in vitro simulation (as explained in Section 6.5), ACL strain was recorded at 1000 Hz and observing the strain pattern (Figure 62), it is evident that peak ACL strain values of 18% occurred while simulating unbraced landing activity of the subject. This observation is in contrary to research findings such as reported by Cassidy et al (2013), Hashemi et al (2007) and Withrow et al (2006) where average strain ranged between 3 to 6% during in vitro simulations, however this can be attributed to the fact that peak GRF values observed in these studies were lower and ranged between 1300 N to 1700 N. Furthermore, observing the peak ACL strain during braced landing condition, it can be noted that the strain values are reduced to about 7% this is clear evidence that prophylactic brace effectiveness in reducing ACL strain and several factors can be attributed to this observation. In study completed by Hashemi et al (2007), they observed that attenuation of peak GRF further reduced the joint reaction forces and contributed in reduction of ACL strain and in current case study, attenuation of peak GRF from 26 milliseconds to 43 milliseconds due to braced condition would be one of the contributors. Besides observing muscle firing pattern in Figure 60 and Figure 61, it can be noted that Hamstring activation was increased, close to 50 milliseconds surrounding the peak GRF during braced landing scenario in comparison to 25- 28 milliseconds as seen during unbraced landing scenario. This longer activation of hamstring muscles has been credited to effective reduction of ACL loads resulting in further decrease in ACL strains (Li et al, 1999). In addition to increased activation of the hamstring muscle, rise in quadriceps activation during braced landing condition surrounding peak GRF and delayed activation of the hip extensor moments at the same instance, that is 0.43 milliseconds in comparison to 26 milliseconds during unbraced landing and reduction in peak hip extensor moments can also lead to significant reductions in ACL strain. In an alternate injury mechanism study completed by Hashemi et al (2007), they observed that increased activation of quadriceps force at the time of landing provided protective effects on ACL by increasing the joint compressive forces thereby reducing ATT (anterior tibial

translation). Hence this combination of protective muscle firing pattern followed by brace attenuating GRF resulted in lesser ACL strain and such neuromuscular changes occurred mostly due to the proprioceptive feedback induced by the brace. Ramsey et al (2003) and Baltaci et al (2011) have reported similar findings with increase in joint stability, coordination due to proprioceptive feedback and similar findings have been noted by Osternig et al (1993).

In order to isolate the effect of mechanical restraint offered by prophylactic brace during jump landing simulation (on the knee simulator), four different scenarios listed in Table 3 were simulated. Observing Figure 62, it can noted that ACL strain patterns were similar when compared between trials (a) with (d) and (c) with (b). This clearly indicates that mounting a brace during replication of jump landing activity on the knee simulator did not alter unique strain patterns observed due to unbraced and braced landing conditions (during motion capturing). This further indicates that brace did not provide mechanical restrain or prevent ATT during the simulation but affected the ACL strain by changing the neuromuscular firing patter of the athlete performing (In vivo) the jump landing activity during motion capture and this further reinforces conclusions of previous researches conducted by Ramsey et al (2003) and Osternig et al (1993).

Although results indicate lack of mechanical restrain offered by the prophylactic brace, these findings might not be true under higher strain conditions occurring due to increase in ATT and such strain levels were not observed during the current case study. It is quite possible that the strain values observed during this simulation were within the laxity range of the knee brace being tested, in other words the internal soft padding (layer) of the brace or the link member might be deflecting enough to absorb the ATT. In addition, it could also be the case that this particular brace design was not offering mechanical restraint and may be another design might provide mechanical restrain at lower strain values. All of these above described scenarios were not under the scope of this study and should be considered for future study.

# Chapter 9
# Conclusions

Ever since Anderson et al (1970) pioneered investigation into knee braces, bio mechanic research community has constantly strived to understand effect of a prophylactic brace in preventing knee ligament injuries and numerous studies have been commissioned to solve this mystery. In the past, scientists have utilized static/quasi static in vivo and in vitro techniques (Beynnon et al, 1993 Erickson et al, 1993), while others have investigated retrospectively studying injured athletes. However, to date no study has ever conducted analysis on dynamic activities (Najibi and Albright 2005). Hence this research study was initiated by combining both in vivo and in vitro techniques, wherein a dynamic motion performed by an amateur athlete was simulated on a hybrid surrogate cadaver specimen and strain on ACL was measured using a micro-strain gauge (DVRT) during both braced and unbraced conditions. The in-vitro simulation was conducted on a dynamic knee simulator that was developed by Cassidy (2009), and the novel aspect of this equipment included capabilities of providing high speed motion along two distinct axes thereby replicating sagittal plane kinematics, combined with high speed force actuators that could emulate high speed dynamic muscle forces. Observing the outcome of the two distinct phases of research study, following conclusions can be derived.

- During first phase of the research, the methodology of testing knee brace was developed utilizing the novel combined in-vivo/in-vitro technique and comparing input and output variable of the dynamic knee simulator, it can be concluded that the dynamic knee simulator was capable of closely replicating the input dynamic in-vivo activity. The standardized root mean square (SRMS) error of the output force profile in comparison to the input muscle profile was within 12%.
- In addition, ACL strain values that were measured during the methodology development phase were similar to findings /predictions of researchers in the past (Cassidy et al, 2013, Withrow et al, 2006). Hence this novel approach was considered an appropriate technique to evaluate the prophylactic brace effectiveness during dynamic activities.
- During second phase of study, reviewing muscle force outputs estimated by Anybody® biomechanical model, two distinctive muscle firing patterns were observed between braced and unbraced landing in-vivo conditions. In light of these findings, it can be

concluded that brace assisted in altering the neuromuscular firing pattern during jump landing, thereby resulting in reducing the antagonistic muscle activation (reduction in net hip extensor moments) and increasing agonistic muscle activation (increase in Hamstring and Quadriceps activation). In addition, it can also be noted that bracing altered the in-vivo landing kinematics by reducing knee abduction angle indicating an important protective feature against valgus loading of knee.

- During braced in-vivo landing state, peak GRF values was reduced and the time to peak GRF at the time of landing seemed to have attenuated when compared to unbraced landing condition. Other researchers have identified these patterns as markers for reduction in ACL strain and current research reinforces these findings.
- After completion of four distinct in-vitro simulations, the ACL strain data indicated high strain values during unbraced jump landing scenario when compared to the braced condition. This signifies previous research findings regarding changes in neuromuscular firing pattern induced by proprioceptive feedback due to bracing. This is an important finding of this novel research approach and identifies the effectiveness of a custom fit brace in reducing ACL strain during dynamic activities such as during a single leg jump landing.
- Furthermore during this research study, in order to understand if the brace mechanically restrained the knee by preventing ATT (anterior tibial translation), four different scenarios were simulated. The resulting ACL strain data indicates that applying the brace during simulation on the hybrid surrogate specimen did not alter strain patterns that were observed during braced and unbraced in-vivo landing conditions. Although this was an important finding, since ACL strain values observed during these testing conditions were low in comparison to actual strain values that create rupture in ligaments, this conclusion must be considered with caution and there is a possibility that brace with different design under higher strain conditions might provide some mechanical restraint and current research does not provide complete insight into this issue.

In light of all above mentioned affirmative discoveries, it is possible to conclude that brace has protective effects on human knee during dynamic activities such as single leg jump landing. The case study indicates that braces impacts neuromuscular activity and reduces ACL antagonistic muscle activation and increasing agonistic muscle activation thereby resulting in reduction of ACL strain.

# Chapter 10
# Limitation of Study and Recommendations for Future Work

The research study provides conclusive evidence that a prophylactic brace exhibits positive effects by reducing ACL strain during a high risk activity such as single leg jump landing however, certain limitations are inherent to the methodology and knee simulator utilized in this research. Cassidy et al (2013) major limitations and assumptions those are inherent to the use of dynamic knee simulator to test dynamic motions. In addition to that, following litany of items must be taken into consideration while evaluating the results of this study.

- Due to the complex process involved in preparing a hybrid specimen, study was limited to one cadaver knee specimen (case study) and further cadaver knee studies are necessary to understand the physiological variances that occur due to multiple cadaver knees, in order to verify the results of this case study and also to apply the study results to a wider population.
- Due to the complex nature of this research study, it was imperative to maintain focus on the primary objective of the study which was to develop a methodology and evaluate effectiveness of a knee brace. Hence Anybody® biomechanical software was utilized to determine resulting muscle forces for the motion captured dynamic activity. This involved modification of an existing gait model by scaling it suit the anthropometrics of the subject. Consequently the research study was limited to utilize the muscle force solver algorithm employed in the downloaded gait model with no additional investigations into other possible muscle solver algorithms. Hence it is recommended that other solver algorithms must be tested to evaluate if the muscle force patterns are significantly different.
- Anybody® Biomechanical software utilizes min-max optimization criterion to resolve muscle recruitment indeterminacy however muscle activation dynamics are not considered in this software (Damsgaard et al, 2006) and hence other software options must be explored to estimate muscle forces.
- Entire study was based on muscle activation profiles of one individual deemed high risky subject and this might not be absolute as the individual studied belonged to a group of ten

volunteers. Hence, further testing using larger number of other individual muscle profiles might be necessary to identify subject related differences and its effects on bracing knees during jump landing.

- Although muscle force profiles were significantly different between braced and unbraced conditions, EMG analysis (electromyography analysis) must be included as an integral component of this methodology to validate the muscle forces estimated by the biomechanical software
- Study results examined ACL strain as a relative measure (relative strain) as validated by Beynnon et al (1993) however, true value of ACL strain was never determined. Hence it is recommended that inflection point of the cadaver knee should be determined prior to the initiation of the tests.
- Further modification of the knee simulator must be completed to obtain simulation of frontal plane kinematics as valgus / varus loading of knee poses higher threats to ACL injuries (Krosshaug et al, 2007).
- In the current study, only one brace was tested and hence it is advisable to test different design of braces to detect if other designs provide any form of mechanical restrain along sagittal plane.
- Current study indicates that brace influenced the neuromuscular activity of the individual due to proprioception and with the current methodology it is not possible to identify if such effects of the brace was present even after the athlete was exposed to braced conditions for longer durations. Further studies are recommended to analyze brace such effects on individuals by administering test at different interval of longer exposure to bracing.

Currently, knee braces are not widely used as preventive interventions due to an absence of direct evidence of their prophylactic effectiveness and current research study clearly shows that knee braces can reduce strain in an intact ACL during a jump landing activity. In light of the current findings, it is further recommended high risk athletes might find it beneficial to wear custom fit prophylactic knee braces while performing high risk activities that pose risk with occurrence of non-contact injuries to ACL.

# Appendix 1

## Section 1

These codes refer to the marker co-ordinate data that was input in "ModelSetup.any" file during first phase of the study to scale biomechanical model.

```
CreateMarkerTD LC (
  MarkerName=PrefixDef(LC),
  MarkerPlacement =Right.Leg.Seg.Thigh,
  OptX="Off",OptY="Off",OptZ="Off",
  WeightX=1.0,WeightY=1.0,WeightZ=1.0,
  Model1=MotionAndParameterOptimizationModel, Model2=
InverseDynamicModel
  )= {sRelOpt= {0.031, -0.400, 0.05};};

  CreateMarkerTD MC (
  MarkerName=PrefixDef(MC),
  MarkerPlacement =Right.Leg.Seg.Thigh,
  OptX="On",OptY="On",OptZ="On",
  WeightX=1.0,WeightY=1.0,WeightZ=1.0,
  Model1=MotionAndParameterOptimizationModel, Model2=
InverseDynamicModel
  )= {sRelOpt= {0.009, -0.383, -0.056};};

  CreateMarkerTD GT (
  MarkerName=PrefixDef(GT),
  MarkerPlacement =Right.Leg.Seg.Thigh,
  OptX="Off",OptY="Off",OptZ="Off",
  WeightX=1.0,WeightY=1.0,WeightZ=1.0,
  Model1=MotionAndParameterOptimizationModel, Model2=
InverseDynamicModel
  )= {sRelOpt = {0.005,-0.020, 0.085}; };


  CreateMarkerTD RASIS (
  MarkerName=PrefixDef(RASIS),
  MarkerPlacement=Trunk.SegmentsLumbar.PelvisSeg,
  OptX="Off", OptY="Off", OptZ="Off",
  WeightX=1.0,WeightY=1.0,WeightZ=1.0,
  Model1=MotionAndParameterOptimizationModel, Model2=
InverseDynamicModel
  ) = {sRelOpt=  {0.080, -0.012, 0.135}; };

  CreateMarkerTD LASIS (
  MarkerName=PrefixDef(LASIS),
```

```
  MarkerPlacement=Trunk.SegmentsLumbar.PelvisSeg,
  OptX="Off", OptY="Off", OptZ="Off",
  WeightX=1.0,WeightY=1.0,WeightZ=1.0,
  Model1=MotionAndParameterOptimizationModel, Model2=
InverseDynamicModel
  ) = {sRelOpt =  {0.085, -0.018, -0.155}; };

  CreateMarkerTD RPSIS (
  MarkerName=PrefixDef(RPSIS),
  MarkerPlacement=Trunk.SegmentsLumbar.PelvisSeg,
  OptX="Off", OptY="Off", OptZ="Off",
  WeightX=1.0,WeightY=1.0,WeightZ=1.0,
  Model1=MotionAndParameterOptimizationModel, Model2=
InverseDynamicModel
  ) = {sRelOpt = {-0.055, 0.035, 0.060}; };

  CreateMarkerTD LPSIS (
  MarkerName=PrefixDef(LPSIS),
  MarkerPlacement=Trunk.SegmentsLumbar.PelvisSeg,
  OptX="Off", OptY="Off", OptZ="Off",
  WeightX=1.0,WeightY=1.0,WeightZ=1.0,
  Model1=MotionAndParameterOptimizationModel, Model2=
InverseDynamicModel
  ) = {sRelOpt ={-0.055, 0.050, -0.070};};

  CreateMarkerTD LM (
  MarkerName=PrefixDef(LM) ,
  MarkerPlacement=Right.Leg.Seg.Shank,
  OptX="Off",OptY="Off",OptZ="Off",
  WeightX=1.0,WeightY=1.0,WeightZ=1.0,
  Model1=MotionAndParameterOptimizationModel, Model2=
InverseDynamicModel
  ) = {sRelOpt = {0.00671602, -0.010, 0.03042605; };

  CreateMarkerTD MT1 (
  MarkerName=PrefixDef(MT1),
  MarkerPlacement=Right.Leg.Seg.Foot,
  OptX="Off",OptY="Off",OptZ="Off",
  WeightX=1.0,WeightY=1.0,WeightZ=1.0,
  Model1=MotionAndParameterOptimizationModel, Model2=
InverseDynamicModel
  ) = {sRelOpt=  {0.22, 0.030, -0.02};};

  CreateMarkerTD TOE (
  MarkerName=PrefixDef(TOE),
  MarkerPlacement=Right.Leg.Seg.Foot,
  OptX="Off",OptY="Off",OptZ="Off",
  WeightX=1.0,WeightY=1.0,WeightZ=1.0,
```

```
  Model1=MotionAndParameterOptimizationModel, Model2=
InverseDynamicModel
  ) = {sRelOpt=  {0.24931776, 0.02168634, -0.01}; };

  CreateMarkerTD MT5 (
  MarkerName=PrefixDef(MT5),
  MarkerPlacement=Right.Leg.Seg.Foot,
  OptX="Off",OptY="Off",OptZ="Off",
  WeightX=1.0,WeightY=1.0,WeightZ=1.0,
  Model1=MotionAndParameterOptimizationModel, Model2=
InverseDynamicModel
  ) = {sRelOpt =  {0.150, 0.0128, 0.085};};

  CreateMarker  T10 (
  MarkerName=T10,
  MarkerPlacement=Trunk.SegmentsThorax.ThoraxSeg,
  OptX="Off",OptY="Off",OptZ="Off",
  WeightX=1.0,WeightY=1.0,WeightZ=1.0,
  Model1=MotionAndParameterOptimizationModel,Model2=
InverseDynamicModel
  ) = {sRelOpt = {-0.095,0.210,-0.020};};

  CreateMarker  C7 (
  MarkerName=C7,
  MarkerPlacement=Trunk.SegmentsThorax.ThoraxSeg,
  OptX="Off",OptY="Off",OptZ="Off",
  WeightX=1.0,WeightY=1.0,WeightZ=1.0,
  Model1=MotionAndParameterOptimizationModel,Model2=
InverseDynamicModel
  ) = {sRelOpt = {-0.035,0.450,0};};

  CreateMarker  SS (
  MarkerName=SS,
  MarkerPlacement=Trunk.SegmentsThorax.ThoraxSeg,
  OptX="Off",OptY="Off",OptZ="Off",
  WeightX=1.0,WeightY=1.0,WeightZ=1.0,
  Model1=MotionAndParameterOptimizationModel,Model2=
InverseDynamicModel
  ) = {sRelOpt = {0.1,0.325,-0.005};};

  CreateMarker  XP(
  MarkerName=XP,
  MarkerPlacement=Trunk.SegmentsThorax.ThoraxSeg,
  OptX="Off",OptY="Off",OptZ="Off",
  WeightX=1.0,WeightY=1.0,WeightZ=1.0,
  Model1=MotionAndParameterOptimizationModel,Model2=
InverseDynamicModel
  ) = {sRelOpt = {0.125,0.135,-0.030};};
```

```
  CreateMarker  RA(
  MarkerName=RA,
  MarkerPlacement=Trunk.SegmentsThorax.ThoraxSeg,
  OptX="Off",OptY="Off",OptZ="Off",
  WeightX=1.0,WeightY=1.0,WeightZ=1.0,
  Model1=MotionAndParameterOptimizationModel,Model2=
InverseDynamicModel
  ) = {sRelOpt = {0.0,0.360,0.165};  };

  CreateMarker  LA(
  MarkerName=LA,
  MarkerPlacement=Trunk.SegmentsThorax.ThoraxSeg,
  OptX="Off",OptY="Off",OptZ="Off",
  WeightX=1.0,WeightY=1.0,WeightZ=1.0,
  Model1=MotionAndParameterOptimizationModel,Model2=
InverseDynamicModel
  ) = {sRelOpt = {0.0,0.395,-0.170}; };};
```

## Section 2

In the main program file, `#include "HumanModel.any"` was selected and file by name `"AnyWomanExtPercentile.any"` was added and initiated. Subsequently in the program file `"AnyWomanExtPercentile.any"`, the following formulae was initiated

"AnyVar `Z = (0.0279*Percentile)-1.3971;`" in order to calculate a linear regression constant "Z" for a 50$^{th}$ percentile woman.

During the second phase of testing, the below listed formulae was initiated

"AnyVar `Z = (0.064*Percentile)-1.96;`" in order to calculate a linear regression constant "Z" for a 15$^{th}$ percentile woman.

## Section 3

Optimization of selected body segment parameters were enable and disabled by turning "On" and "Off" in file `#include "ModelSetup.any"` as shown in the codes below.

```
OptimizeAnthropometricsOnOff OptimizeOnOff (
  PelvisWidthOnOff ="On",
  ThighLengthOnOff="On",
  ShankLengthOnOff="On",
  FootLengthOnOff="On",
```

```
  HeadHeightOnOff="Off",
  TrunkHeightOnOff="On",
  UpperArmLengthOnOff="Off",
  LowerArmLengthOnOff="Off",
  VarusValgusOnOff="Off",
Model1=MotionAndParameterOptimizationModel,
Model2=InverseDynamicModel) = {};
```

## Section 4

These modified portions of codes belong to "BodyPartsSetup2.any" file and initiate corresponding body segments for the biomechanical model

```
// Trunk: 1 included, 0 not included
// ********************************
#define TRUNK 1 Modified
// This is just the bones,
// Choose one of the following options to add muscles
#define TRUNK_SIMPLE_MUSCLES 0 Modified
// Additional stiffness in the lumbar joints can be added.
#define TRUNK_DISC_STIFFNESS_NORMAL 0

// RightLegTD: 1 included, 0 not included
// **********************************
#define RIGHT_LEG_TD 1 Modified
// This is just the bones,
// Choose one of the following options to add muscles
#define RIGHT_LEG_TD_SIMPLE_MUSCLES 0 Modified
#define RIGHT_LEG_TD_MUS_3E 0
```

## Section 5

These codes were added into file "TrunkDrivers.any" and subsequently initiated in the main program file

```
// Neck driver
  AnyKinEqSimpleDriver NeckJntDriver = {
  AnyRevoluteJoint &T12L1Joint =
...HumanModel.BodyModel.Interface.Trunk.NeckJoint;
  DriverPos = pi/180*{.JntPos.NeckExtension};
  DriverVel = pi/180*{.JntVel.NeckExtension};Reaction.Type = {Off}
;};
```

## Section 6

Following codes were modified in the file `#include "ModelSetup.any"` to reflect changes in marker references and orientation that were modified for Right Acromion and Left Acromion markers during second phase of study

```
  CreateMarker  RA(
  MarkerName=RA,
  MarkerPlacement=Right.ShoulderArm.Seg.Scapula,(Modified)
  OptX="Off",OptY="Off",OptZ="Off",
  WeightX=1.0,WeightY=1.0,WeightZ=1.0,
  Model1=MotionAndParameterOptimizationModel,Model2=
InverseDynamicModel
  ) = {
    //sRelOpt = {0.040,0.320,0.165};
    //sRelOpt = {0.0,0.360,0.165};
    //sRelOpt = {-0.03,-0.04,-0.06};
      sRelOpt = {0.03,-0.0,-0.04};
  };

  CreateMarker  LA(
  MarkerName=LA,
  MarkerPlacement=Left.ShoulderArm.Seg.Scapula,(Modified)
  OptX="Off",OptY="Off",OptZ="Off",
  WeightX=1.0,WeightY=1.0,WeightZ=1.0,

  Model1=MotionAndParameterOptimizationModel,Model2=
InverseDynamicModel
  ) = {
    //sRelOpt = {0.0450,0.360,-0.180};
    //sRelOpt = {0.0,0.395,-0.170};
    //sRelOpt = {-0.02,0.04,-0.06};
    sRelOpt = {0.03,0.0,-0.04};
  };
```

## Section 7

This section of the report has the drivers for the arm motion, glenohumeral joint and the clavicular joint of both left and right arms. These codes were input into the `"TrunkDrivers.any"` file in the main program.

```
  // ***********************************
  // Drivers for the right arm
  // ***********************************
  //Sterno clavicular joint driver
  AnyKinEqSimpleDriver SCDriverRight ={
```

```
    AnyKinMeasureOrg &ref1
=...HumanModel.BodyModel.Interface.Right.SternoClavicularProtraction
;
    AnyKinMeasureOrg &ref2
=...HumanModel.BodyModel.Interface.Right.SternoClavicularElevation;
    AnyKinMeasureOrg &ref3
=...HumanModel.BodyModel.Interface.Right.SternoClavicularAxialRotati
on;
    DriverPos = pi/180*{
      .JntPos.Right.SternoClavicularProtraction,
      .JntPos.Right.SternoClavicularElevation,
      .JntPos.Right.SternoClavicularAxialRotation
    };
    DriverVel = {
      .JntVel.Right.SternoClavicularProtraction,
      .JntVel.Right.SternoClavicularElevation,
      .JntVel.Right.SternoClavicularAxialRotation
    };
    Reaction.Type={Off,Off,Off};
  };
  //Glenohumeral joint
  AnyKinEqSimpleDriver GHDriverRightAbduction={
    AnyKinMeasureOrg &ref1
=...HumanModel.BodyModel.Interface.Right.GlenohumeralAbduction;
     DriverPos=pi/180*{.JntPos.Right.GlenohumeralAbduction};
     DriverVel = pi/180*{.JntVel.Right.GlenohumeralAbduction};
     Reaction.Type={Off};
  };
  AnyKinEqSimpleDriver GHDriverRightFlexion={
    AnyKinMeasureOrg &ref2
=...HumanModel.BodyModel.Interface.Right.GlenohumeralFlexion;
     DriverPos=pi/180*{.JntPos.Right.GlenohumeralFlexion};
     DriverVel = pi/180*{.JntVel.Right.GlenohumeralFlexion};
     Reaction.Type={Off};
  };
  AnyKinEqSimpleDriver GHDriverRightExternalRotation={
    AnyKinMeasureOrg &ref3
=...HumanModel.BodyModel.Interface.Right.GlenohumeralExternalRotatio
n;
     DriverPos=pi/180*{.JntPos.Right.GlenohumeralExternalRotation};
     DriverVel =
pi/180*{.JntVel.Right.GlenohumeralExternalRotation};
     Reaction.Type={Off};
  };
  //Elbow flexion driver
  AnyKinEqSimpleDriver ElbowFlexionDriverRight={
    AnyKinMeasureOrg  &Elbow
=...HumanModel.BodyModel.Interface.Right.ElbowFlexion;
```

```
    DriverPos=pi/180*{.JntPos.Right.ElbowFlexion};
    DriverVel = pi/180*{.JntVel.Right.ElbowFlexion};
    Reaction.Type={Off};
  };
  //Elbow pronation driver
  AnyKinEqSimpleDriver ElbowPronationDriverRight={
    AnyKinMeasureOrg &Elbow
=...HumanModel.BodyModel.Interface.Right.ElbowPronation;
    DriverPos = pi/180*{.JntPos.Right.ElbowPronation };

    DriverVel=pi/180*{.JntVel.Right.ElbowPronation };
    Reaction.Type={Off};
  };
  //Wrist driver
  AnyKinEqSimpleDriver WristDriverRightFlexion ={
    AnyKinMeasureOrg &ref1
=...HumanModel.BodyModel.Interface.Right.WristFlexion;
    DriverPos = pi/180*{.JntPos.Right.WristFlexion};
    DriverVel = pi/180*{.JntVel.Right.WristFlexion};
    Reaction.Type={Off};
  };
  AnyKinEqSimpleDriver WristDriverRightAbduction ={
    AnyKinMeasureOrg &ref2
=...HumanModel.BodyModel.Interface.Right.WristAbduction;
    DriverPos = pi/180*{.JntPos.Right.WristAbduction};
    DriverVel = pi/180*{.JntVel.Right.WristAbduction};
    Reaction.Type={Off};
  };
  // ***********************************
  // Drivers for the left arm
  // ***********************************
  //Sterno clavicular joint driver
  AnyKinEqSimpleDriver SCDriverLeft ={
    AnyKinMeasureOrg &ref1
=...HumanModel.BodyModel.Interface.Left.SternoClavicularProtraction;
    AnyKinMeasureOrg &ref2
=...HumanModel.BodyModel.Interface.Left.SternoClavicularElevation;
    AnyKinMeasureOrg &ref3
=...HumanModel.BodyModel.Interface.Left.SternoClavicularAxialRotatio
n;
    DriverPos = pi/180*{
      .JntPos.Left.SternoClavicularProtraction,
      .JntPos.Left.SternoClavicularElevation,
      .JntPos.Left.SternoClavicularAxialRotation
    };

    DriverVel = pi/180*{
      .JntVel.Left.SternoClavicularProtraction,
```

```
      .JntVel.Left.SternoClavicularElevation,
      .JntVel.Left.SternoClavicularAxialRotation
    };
    Reaction.Type={Off,Off,Off};
  };
  //Glenohumeral joint driver
  AnyKinEqSimpleDriver GHDriverLeftAbduction={
    AnyKinMeasureOrg &ref1
=...HumanModel.BodyModel.Interface.Left.GlenohumeralAbduction;
    DriverPos=pi/180*{.JntPos.Left.GlenohumeralAbduction};
    DriverVel = pi/180*{.JntVel.Left.GlenohumeralAbduction};
    Reaction.Type={Off};
  };
    AnyKinEqSimpleDriver GHDriverLeftFlexion={
    AnyKinMeasureOrg &ref2
=...HumanModel.BodyModel.Interface.Left.GlenohumeralFlexion;
    DriverPos=pi/180*{.JntPos.Left.GlenohumeralFlexion};
    DriverVel = pi/180*{.JntVel.Left.GlenohumeralFlexion};
    Reaction.Type={Off};
  };
  AnyKinEqSimpleDriver GHDriverLeftExternalRotation={
    AnyKinMeasureOrg &ref3
=...HumanModel.BodyModel.Interface.Left.GlenohumeralExternalRotation
;
    DriverPos=pi/180*{.JntPos.Left.GlenohumeralExternalRotation};
    DriverVel = pi/180*{.JntVel.Left.GlenohumeralExternalRotation};
    Reaction.Type={Off};
  };
  //Elbow flexion driver
  AnyKinEqSimpleDriver ElbowFEDriverLeft={
  AnyKinMeasureOrg  &Elbow
=...HumanModel.BodyModel.Interface.Left.ElbowFlexion;
    DriverPos=pi/180*{.JntPos.Left.ElbowFlexion};
    DriverVel = pi/180*{.JntVel.Left.ElbowFlexion};
    Reaction.Type={Off};
  };
  //Elbow pronation driver
  AnyKinEqSimpleDriver ElbowPSDriverLeft={
    AnyKinMeasureOrg &Elbow
=...HumanModel.BodyModel.Interface.Left.ElbowPronation;
    DriverPos= pi/180*{.JntPos.Left.ElbowPronation };
    DriverVel = pi/180*{.JntVel.Left.ElbowPronation };
    Reaction.Type={Off};
  };
  //Wrist driver
  AnyKinEqSimpleDriver WristDriverLeftFlexion ={
    AnyKinMeasureOrg &ref1
=...HumanModel.BodyModel.Interface.Left.WristFlexion;
```

```
    DriverPos = pi/180*{.JntPos.Left.WristFlexion};
    DriverVel = pi/180*{.JntVel.Left.WristFlexion};
    Reaction.Type={Off};
  };
  AnyKinEqSimpleDriver WristDriverLeftAbduction ={
    AnyKinMeasureOrg &ref2
=...HumanModel.BodyModel.Interface.Left.WristAbduction;
    DriverPos = pi/180*{.JntPos.Left.WristAbduction};
    DriverVel = pi/180*{.JntVel.Left.WristAbduction};
    Reaction.Type={Off}; };
```

# References

Alexander E, Andriacchi T P, Correcting for deformation in skin based marker systems, Journal of Biomechanics 2000; 34: 355-361

Ambrose T L, The Anterior Cruciate Ligament and functional stability of the knee joint, Journal article, British Columbia Medical Journal 2003; 43: 495-499

Amis A A , Dawkins G P C, Functional Anatomy of the Anterior Cruciate Ligament, Fibre Bundle Actions Related to Ligament Replacements and Injuries, Journal of Bone Joint surgery [Br] 1991; 73-B 260-7

Baltaci G, Aktas G, Camci E, Oksuz S, Yildiz S, Kalaycioglu T, The effect of Prophylactic Knee bracing on performance: balance, proprioception, coordination and muscular power, The journal of Knee Surgery Sports Traumatology Arthroscopy, 2011; 10.1007/s00167-011-1491-3

Beynnon B D, Fleming B C, Churchill D L, Brown D, The effect of Anterior Cruciate ligament deficiency and functional bracing on translation of the tibia relative to the femur during non-weight bearing and weight bearing: The American Journal of Sports Medicine 2003; 31: 99-105.

Beynnon B D, Johnson R J, Abate J A, Fleming B C, Nichols C E, Treatment of Anterior Cruciate Ligament injuries, part 1, American Journal of Sports Medicine 2005; 33: 1579-1602

Beynnon B D, Johnson R J, Fleming B C, Peura D G, Renstorm P A, Nichols C E, Pope M H, The effect of functional knee bracing on the Anterior cruciate ligament in the weight bearing and non-weight bearing knee: The American Journal of Sports Medicine 1997; 25: 353-359.

Birmingham TB, Bryant DM, Giffin JR, Litchfield RB, Kramer JF, Donner A, Fowler PJ.A randomized controlled trial comparing the effectiveness of functional knee brace and neoprene sleeve use after anterior cruciate ligament reconstruction.Am J Sports Med. 2008 Apr;36(4):648-55.

Blackburn JT, Darin A Padua, Sagittal-Plane Trunk Position, Landing Forces, and Quadriceps Electromyographic Activity J Athletics and Training 2009 Mar-Apr; 44(2): 174–179.

Boden B P, Dean G S, Feagin JA Jr, Garrett W E Jr. , Mechanisms of Anterior Cruciate Ligament Injury. Orthopedics 2000; 23 (6) : 573-8 Pubmed PMID: 10875418

Boden BP, Joseph S. Torg, Sarah B. Knowles and Timothy E. Hewett Video Analysis of Anterior Cruciate Ligament Injury : Abnormalities in Hip and Ankle Kinematics. Am J Sports Med 2009 37: 252

Branch T P, Hunter R, Donath M, Dynamic EMG analysis of Anterior Cruciate deficient legs with and without bracing during cutting, The American Journal of Sports Medicine, 1989; 17-1:35:41

Carey JL, Huffman GR, Parekh SG, Sennett J B. Outcomes of anterior cruciate ligament injuries to running backs and wide receivers in the National Football League. Am J Sports Med 2006 Dec; 34: 1911-7

Cassidy Karla, Design and Validation of a Dynamic Knee Injury Simulator 2009, Master of Applied Science Thesis, University of Waterloo.

Cassidy K, Hangalur G, Sabharwal P, Chandrashekar N, Combined In Vivo/In Vitro Method to study Anteriomedial Bundle Strain in the Anterior Cruciate Ligament Using a Dynamic Knee Simulator. Journal of Biomechanical Engineering 2013; 135: 35001

Chaffin D B, Andersson G B J, Martin B J, Occupational Biomechanics- 4th edition, published by John Wiley & Sons, Inc. 2006.

Chandrashekar Naveen Kugwe M S., Sex Based Difference in the Morphology, Tensile properties and Ultra Structure of the Human Anterior Cruciate Ligament and Patellar Tendon,2005, Doctor of Philosophy Thesis, Texas Tech

Chew KTL, Lew HL, Date E, Fredericson, M: Current Evidence and Clinical Applications of Therapeutic Knee Braces. American Journal of Physical Medicine and Rehabilitation 2007; 86:678-686.

Damsgaard M, Rasmussen J, Christensen S T, Surma E, Zee M, Analysis of musculoskeletal systems in the AnyBody® Modeling System, published journal article in Simulation Modelling Practice and Theory 2006; 14:1100-1111

Deacon A, Bennell K, Kiss ZS, et al. Osteoarthritis of the knee in retired, elite Australian rules footballers, Med J Aust 1997; 166: 187-90.

de Loës M, Dahlstedt J L, Thomée R, A 7 year study on risks and costs of knee injuries in male and female youth participants in 12 sports. Scand J Med Sci Sports 2000; 10: 90-97

Delp L S, Ringwelski D A, Carroll N C, Transfer of the Rectus Femoris: Effects of Transfer site on Moment Arms About the Knee and Hip, Journal of Biomechanics, 1994; 27-10: 1201:1211

Department of Research & Scientific Affairs, American Academy of Orthopaedic Surgeons. Rosemont, IL: AAOS; February 2014. Based on data from the National Ambulatory Medical Care Survey, 2010; Centers for Disease Control and Prevention retrieved from webpage http://orthoinfo.aaos.org/topic.cfm?topic=a00325

Dr.Kevin G Shea, report on worldwide web, article "ACL injury prevention: Does it work?" – Study calls for more research on ACL, knee injury prevention programs, published by American Academy of Orthopaedic Surgeons, August 2010. Retrieved from - http://www.aaos.org/news/aaosnow/aug10/clinical6.asp

Duthon V B, Barea C, Abrassart S, Fasel J H, Fritschy D, Menetrey J, Anatomy of the anterior cruciate ligament, Journal article Knee Surg sports Traumatol Arthrosc 2006, 14:204-213

Ebstrup J F, Bojsen-Moller F, Case Report Anterior Cruciate Ligament Injury in indooe ball games, Sc and J Med Sci Sports 2000; 10: 114-116

Erickson A R, Yasuda K, Beynnon B, Johnson R, Pope M. An in vitro dynamic evaluation of prophylactic knee braces during lateral impact loading. Am J Sports Med. 1993; 21:26-35.

Fleming B C, Beynnon B D, Tohyama H, Johnson R J, Nichols C E, Renstrom P, Pope M H, Determination of a Zero strain reference for the anteromedial band of the anterior cruciate ligament, Journal of Orthopaedic Research 1994 Nov; 12(6):789-795

Fleming BC, Renstrom PA, Beynnon BD, t al. The influence of functional knee bracing on the anterior cruciate ligament strain biomechanics in weight bearing and non-weight bearing knees, American Journal of Sports Medicine, 2000 Nov-Dec;28(6):815-24.

Flynn RK, Pedersen CL, Birmingham TB, Kirkley A, Jackowski D, Fowler PJ. The familial predisposition toward tearing the anterior cruciate ligament: a case control study. Am J Sports Med. 2005;33: 23-28.

Freedman KB, Glasgow MT, Glasgow SG, et al. Anterior cruciate ligament injuries and reconstruction among university students, Clin Orthop Relat Res 1998; 356: 208-12

Gabriel M T, Wong E K, Woo S L Y, Yagi M, Debski R E, Distribution of in situ forces in the Anterior Cruciate Ligament in response to rotary Loads. 2004, Journal of Orthopaedic Research; 22: 85-89

Garrett WE Jr. Anterior cruciate ligament injury: pathophysiology and current therapeutic principles. Paper presented at: 71st Annual Meeting of the American Academy of Orthopaedic Surgeons; March 10-14, 2004; San Francisco, California.

Girgis FG, Marshall JL, Monajem ARSA, The cruciate ligaments of the knee joint, Anatomical, functional and experimental analysis 1975, Clin Orthop 106:216–231

Griffin LY. Agel J, Albohm MJ, et al (2000) Noncontact anterior cruciate ligament injuries: risk factors and prevention strategies. Journal of American Academy of Orthopedic Surgeons 8:141-150 (google books)

Griffin L Y, Agel J, Albohm M J, Arendt E A, Dick R W, Garrett W E, Garrick J G, Hewett T E, Huston L, Ireland M L, Johnson R J, W. Kibler B, Lephart S, Lewis J L, Lindenfeld T N, Mandelbaum B R, Marchak P, Teitz C C, and Wojtys E M, Noncontact Anterior Cruciate Ligament Injuries: Risk Factors and Prevention Strategies, Journal article, American Academy of orthopaedic surgeons, 2008; 8:141-150

Griffin LY, Albohm MJ, Arendt EA, et al. Understanding and preventing noncontact anterior cruciate ligament injuries – A review of the Hunt Valley 2 Meeting, American Journal Sports Medicine 2006; 34: 1512-32.

Hashemi J, Chandrashekar N, Jang T, Karpat F, Oseto M, Ekwardo-Osire S, An Alternative Mechanism of Non-contact Anterior Cruciate Ligament Injury during Jump-Landing: In-vitro Simulation, Journal for Society for Experimental Mechanics, 2007; 47: 347 – 354

Hewett TE, Lindenfield TN, Riccobene JV, et al. The effect of neuromuscular training on the incidence of knee injury in female athletes: a prospective study. Am J Sports Med 1999; 27: 699-706.

Hewett TE, Myer GD, Ford KR. Anterior cruciate ligament injuries, Part I: mechanisms and risk factors. Am J Sports Med 2006; 34: 299-311

Hewett TE, Myer GD, Ford KR, Heidt RS Jr, Colosimo AJ, McLean SG, van den Bogert AJ, Paterno MV, Succop P. Biomechanical measures of neuromuscular control and valgus loading of the knee predict anterior cruciate ligament injury risk in female athletes: a prospective study.Am J Sports Med. 2005 Apr;33(4):492-501.

Hinterwimmer S, H Graichen, R Baumgart, W Plitz, Influence of a mono-centric knee brace on the tension of the collateral ligaments in knee joints after sectioning of the anterior cruciate ligament – an in vitro study- Clinical Biomechanics, 2004, 19; 719-725

Hollis JM, Takai S, Adams DJ, Horibe S, Woo SL-Y (1991) The effects of knee motion and external loading on the length of the anterior cruciate ligament (ACL): a kinematic study. J Biomech Eng 113:208–214

Horikawa M, Ebihara S, Sakai F, Akiyama M, Non-invasive measurement method for hardness in muscular tissues, Journal of Medical and Biological Engineering and Computing 1993; 31: 623-627

Hurley W L, Boros R L, Challis J H, Influences of variation in Force Application on Tibial Displacement and Strain in the Anterior Cruciate Ligament during Lachman test, Journal of Clinical Biomechanics, 2004; 19:95-98

Krosshaug T, Nakamae A, Boden B P, Engebresten L, Smith G, Slaterbeck J R, Hewett T E, Bahr R, Mechanisms of Anterior Cruciate Ligament Injury in Basketball - Video Analysis of 39 cases, American Journal of Sports Medicine 2007; 35:359,367

Lamontagne M, Brisson N, Review article, University of Ottawa, ISBS Conference proceeding 2009

Laughlin W A, Weinhandl J T, Kernozek T W, Cobb. S C, Keenan K G, The effects of Single-leg Landing Technique on ACL loading, Journal of Biomechanics, 2011; 44:1845-1851

Li G, Rudy T W, Sakane M, Kanamori A, Ma C B, Woo S L Y, The importance of quadriceps and hamstring muscle loading on knee kinematics and in-situ forces in the ACL, Journal of Biomechanics 1999;32: 395-400

Liu S H, Lunsford T, Gude S, Vangsness T C, Comparison of Functional Knee Braces for Control of Anterior Tibial Displacement, Journal of Clinical Orthopaedics 1994; 303: 203-210

Lu TW, Lin HC, Hsu HC.Influence of functional bracing on the kinetics of anterior cruciate ligament-injured knees during level walking.Clin Biomech (Bristol, Avon). 2006 Jun;21(5):517-24.

Medical dictionary, 2013 information retrieved from webpage http://medical-dictionary.thefreedictionary.com during June 2013

Mihata L C S, Beutler A I, Boden B P- Comparing the incidence of Anterior Cruciate Ligament Injury in Collegiate Lacrosse, Soccer and Basketball Players- Implications for Anterior Cruciate Ligament Mechanism and Prevention, The American Journal of Sports Medicine, 2006; 34:899-904

Mohseni SS, Farahmand F, Karimi H and Kamali M. Arthrometric evaluation of stabilizing effect of knee functional bracing at different flexion angles. Journal of Sports Science and Medicine (2009) 8, 247 – 251

Moore Keith L, Dalley Arthur F, Clinical Oriented Anatomy, Fourth Edition 1999, published by: Lippincott Williams and Wilkins

Najibi S, Albright JP. The use of knee braces, part 1: prophylactic knee braces in contact sports. American Journal of Sports Medicine, 2005; 33:602-611.

Noyes FR, Mooar PA, Matthews DS, et al: The symptomatic anterior cruciate-deficient knee. Part I: The long-term functional disability in athletically active individuals. J Bone Joint Surg 65A: 154–162, 1983

Onate, J.A., Guskiewicz, K.M., Marshall, S.W., Giuliani, C., Yu, B., Garrett, W.E., 2005. Instruction of jump-landing technique using videotape feedback: altering lower extremity motion patterns. Am. J. Sports Med. 33 (6), 831–842.

Osternig L R, Robertson R N- Effects of prophylactic knee bracing on lower extremity joint position and muscle activation during running- The American Journal of Sports Medicine 1993; 21:733-737

Paessler H H, Michel D, Historical Note, How new is the Lachman test?, American Journal of Sports Medicine, 1992; 20:95-98

Paulos L E, Cawley P W, France E P. Impact biomechanics of lateral knee bracing: the anterior cruciate ligament. Am J Sports Med. 1991; 19:337-342.

Ramsey D K, Lamontagne M, Wretenberg PF, Valentin A, Engström B, Németh G. Assessment of functional knee bracing: an in vivo three-dimensional kinematic analysis of the anterior cruciate deficient knee. Clin Biomech (Bristol, Avon). 2001 Jan;16(1):61-70.

Ramsey D K, Wrentenberg P F, Lamontagne M, Nemeth G, Electromyographic and biomechanics analysis of anterior cruciate ligament deficiency and functional knee bracing. Journal of Clinical Biomechanics 2003; 18:28 – 34

Risberg A M, Holm I, Steen H, Eriksson J, Ekeland A, The Effect of Knee Bracing After Anterior Cruciate Ligament Reconstruction- A Prospective Randomized study with two years' Follow-up, The American Journal of Sports Medicine 1999; 27: 76-83

Rishiraj N, Taunton JE, et al., The potential role of prophylactic/functional knee bracing in preventing knee ligament injury. Sports Med. 2009; 39(11):937-60.

Rishiraj N, Taunton J E, Lloyd-Smith R, Regan W, Niven B, Woolard R, Functional Knee brace use effect on peak vertical ground reaction forces during drop jump landing. Journal of Knee Surgery Sports Traumatology Arthroscopy 2012; 20: 2405 – 2412

Roos H, Ornell M, Gardsell P, Lohmander L S, Lindstrand A, Soccer after anterior cruciate ligament injury- and incompatible combination? A national Survet of incidence and risk factors and a 7-year follow-up of 310 players, Acta Orthop Scand, 1995 Apr, 66(2) 107-112

Sabharwal P, A combined In-vivo/In-vitro approach to study knee injury mechanism, Master of Applied Science Thesis 2011, University of Waterloo

Sitler M, Ryan J, Hopkinson W, Wheeler J, Santomier J, Kolb R, et al. The efficacy of a prophylactic knee brace to reduce knee injuries in football: a prospective, randomized study at West Point. Am J Sports Med, 1990; 18:310-5.

Sportsinjuryclinic.net, 2013 information retrieved from webpage http://www.sportsinjuryclinic.net/anatomy/knee-anatomy during July 2013

Taylor KA, Terry ME, Utturkar GM, Spritzer CE, Queen RM, Irribarra LA, Garrett WE, DeFrate LE, Measurement of in vivo anterior cruciate ligament strain during dynamic jump landing, Journal of Biomechanics 2011; 44: 365-371

Tegner Y, Lorentzon R, Evaluation of Knee braces in Swedish Ice Hockey players, British Journal of sports medicine 1991; 25:159-161

Théoret D, Lamontagne M.. Study on three-dimensional kinematics and electromyography of ACL deficient knee participants wearing a functional knee brace during running. Knee Surgery Sports Traumatology Arthroscopy 2006 Jun; 14(6):555-63. Epub 2006 Apr 6.

Wikibooks.org, 2013 information retrieved from webpage http://en.wikibooks.org/wiki/Human_Anatomy/Terminology_and_Organization during June of 2013

Wilson Ross B S (2007). Anterior Cruciate Ligament Injury And Impingement Against Intercondylar Notch: An In-Vitro Study Using Robots, M.Sc.thesis Texas Tech

Withrow TJ, Huston LJ, Wojtys EM, Ashton-Miller JA, The relationship between quadriceps muscle force, knee flexion, and anterior cruciate ligament strain in an in vitro simulated jump landing, American Journal of Sports Med, 2006; 34(2), 269-74

Wojtys E, Kothari S U, Huston L, Anterior Cruciate Ligament Functional Brace Use in Sports, The American Journal of Sports Medicine, 1996; 24-4: 539- 546

World of Sports science, 2013 information retrieved from webpage http://www.faqs.org/sports-science/Je-Mo/Lower-Leg-Anatomy.html#b) during July 2013

Wright RW, Fetzer GB.Bracing after ACL reconstruction: a systematic review.Clin Orthop Relat Res. 2007 Feb; 455:162-8

Yeow C H, Gan W L, Lee P V S, Goh J C H, Effect of an anterior-sloped brace joint on anterior tibial translation and axial tibial rotation: A motion analysis study, Journal of Clinical Biomechanics 2010; 25: 1025-1030

Yeow C H, Khan R S, Lee P V S, Goh J G H, Preventing Anterior Cruciate Ligament Failure During Impact Compression by Restraining Anterior Tibial Translation or Axial Tibial Rotation, The American Journal of Sports Medicine, 2009; 37:813 – 821

Yu B, Gabriel D, Noble L, An K N, Estimate of the Optimum Cutoff Frequency for the Butterworth Low-Pass Digital Filter, Journal of Applied Biomechanics, 1999; 15:318-329
Yu B, Garrett WE, Mechanisms of non-contact ACL injuries, Br J Sports Med 2007; 41: 47-51

# References for Figures

Figure 1: Retrieved from website: http://kneestability.weebly.com/anatomy.html

Figure 2: Retrieved from website: http://www.pt.ntu.edu.tw/hmchai/Kinesiology/KINlower/Knee.htm

Figure 3: Retrieved from website: http://www.cea1.com/anatomy-sistems/leg-muscle/

Figure 4: Retrieved from website: http://www.vitalityplusaustralia.com/news/Knee-Anatomy_361.htm

Figure 5: Retrieved from website: http://stemcelldoc.wordpress.com/tag/acl-tear-treatment-without-surgery/

Figure 6: Retrieved from Beynnon B D, Fleming B C, Churchill D L, Brown D, The effect of Anterior Cruciate ligament deficiency and functional bracing on translation of the tibia relative to the femur during non-weight bearing and weight bearing: The American Journal of Sports Medicine 2003; 31: 99-105.)

Figure 7: Retrieved from Mohseni SS, Farahmand F, Karimi H and Kamali M. Arthrometric evaluation of stabilizing effect of knee functional bracing at different flexion angles. Journal of Sports Science and Medicine (2009) 8, 247 – 251

Figure 8: Retrieved from Paulos L E, Cawley P W, France E P. Impact biomechanics of lateral knee bracing: the anterior cruciate ligament. Am J Sports Med. 1991; 19:337-342.

Figure 9: Retrieved from Erickson A R, Yasuda K, Beynnon B, Johnson R, Pope M. An in vitro dynamic evaluation of prophylactic knee braces during lateral impact loading. Am J Sports Med. 1993; 21:26-35.

Figure 10: Retrieved from S. Hinterwimmer, H Graichen, R Baumgart, W Plitz, Influence of a mono-centric knee brace on the tension of the collateral ligamfrents in knee joints after sectioning of the anterior cruciate ligament – an in vitro study- Clinical Biomechanics, 2004, 19; 719-725